

Investigating the impact of two submerged sills  
on the physical habitat of Yangtze finless  
porpoise in Hechangzhou reach, China



Chu Chen





# Investigating the impact of two submerged sills on the physical habitat of Yangtze finless porpoise in Hechangzhou reach, China

by

Chu Chen

to obtain the degree of Master of Science  
at the Delft University of Technology,  
to be defended publicly on 30th October, 2020

Student number: 4748999

Thesis committee:

Prof. Stefan Aarninkhof	TU Delft
Dr. Qinghua Ye	TU Delft, Deltares
Dr. Bas van Maren	TU Delft, Deltares
Dr. Sien Liu	TU Delft, NHRI

An electronic version of this thesis is available at <http://repository.tudelft.nl/>.



# Contents

<b>Summary</b>	<b>v</b>
<b>Acknowledgement</b>	<b>vii</b>
<b>List of Figures</b>	<b>viii</b>
<b>List of Tables</b>	<b>xiii</b>
<b>List of Abbreviations</b>	<b>xiv</b>
<b>1 Introduction</b>	<b>1</b>
1.1 Background . . . . .	1
1.2 Problem statement . . . . .	3
1.3 Research questions . . . . .	4
1.4 Methodology and thesis outline . . . . .	4
1.4.1 Methodology . . . . .	4
1.4.2 Thesis outline . . . . .	5
<b>2 Literature Review</b>	<b>7</b>
2.1 Population status of Yangtze finless porpoise . . . . .	7
2.1.1 Population abundance of Yangtze finless porpoise . . . . .	7
2.1.2 Distribution of Yangtze finless porpoise population in the trunk of Yangtze River and adjacent lakes . . . . .	8
2.1.3 Hazard factors of Yangtze finless porpoise abundance . . . . .	8
2.2 Ecological habit of Yangtze finless porpoise . . . . .	11
2.2.1 Ecological behaviors of Yangtze finless porpoise . . . . .	11

---

2.2.2	Feeding habit and food choice of Yangtze finless porpoise . . . . .	13
2.2.3	River and lake migration . . . . .	14
2.2.4	Characteristics of habitat . . . . .	15
2.3	Habitat suitability index model . . . . .	16
2.3.1	Basic concept of model . . . . .	16
2.3.2	Procedures of model set-up . . . . .	17
<b>3</b>	<b>Study area</b>	<b>20</b>
3.1	General . . . . .	20
3.2	Hydrodynamic characteristics . . . . .	21
3.2.1	Upstream discharge . . . . .	21
3.2.2	Tide and currents . . . . .	24
3.2.3	Suspended sediment and transport . . . . .	25
3.3	Bed material . . . . .	27
3.4	Historical morphological changes . . . . .	28
3.5	Submerged sills . . . . .	30
<b>4</b>	<b>Method</b>	<b>31</b>
4.1	Habitat suitability index model application . . . . .	31
4.1.1	Ecological components . . . . .	31
4.1.2	Habitat variables of each ecological components . . . . .	35
4.1.3	Suitability index curve of each habitat variable . . . . .	36
4.1.4	Approach to derive the SI curve of V6 . . . . .	39
4.1.5	Equations in the HSI model . . . . .	40
4.2	Numerical model configuration . . . . .	41
4.2.1	Basic Lower Yangtze River model . . . . .	41

---

4.2.2	Domain and computational grids . . . . .	42
4.2.3	Boundary conditions . . . . .	43
4.2.4	Bathymetry . . . . .	43
4.2.5	Scenario description . . . . .	43
4.2.6	Simulation time and morphological scale factor . . . . .	44
4.2.7	Physical factor and median sediment diameter . . . . .	44
4.2.8	Calibration method . . . . .	44
<b>5</b>	<b>Results</b>	<b>46</b>
5.1	Numerical model performance . . . . .	46
5.1.1	Visual calibration . . . . .	46
5.1.2	Statistical calibration . . . . .	48
5.2	Numerical model results . . . . .	49
5.2.1	Changes of morphology . . . . .	49
5.2.2	Changes of hydrodynamic condition . . . . .	52
5.3	HSI model performance . . . . .	61
5.3.1	Visual validation . . . . .	61
5.4	Results of hydraulic-habitat model . . . . .	62
5.4.1	Water depth impact . . . . .	62
5.4.2	Flow velocity impact . . . . .	66
5.4.3	Substrate type impact . . . . .	70
5.4.4	Changes of composited suitability index(CSI) . . . . .	72
5.4.5	Changes of habitat area and quality . . . . .	75
5.5	Tidal effects . . . . .	78
5.5.1	Flow velocity during tidal ebbing period . . . . .	78

---

5.5.2	Flow velocity impact . . . . .	81
5.5.3	Changes of habitat area and quality . . . . .	86
<b>6</b>	<b>Discussions</b>	<b>88</b>
6.1	Habitat suitability index model . . . . .	88
6.1.1	Ecological component . . . . .	88
6.1.2	Habitat variable . . . . .	88
<b>7</b>	<b>Conclusions and Recommendation</b>	<b>89</b>
7.1	Conclusions . . . . .	89
7.2	Recommendation . . . . .	92
<b>A</b>	<b>Related graphs</b>	<b>93</b>
A.1	Hydrodynamic conditions . . . . .	93
A.2	Morphology . . . . .	94
A.3	HSI model results . . . . .	94
	<b>Bibliography</b>	<b>101</b>



# Summary

As Chinese economy booms during recent decades, river management attains more investment, and is required to develop more rapidly for flood defense as well as facilitating navigation, which brings a lot of changes and threat to most of aquatics, especially those endangered species. Yangtze finless porpoise is one of those endangered species, of which the habitat is faced up with severe threats from hydraulic engineering. Hechangzhou reach, situating in the lower Yangtze river and 250km upstream from the Yangtze river estuary(Shanghai), is one of the important navigation channels in Yangtze river and is also one of the main nature reserves for Yangtze finless porpoise. In order to adjust the discharge distribution of the two branches in Hechangzhou reach, Chinese Department of Water Resources conducted a project to construct 2 submerged sills in the north branch of Hechangzhou reach. This project aimed to deepen the south branch of Hechangzhou reach and to improve the navigation condition in the south branch. Acknowledging the importance of both navigation development and protection of endangered Yangtze finless porpoise, investigating the impact of two submerged sills on the physical habitat of Yangtze finless porpoise is necessarily. This requires a good understanding of the hydrodynamics changes caused by two submerged sills as well as the requirements from Yangtze finless porpoise on its physical habitat.

In this thesis, a study is performed to find a reliable evaluating system of Yangtze finless porpoise's physical habitat quality under the impact of hydraulic engineering. It aims to build the connection between engineering and ecological point of view. Habitat suitability index model, developed by the United States Fish and Wildlife Service(USFWS or FWS), is applied to the physical habitat of Yangtze finless porpoise. By literature reviewing and inquiring biologists, the vital ecological behaviors of Yangtze finless porpoise are identified as movement and feeding, and vital habitat variables are identified as water depth, flow velocity and substrate type. After summarizing and analyzing data from literature, the ranges of suitable water depth, flow velocity and substrate type are determined considering Yangtze finless porpoise's movement and feeding.

A previous developed hydro-morphodynamic numerical model was made available and is further developed to gain a better understanding of the changes to local hydrodynamic variables such as water depth, flow velocity. Substrate type, as one of the identified habitat variable from the results of habitat suitability index model, is determined by taking a simplified method of comparison between soil critical shear stress and local bed shear stress. Three scenarios are designed to simulate the situation in the dry, normal-water and monsoon season. Model results show an additional inward flux of water discharge though the south branch and a declining inward flux of water discharge though the north branch. In order to model the morphology in Hechangzhou reach in an efficient manner, a morphological acceleration factor was used to simulate more critical situations. The changes to water depth highly correspond with the changes to bed elevation caused by the sills. In the dry season, the changes of water depth, flow velocity

and substrate type are rare from the view of the whole reach. In the normal-water season, the submerged sills induce reduction of water depth and flow velocity in the north branch and the areas downstream the confluence close to Dagang while the sills lead to slight growth of water depth and velocity in the south branch. Soil with smaller grain size are retained due to the declining bed shear stress in most areas of the reach. In the monsoon season, the reduction and the growth of velocity are enhanced. The sills lead to a larger surface area where small grain soil can retain and deposit.

This thesis forecasts the changes to the physical habitat quality of Yangtze fineless porpoise through understanding the changes to local hydrodynamic condition and combining the results from habitat suitability index model. The adjacent area of Zhengrunzhou Dune and Luochengzhou Dune, the floodplain of the whole reach as well as the northern area in the north branch are classified as high quality habitat. In all three scenarios, the two submerged sills deteriorate the physical habitat quality in the south branch of Hechangzhou reach. In the normal-water and monsoon season, the sills improve the area upstream the bifurcation area, adjacent area of Luochengzhou Dune and the side channel near Wufengshan hill. Overall, the submerged sills offer limited potential habitat area, slightly extend the high-quality habitat area and improve the existing habitat. This study could be used to evaluate the impact of hydraulic engineering on Yangtze fineless porpoises' physical habitat and guide engineers to consider the quality of endangered species' physical habitat.

# Acknowledgement

This thesis shows the process and results of the master graduation project. The thesis concerns a study to investigate the impact of two submerged sills on the physical habitat of Yangtze finless porpoise in Hechangzhou reach, China. It is the final deliverable of the Master Program Hydraulic Engineering at the Delft University of Technology. I want to express my sincere gratitude to some people for their supports during this graduation project.

I would like to thank my supervisor team, Prof.Stefan Aarninkhof, Dr.Qinghua Ye, Dr.Bas van Maren and Dr.Sien Liu for supporting, guiding and encouraging me throughout the process. Thank you for overcoming the distance barrier and assisting me online to complete and improve my thesis when we all worked from home. You gave valuable insights and suggestions, shared knowledge and experience on my project. Thank Dr.Qinghua Ye for giving me much advise on the thesis methodology patiently when I was very confused at the start of the project. Thank Dr.Sien Liu for supervising my work and examining the thesis carefully and patiently, and even helping me to relieve my stress and anxiety during the project. Your help and understanding always motivate me to do it better. It is so great to work with you.

Also, thank Dr.Luca van Duren from Deltares, who participated in my researches. Thanks for taking the time, sharing the opinions and giving the inspirations for my project.

Thank all my friends for being with me. Thank my peers and friends in TU Delft, it is great to study and work with you all together for our similar goals. Also, thank you for giving me suggestions and inspiration whenever I need it. Thank my friends, who are not by my side. Thank you for listening to me, cheering me up and motivating me to believe in myself.

The greatest thanks to my parents. Thank you for supporting, encouraging and sometimes comforting me in the past years. Thank you for telling me 'you can do it' every time I feel frustrated.

At last, I would like to express my sincere gratitude to all people who accompanied me by my side or by remote communications during the tough and lonely time due to COVID-19.

Chu Chen  
Yangzhou, October 2020

# List of Figures

1.1.1 Sketch map showing locations of Yangtze finless porpoise reserves (Magenta numbers and names) and major cities, with downstream distance in km from Yichang along the Yangtze main stem. . . . .	3
1.4.1 Schematic overview of the structure of the thesis. Indicated within the parentheses are the corresponding chapters and sections of each process. The colored blocks correspond with the three phases as described . . . . .	6
2.3.1 Example SI curve from HSI model of SHORTNOSE STURGEON (SUITABILITY, 1986) . . . . .	17
2.3.2 Flowchart of procedures for establishing HSI model . . . . .	18
2.3.3 Example diagram of model structure showing how model variables combine to determine an HSI. Dashed lines indicate optional variables.(Terrell, 1982) . . . .	19
3.1.1 Schematic diagram of the Yangtze River from Datong to the estuary. . . . .	20
3.1.2 Schematic diagram of Hechangzhou reach. . . . .	21
3.2.1 Monthly distribution of yearly mean discharge measured measured at Datong gauge station(percentage above column indicating monthly distribution). . . . .	22
3.2.2 The annual (a)average (b)maximum and (c)minimum discharge measured at Datong gauge station (Ai, 2018) . . . . .	23
3.2.3 Variations of monthly discharge measured at Datong gauge station in the pre- and post- dam periods (Ai, 2018) . . . . .	23
3.2.4 Average monthly sediment transport rate and concentration at Datong gauge station. . . . .	26
3.2.5 Annual runoff volume and sediment input volume measured at Datong gauge station in 1950-2007. . . . .	26
3.2.6 Variations of monthly sediment discharge of Datong station in the pre- and post-dam periods, percentage above column indicating decreasing proportion. (Ai, 2018) . . . . .	27
3.2.7 Variations of monthly sediment concentration of Datong station in the pre- and post- dam periods. . . . .	27

3.3.1 Riverbed surface sediment grain size for the tidal reach of the Yangtze River. (Shuwei et al., 2017) . . . . .	28
3.4.1 Changes of the river plane morphology of the reach downstream Nanjing in the last 50 years. (LIU et al., 2011) . . . . .	29
3.5.1 Section of the two newly-built submerged sills and layout of the submerged sills.	30
4.1.1 Diagram illustrating the relationship among model variables, components, and HSI in the model for the brown trout.(Raleigh et al., 1984) . . . . .	32
4.1.2 Tree diagram illustrating relationships of habitat variables and life requisites in the riverine model for the carp. Dashed line indicates optional variable in the model.(Edwards and Twomey, 1982) . . . . .	33
4.1.3 Tree diagram illustrating relationships of habitat variables and life requisites in the riverine model for Yangtze finless porpoise. . . . .	34
4.1.4 Illustration of the derived SI curves for (a) Water depth regarding of movement (V1); (b) Flow velocity regarding of movement (V2); (c) Substrate type regarding of movement (V3); (d) Water depth regarding of feeding (V4); (e) Flow velocity regarding of feeding (V5); (f) Substrate type regarding of feeding (V6) . . . . .	37
4.1.5 Suitability index graphs for (a)water depth and (b) flow velocity of Cyprinidae's HSI model from literature (Chou and Chuang, 2011; WANG and YAN, 2008; WANG et al., 2009; Tan et al., 2011; Yang et al., 2010; Im et al., 2011) . . . . .	39
4.2.1 Domain map of Lower Yangtze River Model . . . . .	42
4.2.2 Domain map of Hechangzhou Reach Model . . . . .	42
4.2.3 Bathymetry map of Hechangzhou Reach Model . . . . .	43
5.1.1 Sketch of locations of 7 waterlevel measuring stations . . . . .	46
5.1.2 Calculated and measured waterlevels at (a) K1R Station, (b) K7R Station, (c) YZ10L Station, (d) YZ11L Station, (e) YZ14L Station, (f) YZ18L Station and (g) Zhenjiang Station . . . . .	47
5.1.3 Model Efficiency for the calculated waterlevels at the 7 measuring stations . . . . .	48
5.1.4 Percentage Bias for the calculated waterlevels at the 7 measuring stations . . . . .	48

5.2.1 Differences of bed level change caused by the submerged sills in the (a)normal-water season and (b)monsoon season . . . . .	50
5.2.2 Distribution map of bed level changes of the three scenarios with- or without-submerged sills. . . . .	51
5.2.3 Differences of flow velocity caused by the submerged sills in the (a)dry season (b)normal water season and (c)monsoon season. . . . .	54
5.2.4 Distribution map of flow velocity of the three scenarios with- or without- submerged sills. . . . .	55
5.2.5 Differences of water depth caused by the submerged sills in the (a)dry season (b)normal-water season (c)monsoon season . . . . .	57
5.2.6 Distribution map of water depth of the three scenarios with- or without- submerged sills. . . . .	58
5.2.7 Distribution map of tidal range of the three scenarios with- or without- submerged sills. . . . .	60
5.3.1 Distribution map of YFP's occurrence and composite suitability index in the normal-water season . . . . .	61
5.4.1 Differences of SI of V1 caused by the submerged sills in the (a)dry season (b)normal-water season and (c)monsoon season . . . . .	63
5.4.2 Distribution map of SI of V1 of the three scenarios with- or without- submerged sills. . . . .	64
5.4.3 Distribution map of SI of V4 with submerged sills and differences of SI of V4 caused by the submerged sills in the three scenarios. . . . .	65
5.4.4 Differences of SI of V2 caused by the submerged sills in the (a)normal-water season and (b)monsoon season . . . . .	66
5.4.5 Distribution map of SI of V2 of the three scenarios with- or without- submerged sills. . . . .	67
5.4.6 Distribution map of SI of V5 with submerged sills and differences of SI of V5 caused by the submerged sills in the three scenarios. . . . .	69
5.4.7 Distribution map of SI of V6 with submerged sills and differences of SI of V6 caused by the submerged sills in the three scenarios. . . . .	71



5.4.8 Differences of CSI caused by the submerged sills in the (a)dry season, (b)normal-water season and (c)monsoon season. . . . .	73
5.4.9 Distribution map of CSI of the three scenarios with- or without- submerged sills.	74
5.4.10Growth/Decline ratio of habitat areas and effective habitat areas with the submerged sills in the three scenarios. . . . .	76
5.4.11The growth/decline ratios of habitat areas or weighted areas(product of CSI multiplied by area) with the submerged sills in the (a)dry season (b)normal-water season and (c)monsoon season. . . . .	78
5.5.1 Distribution map of flow velocity of the three scenarios with- or without- submerged sills during tidal ebbing period. . . . .	80
5.5.2 Differences of flow velocity caused by the submerged sills during the tidal ebbing period in the (a)normal-water (b)monsoon season and (c)dry season . . . . .	81
5.5.3 Distribution map of SI of V2 with submerged sills and differences of SI of V2 caused by the submerged sills in the three scenarios during tidal ebbing period. .	83
5.5.4 Distribution map of SI of V5 with submerged sills and differences of SI of V5 caused by the submerged sills in the three scenarios during tidal ebbing period. .	85
5.5.5 Growth/Decline ratio of habitat areas and effective habitat areas in the three scenarios caused by the submerged sills during the tidal ebbing period. . . . .	87
A.1.1Distribution map of bed shear stress in the three scenarios with- or without- submerged sills and the distribution difference caused by the submerged sills. . .	93
A.2.1Differences of bed level change caused by the submerged sills in the dry season. .	94
A.3.1Differences of SI of V2 caused by the submerged sills in the dry season. . . . .	94
A.3.2Distribution map of SI of V4 without submerged sills in the three scenarios. . . .	95
A.3.3Distribution map of SI of V5 without submerged sills in the three scenarios. . . .	96
A.3.4Distribution map of SI of V6 without submerged sills in the three scenarios. . . .	97
A.3.5Distribution map of CSI with- or without- submerged sills and the distribution difference caused by the submerged sills in the three scenarios during tidal ebbing period. . . . .	98

---

A.3.6 The growth/decline ratios of habitat areas or weighted areas (product of CSI multiplied by area) with the submerged sills during tidal ebbing period in the (a) dry season (b) normal-water season and (c) monsoon season. . . . .	100
------------------------------------------------------------------------------------------------------------------------------------------------------------------------------------------------------------------------------------------	-----

# List of Tables

1.1	Summary of Yangtze finless porpoise reserves in the Yangtze river trunk and 2 main lakes . . . . .	2
2.1	Summary of bait fish of Yangtze finless porpoises. . . . .	14
3.1	Several important hydrological indices measured measured at Datong gauge station from 1950 to 2007 . . . . .	22
3.2	Tidal characteristic values from 2 tide stations in HCZR . . . . .	24
3.3	Several sediment characteristic values at Datong gauge station from 1950 to 2007	25
3.4	Annual sediment input volume and concentration in the post-TGD period at Datong gauge station . . . . .	25
4.1	Data sources for Yangtze finless porpoise suitability indices . . . . .	38
4.2	Critical shear stress and suitability index of different fractions of sediment . . . .	40
5.1	Changes of habitat area and quality . . . . .	75
5.2	Changes of habitat area and quality in the tidal ebbing period . . . . .	86

# List of Abbreviations

CSI Composite suitability index

HCZD Hechangzhou Dune

HCZR Hechangzhou reach

HSI Habitat suitability index

LCZD Luochengzhou Dune

TGD Three Gorges Dam

WFSH Wufengshan Hill

YFP Yangtze finless porpoise(s)

ZRZD Zhengrunzhou Dune

ZYR Zhenyang reach

# Chapter 1 Introduction

In this chapter, an overall introduction is given to the area and problem of interest, which is the subject of this thesis. Next, from the problem definition, the objective and corresponding research questions are formulated. Finally, the general structure of this thesis is outlined as a reading guide.

## 1.1 Background

The People's Republic of China is one of the most populated and developing countries in the world. With the world's second largest GDP of 11,200,000 million USD and a net growth of 6.7% in 2016, China has become a major global economy (Salaam, 2017; Bank, 2017). As Chinese economics booms from recent decades, river management attains more investment and is required to develop rapidly for flood defense and facilitating navigation, which brings a lot of changes and threat on most of aquatics, especially those endangered species. Yangtze finless porpoise(YFP) is one of those endangered species, of which the habitat is faced up with severe threats from hydraulic engineering (Yu et al., 2002).

Yangtze finless porpoise (*Neophocaena asiaeorientalis asiaeorientalis*) is a critically endangered sub-species of the narrow-ridged finless porpoise (*Neophocaena asiaeorientalis*) that exclusively occurs at the Yangtze River and the adjacent Poyang Lake and Dongting Lake (Gao, 1995; Jefferson and Wang, 2011). This sub-species of porpoise was previous occurred throughout the 1700km Yangtze River mainstream from Yichang to Shanghai (Gao, 1995), but its distribution is now primarily confined to about 1000 km of the Yangtze River mainstream, from Ezhou to Shanghai(Mei et al., 2012). The latest Yangtze Freshwater Dolphin Expedition (YFDE2012) revealed that at the end of 2012, there were only approximately 1,040 individuals remaining (Mei et al., 2012) and YFP was listed as Endangered by IUCN in 1996 (IUCN, 1996) in terms of the criteria that fewer than 2500 mature individuals remained and the population was continuing to decline. This sub-species has been affected by a sharp decline in the population and population fragmentation (Mei et al., 2012). The heavy impact of human activities in the Yangtze River, including overfishing of prey species, water development projects, water pollution and accidental deaths was considered as the primary threaten to this sub-species (Wang, 2009).

In order to protect YFP, Chinese government has established several natural reserves, including: Tongling national natural reserve in Anhui province, Honghu national natural reserve in Hubei province, Poyang lake provincial natural reserve in Jiangxi province, Zhenjiang provincial natural reserve in Jiangsu province, and Dongting Lake municipal natural reserve in Hunan province (see Figure.1.1.1 and Table.1.1). Many hydraulic engineering projects have been implemented

in recent decades in these natural reserves. One of these reserves is Zhenjiang Provincial Nature Reserve in Jiangsu province, which is a representative area revealing the conflict between hydraulic engineering and YFP's living.

Zhenjiang Provincial Nature Reserve situates in the north branch of Hechangzhou reach(HCZR) which is located in the lower Yangtze River, adjacent to Dantu District, Zhenjiang City. HCZR is one of the most unstable reaches in the lower Yangtze River. The south branch, as the main shipping channel, was being narrowed continually. To stabilize the river regime, after a previous submerged sill was built in 2003, the construction of two following submerged sills, which locates 2km downstream from the old sill in the north branch, started in 2015 and was completed in 2018, resulting in the substantial change of morphology and hydrodynamics in HCZR. The implement of the two newly-built sills is going to have deep and systematic impact on the hydrodynamics, morphology and ecology of this reach. Considering that the protection of YFP is so urgent, study on the impact of the engineering on YFP's habitat is apparently necessary in HCZR.

Table 1.1: Summary of Yangtze finless porpoise reserves in the Yangtze river trunk and 2 main lakes

Reserves name	Upper limit index(km)	Lower limit index(km)	Position $DD^{\circ}MM'$	Grade	Length(km)
Shishou	Xichang 214	Wumakou 303	E $112^{\circ}25'$ , N $29^{\circ}57'$ E $112^{\circ}51'$ , N $29^{\circ}46'$	National	89
Honghu	Xintankou 410	Luoshan 546	E $113^{\circ}16'$ , N $29^{\circ}36'$ E $113^{\circ}52'$ , N $30^{\circ}13'$	National	136
Anqing	Sanhaozhou 919	Zongyang 1142	E $116^{\circ}22'$ , N $29^{\circ}51'$ E $117^{\circ}39'$ , N $30^{\circ}46'$	Municipal	222
Tongling	Zongyang 1142	Jinniudu 1180	E $117^{\circ}39'$ , N $30^{\circ}46'$ E $117^{\circ}55'$ , N $30^{\circ}46'$	National	58
Zhenjiang	- 1458	- 1473	E $119^{\circ}24'$ , N $32^{\circ}15'$ E $119^{\circ}32'$ , N $32^{\circ}13'$	Provincial	15
Poyang Lake	-	-	-	Provincial	-
Dongting Lake	-	-	-	Municipal	-



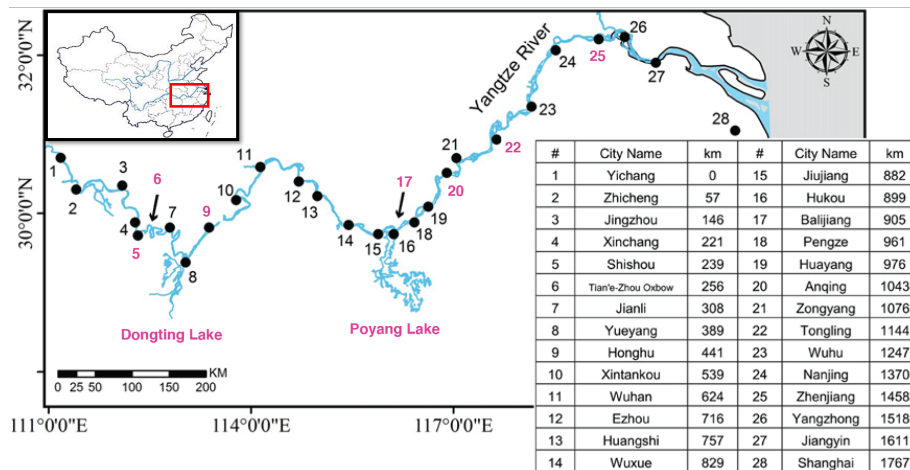


Figure 1.1.1: Sketch map showing locations of Yangtze finless porpoise reserves (Magenta numbers and names) and major cities, with downstream distance in km from Yichang along the Yangtze main stem.

## 1.2 Problem statement

The channels from Nanjing to the Yangtze River Estuary, with superior natural conditions for navigation are currently the ones with the highest inland waterway level and navigation development potential in China. But there are navigation-obstructing shallow reaches in the channels, hence calling for implementing a deep-water channel regulation projects including two submerged sills to be constructed in HCZR, where a crucial nature reserve for YFP is also located.

Although the sill benefit for channel regulation, its influence on YFP's physical habitat can not be neglected and is still unclear to engineers. In recent years, Chinese government has paid more attention on the balance between engineering effectiveness and deterioration of river ecological environment as well as loss of biodiversity. Natural ecosystems are highly dependent on rivers environment and freshwater resources. The destruction of river ecosystems will eventually affect humans, so how to protect and repair river ecosystems has become a hot topic in the world. European and American countries started research in this area earlier, and have carried out a series of river ecological assessment and restoration work since the middle of the last century. However, the research in China still needs to be developed more. Due to the complex requirements of wild species for its habitat, several problems such as how to quantify the ecological impact of hydraulic engineering, and how to scientifically establish the relationship between water environment and aquatics' habitat are worthy of further study.

Furthermore, it is known that YFP is an endangered aquatic species. The most common and reliable method on studying species' habitat preference is to investigate the relationship between

the occurrence of its fixed nest and corresponding physical indices. In other words, animals such as birds usually prefer the habitat where their nests are spotted more. However, unlike the animals having fixed nests, YFP's habitat extent is usually rougher than that of those animals. As a result, the previous method may not be suitable for YFP. In addition, since YFP is endangered nowadays and the measurements of hydrodynamics indices can not cover the whole habitat, there is inadequate quantitative data about its occurrence and corresponding hydrodynamics indices, which brings more difficulties on quantifying its habitat preferences. Therefore, how to quantify endangered species' habitat preferences based on existing limited quantitative data needs to be addressed.

### 1.3 Research questions

In order to further investigate the main objectives, the following three sub-research questions are expected to be answered with the results of this thesis.

- (1) What is the preference of Yangtze finless porpoise towards its habitat? (Which habitat variables are important? What is the suitable range of each variable for YFP?)
- (2) What morphology and hydrodynamics which will affect the Yangtze finless porpoise's habitat will be changed by the two submerged sills? (How will the submerged sills change the habitat variables mentioned in 1st research question?)
- (3) How does the changed morphology and hydrodynamics affect the Yangtze finless porpoise's living? (How to evaluate the changes mentioned in 2nd research question?)

### 1.4 Methodology and thesis outline

#### 1.4.1 Methodology

In this thesis, a hydraulic-habitat model which is a combination of a habitat suitability index model and a 2-D processed-based numerical model(Delft3D) is applied. The habitat suitability index model is used to indicate the quality of each habitat grid by habitat suitability index ranging between 0 and 1. During the process of establishing the habitat suitability index model, several habitat variables which are important to the quality of habitat are identified. The numerical model is used to obtain the changes of morphology and local hydrodynamics after the submerged sills are built in different scenarios.

After obtaining the changes of suitability index of each habitat grid due to the changes of morphology and local hydrodynamics, the effect of submerged sills on YFP's habitat can be

discussed by "weighed usable area" value, which is the aggregation of the area of a river unit multiplied by this unit's composited suitability index.

### 1.4.2 Thesis outline

According to the questions that need to be answered, this thesis is divided into 3 phases. These phases are further divided into several processes as shown in Figure 1.4.1.

The first phase is aimed at understanding the preference of YFP towards its physical habitat. This is done by means of a review of the literature on the YFP's population abundance as well as its ecological habit and can be found in Chapter 2. Subsequently, in order to further study and quantify YFP's preference towards its habitat, a habitat suitability index model(HSI) of YFP is developed. With the HSI model, on one hand, which habitat variables are most important can be determined in order to give instructions on which variables' changes of morphology and hydrodynamics need to be obtained in the second phase; on the other hand, how the quality of habitat will be changed by different habitat variables can be answered in order to quantify the effects of morphology and hydrodynamics. The model description will be covered in Chapter 2.3 and its application will be covered in Chapter 4.1.

In the 2nd phase, the changes of morphology and local hydrodynamics due to submerged sills will be studied. After collecting the basic information of the morphology and hydrodynamics in Hechangzhou reach covered in Chapter 3, in order to study the region and test different scenarios, a 2D hydro-morphodynamic numerical model, previously setup for the lower section of Yangtze river was further developed and applied on the Hechangzhou reach. The model description and setup will be covered in Chapter 4.2. Subsequently, the model results will be calibrated with help of earlier work, such as field observations and measurements(See Chapter 5.1). These modeling results are the first part of the overall results and can be found in Chapter 5.2.

In the 3rd phase, the results from the previous 2 phases are combined for quantifying the impact of submerged sills on YFP's physical habitat. The combination of the HSI model and 2D numerical model, which is called hydraulic-habitat model, can be used to test the results in different hydrology scenarios. The set-up of several conceived scenarios are described in Chapter 4.2. The results with different scenarios during the tidal flooding period are further discussed in Chapter 5.4. After comparing with the results during the tidal ebbing period, the differences of the impacts induced by the tidal effect are treated in Chapter 5.5.

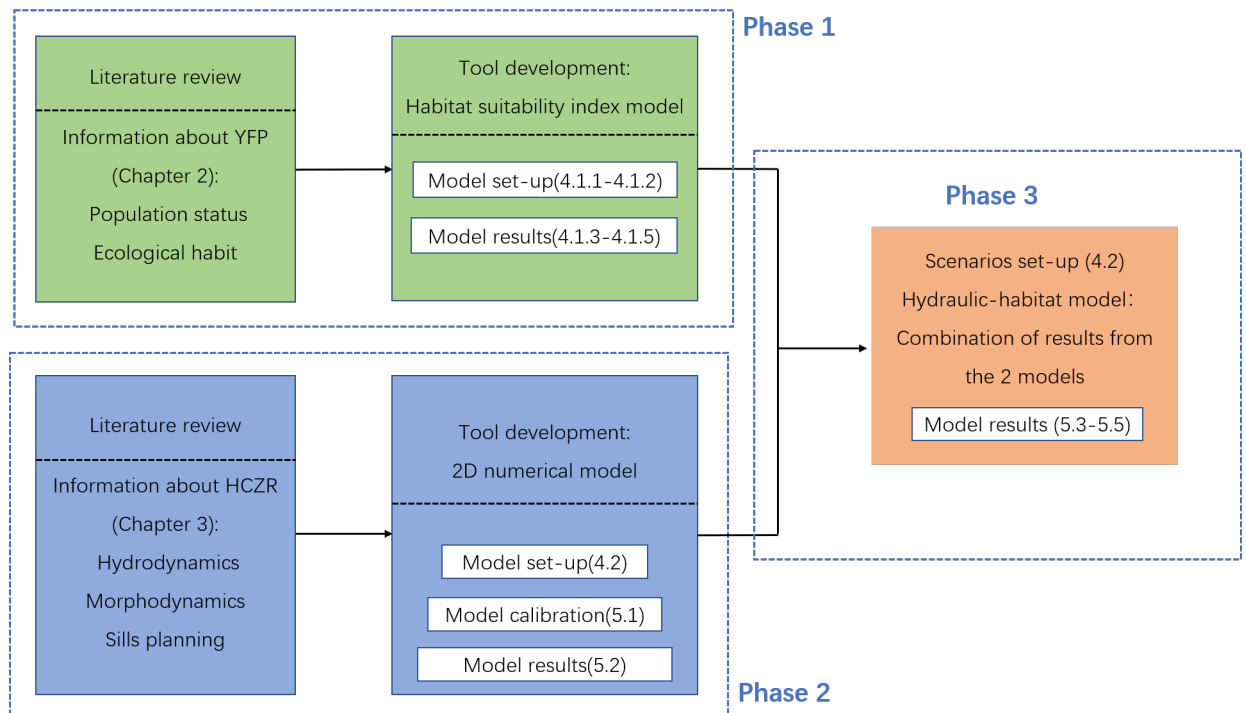


Figure 1.4.1: Schematic overview of the structure of the thesis. Indicated within the parentheses are the corresponding chapters and sections of each process. The colored blocks correspond with the three phases as described

# Chapter 2 Literature Review

## 2.1 Population status of Yangtze finless porpoise

### 2.1.1 Population abundance of Yangtze finless porpoise

Finless porpoise, as the name indicated, is the only porpoise that has a low, narrow ridge covered in thick skin bearing several lines of tiny tubercles instead of a true dorsal fin. In addition, the forehead is unusually steep compared with those of other porpoises (Jefferson et al., 2011).

Yangtze finless porpoise (*Neophocaena phocaenoides*), belonging to kingdom *Animalia*, phylum *Chordata*, class *Mammalia*, order *Artiodactyla*, infraorder *Cetacea*, family *Phocoenidae*, genus *Neophocaena*, Species *N. phocaenoides*, is the only freshwater subspecies of the narrow-ridged finless porpoise (Wang, 1992). Adult YFP can grow to as much as 1.3-1.7 m in length, with its body in dark or black. It is found to be sexual mature at the age of 4 or 5. The pregnancy period is around 10-11 months and the suckling period is around half a year. YFP is recorded to give birth on April or May in spring, or on September or October in autumn (Wei et al., 2002, 2003).

Based on the results of the investigation of YFP in the middle and lower reaches of the Yangtze River in 1984-1991, Zhang et al. believed that the population of YFP in the Yangtze River was about 2700, of which 500 were in the reach from Yichang to Wuhan and 2200 were in the reach below Wuhan, of which 1652 were in the reach from Jiangyinv to Wuhan is 1652 (Zhang et al., 1993). Zhou et al. (1998) extrapolated from the results of four investigations in the Nanjing-Hukou reach from 1989 to 1992 and believed that the population of YFP in the reach from Jiangyin to Wuhan section was about 1481 which decreases 10.35% compared with that from Zhang et al. (1993). Yu et al. (2001) estimated that the number of YFP in the Anhui reach of the Yangtze River (Hukou to Nanjing) was 1054 based on 11 ecological surveys in the reach from Hukou to the Nanjing in 1993-1999.

In the Dongting Lake, YFP are concentrated in the lake area from Chenglingji to Saiyukou, and their population is approximately 100,150; during the monsoon season, the lake surface expands, and the distribution of YFP groups in the Dongting Lake can extend from Saiyukou to Leishi, 20km upstream (Yang et al., 2000; Xiao and Zhang, 2002). In the Poyang Lake, during the dry season, YFP are concentrated in the area from Hukou to Laoyemiao; during the monsoon season, the lake surface expands, and the distribution of YFP is relatively wide, with the number about 450 (Yang et al., 2000; Zhao et al., 2008). According to the latest survey data of the Dongting Lake by the Yangtze River Aquatic Institute in January 2012, the population of YFP in the Dongting Lake is only 85 , which is greatly declining. According to a large number of existing

studies, the population level of Yangtze finless porpoise is low and has declined year after year (Ding et al., 2000; Wang et al., 1998; Wei et al., 2002; Yang et al., 2000; Yu et al., 2001). The number of YFP decreased from about 2700 in 1991 (Zhang et al., 1993) to about 1800 in 2006 (Zhao et al., 2008). Although the exact population of marine subspecies is currently unknown, it is generally considered to range between tens of thousands and hundreds of thousands (Jefferson et al., 2011). Combined with the survey data of 2700 in the early 1990s (Zhang et al., 1993), it can be considered that the number of YFP was only a few tenths to a few hundredths of the marine subspecies at that time, indicating that YFP is the most rare one among the subspecies.

### **2.1.2 Distribution of Yangtze finless porpoise population in the trunk of Yangtze River and adjacent lakes**

YFP is only distributed in the trunk of the middle and lower reaches of the Yangtze River and two large adjacent lakes (Poyang Lake and Dongting Lake) connected to the Yangtze River. Historically, YFP once lived in some large tributaries, such as in the Han River in the 1960s, but it soon disappeared (Zhang et al., 1993). There are also sporadic discoveries in the tributaries of the two lakes, but researchers believe that the distribution of YFP in most tributaries is rare or even disappeared (Xiao and Zhang, 2002; Yang et al., 2000). Compared with its marine subspecies (northern subspecies), the habitat of YFP is much narrower (Kasuya, 1999). The distribution of YFP is neither uniform nor continuous in the trunk of the Yangtze River, and it is more concentrated in Wuxue reach, Nanjing to Zhenjiang reach, Balijiang reach, Xinluo reach and others, but no distribution is found within about 100km downstream of Yichang (Xiong and Zhang, 2011; Zhao et al., 2008). There is a higher population density in the reaches below Wuhan than those above Wuhan. The relatively concentrated reaches are from Wuxue to Sanhaozhou and from Nanjing to Zhenjiang (Zhao et al., 2008). The distribution range of YFP in the Dongting Lake and the Poyang Lake is also directly affected by the size of the water area. During the dry season, the water levels of the two lakes are low, and the lake surface is shrinking. In the Dongting Lake, YFP are concentrated in the lake area from Chenglingji to Saiyukou, and their population is approximately from 100 to 150; during the flood season, the lake surface expands, and the distribution of YFP in Dongting Lake can extend from Nianyukou to 20km upstream Leishi (Yang et al., 2000; Xiao and Zhang, 2002). In Poyang Lake, YFP are concentrated in the area from Hukou to Laoyemiao during the dry season; the lake surface expands during the monsoon season, and the distribution of YFP of which the number is about 450 is relatively wide (Yang et al., 2000; Zhao et al., 2008).

### **2.1.3 Hazard factors of Yangtze finless porpoise abundance**

(1) Fishing resource decline



Since 1980s, the fishing resource in the middle and lower Yangtze river has been declining continuously. In 21th century, the annual fishing production in the middle and lower Yangtze river is less than 20% of the highest production in history.

The decline in the amount of food resources has caused great harm to the survival of YFP. Since March 2012, YFP distributed in the Dongting Lake have gradually died. Before February 2013, more than 20 YFP died in Poyang Lake. Experts dissected the bodies of these dead YFP and found that YFP may have been starved to death due to lack of food supply, and there was almost no food remained in their digestive system. Insufficient bait has forced them to prey in some dangerous areas at risk of their lives, and sometimes even some garbage will be swallowed due to hunger. The Nanjing Fisheries Administration had dissected the dead YFP and found plastic bags and garbage in its stomach. Apparently YFP swallowed the plastic bag and was difficult to digest.

### (2) Illegal fishing and illegal fishing gear use

Illegal and overfishing of wild fish species and the use of harmful fishing gear are threats to the Yangtze finless porpoise. Hooks and some illegal fishing gears that function similarly to hooks can directly do harm to YFP, can kill YFP directly, or at least make them injured and infected with germs and viruses that could affect their living and reproduction. If YFP touch the electrofishing net, there may be cases of direct electric shock death or drowning. According to the incomplete statistics in Tongling nature reserve, there are nine YFP death reported caused by harmful fishing gears from 1995 to 2013 (WANG et al., 2003).

### (3) Shipping and waterway transport

In recent years, China's water shipping industry has developed rapidly, and the number of large vessels passing by in the Yangtze River and its tributaries has increased sharply every day. It is also one of the direct causes of the decline of YFP's population. YFP rely on their sonar system for positioning to seek food and contact with their peers. A large number of shipping vessels bring noise disturbance which causes YFP failing to perform fast and accurate positioning, seriously affects their normal activities, especially preying. Previous studies have found that excessively strong underwater noise may lead to changes of physiological and behavioral adaptation of cetaceans, and severely cause hearing damage and even death (Malakoff, 2001; Foote et al., 2004). YFP usually takes temporary escaping action from ship interference, but considering the waterways in some areas are relatively narrow, combined with the fast speed of some ships, even if the finless porpoise has certain sensitivity to ship interference, it is difficult to escape. In addition, YFP may have a certain "adaptability" to the noise of long-term high-density sailing ships in the waters, resulting in YFP not responding strongly to noise when encountering sailing ships (Dong et al., 2012).

YFP has a special living habit, which is that it floats on the water during the rest period. Because some ships are sailing fast and often do not have time to dodge, it is easy for YFP to be injured

or even killed by the propeller of the ship. The rapid development of the shipping industry has severely reduced the space where finless porpoises can live freely; ship accidents can cause direct or indirect deaths of YFP. According to incomplete statistics, more than 50% of dead dolphins are caused by ship.

#### (4) Water environment pollution

The rapid development of industry and economy has caused serious pollution of industrial waste water and domestic sewage to the Yangtze River water resources, and it is also a huge threat to the survival of YFP. Because YFP plays the top role in the food chain, some harmful components will be enriched in its body by the cascading effect of the food chain, which can have a certain toxic effect on its survival and reproduction (WANG et al., 2003). According to reports, from April to June 2004, there were multiple collective casualties of YFP in the East Dongting Lake area and nearby waters. Expert analysis the death was mainly caused by the discharge of organic pesticides, heavy metals and industrial sewage.

#### (5) Hydraulic engineering

Excessive development and utilization of water resources has worsened the water environment. The ecological environment in the Yangtze River Basin has been severely damaged, and biodiversity has been unprecedentedly destroyed (Jianhua, 2010). YFP is particularly sensitive to the response of water conservancy and hydropower projects, such as dredging, river regulation, water conservancy construction, etc. (Yu et al., 2002). Some large-scale water conservancy and hydropower projects have completely changed the aquatic ecological environment and hydrological conditions of the Yangtze River, severely damaged the habitat of YFP,. For example, the renovation of the east channel of the Yangtze River has obviously changed the habitat area of YFP. Originally, the main habitat of YFP was in the separation area of the sand bar and the other habitat was in the bifurcation area upstream of the sand bar. However, after construction, it was found that the occurrence of finless porpoise in the separation area has been sharply declined, the group size in the separation area is relatively small, and the number of finless porpoises there has dropped significantly (Yu et al., 2012); after the implementation of the Yangtze River Flood Control Project, a series of changes have occurred in the river channel, which has brought some Serious indirect impacts, such as the reduction of the movement area. In dry season, shipping and some construction and blasting operations increase the chance of accidental casualties, such as the reduction of bait (Xian-feng and Jian-bo, 2001).

The construction of the Three Gorges Dam forced the upper limit of the distribution of finless porpoises to retreat downstream, and due to the large amount of siltation in the reservoir area, the downstream riverbed was scoured, which changed some characteristics of its breeding and thus affected its reproduction a lot (Jin et al., 2009). After the Three Gorges Dam started to impound water, the number of four major Chinese carps downstream the dam drastically decreased, causing a sharp drop in porpoise bait resources. Many finless porpoises travelled long

distances because they did not get enough food, and some even starved to death. During the implementation of the Jiepai River Rehabilitation Project, the monitoring data showed that the river section where the finless porpoise was distributed in the middle reaches of the Yangtze River was segmented.

#### (6) Climate change

Global climate change will affect the changes in the hydrological cycle. In recent years, it has affected the ecological environment of rivers and oceans, which has exacerbated the uneven distribution of water resources in some regions (Jin et al., 2009). Due to the effects of extreme climates, such as global warming and persistent dry climate, the unusually low water levels of Dongting Lake and Poyang Lake which are the main habitats of YFP, pose a great threat to the survival of Yangtze finless porpoises. Because the rapid changes in the climate have caused the water level to drop suddenly, YFP have more difficulty finding food, which may starve them to death, as evidenced from autopsy report showed nothing remained in their stomachs.

## 2.2 Ecological habit of Yangtze finless porpoise

### 2.2.1 Ecological behaviors of Yangtze finless porpoise

Based on the extant study on YFP's behavior characteristics in different habitats, five basic behavioural patterns commonly observed of Yangtze finless porpoise have been defined:

#### (1) Swarming

YFP often live as a group called "core unit" of 2-3 members in Yangtze river. The basic unit commonly consists of mother porpoise and its infant, or a male porpoise and a female one (Wenhua, 2000; Wang et al., 1997; Wei et al., 2004). The larger group of more than 5 ind consists of several sub-groups of 2-3 ind. During the swarming period, sub-groups usually keep certain distance away from each other.

In the dry season, YFP tend to assemble and only make short-distance migrations. In Balijiang reach, the average number of individuals is 150. The whole big group can be divided into several concentrated small sub-groups which occupy different water areas at the same time. Each sub-group is basically composed of several core groups of 2-3 heads. Part of the core groups contain a juvenile porpoise, and its structure indicates that the core group is composed in the form of family (Wei et al., 2002). In Tian-E-Zhou national reserve, the average number of finless porpoise groups was 5 ind in dry season, which was higher than the number of that in other non-flood seasons (Wang et al., 1997).

#### (2) Foraging

YFP were observed to forage individually or in a group. Individual foraging is generally in the shallow water near the river bank (the water depth is about 3m) (Wei et al., 2002). When YFP are foraging, they firstly swim fast, mostly dive deep and frequently emerges out of the water, making loud breathing sound, provoking a few centimeters of high waves on the water surface, with birds hovering overhead. After locking the prey, it rushes forward, then quickly swivel, hit the water with the leaf-shaped tail, stir the water, and drive the bait separating. Then it swims and gets close to the prey quickly, turns its head flexibly in order to lock the target accurately. After biting the prey, it adjusts its head to swallow the prey in the direction of the throat, then take the next predation, and sometimes hold several small fish in the mouth and swallow it together (Yang and Chen, 1996). After eating, it slowly swim or suspend in the water. For group preying, 3-5 porpoises converge in a water area of less than 100 m<sup>2</sup>, forming an irregular semi-arc shape. YFP swim apart from each other, plunge into the water from different directions and stir the water. YFP respond slowly to disturbances when preying, especially during group preying. Yu et al. (2003) deemed that YFP's foraging behavior is consistent with its bait fish's movement behavior.

### (3) Oestrus and mating

According to observation results in Tian-E-Zhou reserve, Tongling reserve and Wuhan human-raising reserve, oestrus and mating of YFP mainly occurs in spring and autumn (Wei et al., 2002, 2004; Hao et al., 2006). Adult YFP are often observed to swim in pairs, chasing each other in secluded shallow low-velocity water area (within a depth of 3 m), and splashing water on the water surface. 2 YFP often make their tails to get close, and hit the water at the same time, then dive together. After two to three minutes, the two YFP come out of the water to breathe quickly and finally separated.

### (4) Infant care

During infant-care processing, the baby YFP commonly follows two large YFP, forming a infant-care group of 3 YFP. Newborn YFP often swims slowly above the left or right fin of large YFP, closely following the group, and keeps the swimming direction basically the same as that of large YFP (Wei et al., 2002).

### (5) Resting

YFP moves slowly at the surface or stays afloat for at least five seconds.

### (6) Playing

YFP's playing behavior commonly occurs when YFP group swims upstream in low-velocity water area. Typical playing behaviors are wave riding, jumping, milling, and chasing each other. In Balijiang River, when the wind speed excesses 10 m/s on the surface of the water, and the wave is 0.5 m high, YFP rides on waves, and commonly takes out-of-water breathe at the crest of the

wave instead of at the trough. When the air pressure is low, YFP chases and plays with each other, jumping out of the water, with most of the body or even the whole body being exposed. Sometimes, several YFPs make a circle in a smaller water area, hardly moving or just migrating slowly during a certain period of time. This is the process of milling.

### 2.2.2 Feeding habit and food choice of Yangtze finless porpoise

The range of YFP's food is relatively wide. The food found in the stomach of YFP living in the middle section of Yangtze river includes common carp (*Cyprinus carpio*), yellowhead catfish (*Pelteobagrus fulvidraco*), crucian carp (*Neophocaena asiaeorientalis asiaeorientalis*), shrimp and some cereals (Chen et al., 1997). YFP living in the confluence area of Yangtze river prey *Protosalanx hyalocranius*, *Coilia nasus*, *Coilia ectenes Jordan et Seale*. Institute of Hydro-biology, Chinese Academy of Sciences feeds YFP with crucian carp as its only food, which can also sustain YFP to live healthily.

Yu et al. (2003) made a study on the YFP's feeding habit in Tongling semi-nature reserve which indicated that: from the view of palatability of their baits, catfish (*Silurus asotus*), black carp (*Mylopharyngodon piceus*) and *Channa argus* (*Ophiocephalus argus*) were considered as the best choice; grass carp (*Ctenopharyngodon idellus*), common carp (*Cyprinus carpio*) and bream (*Parabramis pekinensis*) were the second; crucian carp (*Carassius auratus*) and silver carp (*Hypophthalmichthys molitrix*) seem to be the least-favorite one.

Yang et al. (2019) updated the study by conducting experiments during 2016 and 2017 in the same reserve and the results showed that: from the view of palatability of their baits, among 8 different baits, common carp (*Cyprinus carpio*) and wild carp (*Hemiculter leucisculus*) were considered as the best choice; silver carp (*Hypophthalmichthys molitrix*) and crucian carp (*Carassius auratus*) were the second; grass carp (*Ctenopharyngodon idellus*) and bream (*Parabramis pekinensis*) become the least-favorite one. From the perspective of sex there was no significant difference between male and female individuals in the selection of bait fish; the food choice of juvenile is significantly different from that of adult finless porpoises, and it is speculated that young dolphins choose more nutritious food for growth

Because YFP can only swallow their food, they have a certain selectivity to the size of the bait fish, and usually prey on smaller bait fish. By making the feeding choice of baiji (another endangered Yangtze river dolphin) as an analogy, the criterion for the selection of YFP is the bait fish's body height of no more than 6 cm or body length of no more than 25 cm.

Table 2.1 summarizes the bait fish of YFP and the abundance of each bait fish in Hechangzhou reach. Relative importance index in the table reveals the abundance of each bait fish in Hechangzhou reach. In summary, Cyprinidae Family fish is chosen as the main bait for YFP in Hechangzhou reach.

Table 2.1: Summary of bait fish of Yangtze finless porpoises.

English name	Latin name	Family	Sub-family	Genus	Relative importance index in HCZR
Common carp	<i>Cyprinus carpio</i>	<i>Cyprinidae</i>	<i>Cyprininae</i>	<i>Cyprinus</i>	803
Wild carp	<i>Hemiculter leucisculus</i>	<i>Cyprinidae</i>	<i>Cultrinae</i>	<i>Hemiculter</i>	511
Silver carp	<i>Hypophthalmichthys molitrix</i>	<i>Cyprinidae</i>	<i>Xenocyprinae</i>	<i>Hypophthalmichthys</i>	4129
Crucian carp	<i>Carassius auratus</i>	<i>Cyprinidae</i>	<i>Cyprininae</i>	<i>Carassius</i>	714
Grass carp	<i>Ctenopharyngodon idellus</i>	<i>Cyprinidae</i>	<i>Squaliobarbinae</i>	<i>Ctenopharyngodon</i>	720
Bream	<i>Parabramis pekinensis</i>	<i>Cyprinidae</i>	<i>Culterinae</i>	<i>Parabramis</i>	4559
Bighead carp	<i>Aristichthys nobilis</i>	<i>Cyprinidae</i>	<i>Xenocyprinae</i>	<i>Hypophthaemichthyinae</i>	1293
-	<i>Xenocypris argentea</i>	<i>Cyprinidae</i>	<i>Cyprininae</i>	-	634
-	<i>Pseudobrama simoni</i>	<i>Cyprinidae</i>	<i>Xenocyprininae</i>	<i>Pseudobrama</i>	1154

### 2.2.3 River and lake migration

At present, it is generally believed that YFP in the main stream of the Yangtze River is not different from those living in the Dongting Lake and the Poyang Lake in terms of historical geographical distribution and shape (Yu et al., 2005). In addition, There are large differences in numbers of YFP observed in different seasons in the Dongting Lake and the Poyang Lake (Yang et al., 2000; Xiao and Zhang, 2002). From 2007 to 2008, the Institute of Hydrology of the Chinese Academy of Sciences used acoustic recorders to conduct fixed-point observations of porpoise activities in the Hukou reach. The number of YFP that entered the main stream of Yangtze River was 1.3 times of the number of YFP entering Poyang Lake in the dry season, and the number of Yangtze River entering Poyang Lake is 1.4 times of the number of YFP entering the main stream of Yangtze River in the monsoon season (Dong, 2009). Zhao and Wang (2011) forecasts that 40 YFP migrates from the Balijiang reach during the flood period. Therefore, it can be preliminarily concluded that there may be migration behaviors of YFP between the main stream of the Yangtze river and the Dongting Lake as well.

## 2.2.4 Characteristics of habitat

Part of the main stream of the Yangtze River and the two lakes (Poyang and Dongting) are the habitats of Yangtze finless porpoises. Observation of the behavior of Yangtze finless porpoises in Tian-E-Zhou, Xinluo and Tongling reach of Yangtze River in Hubei Province shows that Yangtze finless porpoises have certain requirements for water depth, topography, flow velocity and water quality when choosing habitats.

In terms of topography, Yu et al. (2005) uses the selection weighted coefficient and selection weighted index to study the selection of ecological factors for YFP in Tongling Nature Reserve of Anhui Province. The study indicates that YFP has preference towards goosehead-shaped river, shoals, river bank with reeds. Wei et al. (2003) uses behavior index and habitat utilization index to evaluate the habitat selection of YFP in the Bali Jiang reach, and the study indicates that the bifurcation and confluence areas, shoals, adjacent areas of sand bars are important habitat for YFP's feeding and baby-caring. Xiong and Zhang (2011) believes that more than 90% of YFP in the Xinluo reach are distributed within 200m from the river bank. It can be seen that YFP prefer to select nearshore, shoals, shallow water with reed growth or large backwaters.

In terms of water depth, the distribution of YFP decreases with increasing water depth. Wei et al. (2003) believes that 73% of YFP are distributed in waters with water depth less than 9m. Zhao and Wang (2011) believes that porpoises will not occur in waters with water depth less than 1.5m. Dong (2009) believes that it was observed that the water depth of finless porpoises's occurrence in the estuary of Hukou ranged from 2 to 14 m. It can be generalized that the distribution depth of finless porpoises is between 2m and 14m, of which 2m to 9m is the most suitable water depth for finless porpoises.

In terms of flow velocity, Yu et al. (2005) believes that finless porpoises prefer a slow-flow area with a flow velocity of less than 0.5 m/s, and have no obvious preference for a flow velocity ranging from 0.5m/s to 1.0 m/s. Wei et al. (2003) believes that the flow velocity in the area of finless porpoise in the Bali River ranged from 0.3m/s to 1.2 m/s. It is also noticed that the flow velocity in Tian-E-Zhou reach is basically 0m/s, and finless porpoises can breed in both environments, indicating that finless porpoise activities have no obvious selectivity for flow velocity ranging from 0m/s to 1.2 m/s.

YFP is very sensitive to water quality. When living in water bodies with poor water quality, YFP are easily infected with various skin diseases, which has been proven in the practice of artificial feeding of finless porpoises (Yu et al., 2005; Chen et al., 1997). The finless porpoise avoids water bodies with poor water quality (Yang and Chen, 1996). The water quality of Tongling River in Anhui Province and Tian-E-Zhou reach are above Class II water (Dong et al., 2000; Wu et al., 2006).

In addition, finless porpoises often have a certain preference for the river's graphic shape, sub-

strate type, food resources, etc. The finless porpoise is mostly distributed in bends, bifurcations, the intersection of lakes and the Yangtze River, and nearshore areas (Zhang et al., 1993; Renjun and Kejie, 1986), with substrate being silt (Zhang et al., 1993; Wei et al., 2002).

## 2.3 Habitat suitability index model

### 2.3.1 Basic concept of model

#### Concept of riverine habitat

Riverine habitat offers physical, chemical and biological space for fish and other aquatic organisms to survive, reproduce and complete other life stages suitably (Orth, 1987; Poff and Ward, 1990). It refers to the environmental conditions of the multidimensional niche required by a certain life cycle of the organism (such as water depth, velocity, substrate and water temperature) and resources' conditions (such as food and space) (Hardy and Addley, 2001). Suitable environmental and resource conditions must be available with ensuring quality, quantity, and in time in order to maintain long-term survival and reproduction of species (Statzner et al., 1988). According to Karr and Dudley (1978) (Karr and Dudley, 1978), the productivity of river ecological habitats is mainly determined by four aspects:

Water flow (discharge, velocity and water depth)

River bed and substrate (channel form, substrate composition and sediment concentration)

Water quality (concentration of pollutants in water, water temperature)

Nutrients and organics

The above dynamic factors jointly determine the primary, intermediate productivity of the river and the survival state of fish, invertebrate animals and plants. These basic factors and intermediate productivity must meet the conditions required for long-term survival of the organism, and the number of species will be affected by any single factor or multiple factors.

#### Introduction of habitat suitability index model

An HSI, a unitless number bounded by 0 and 1, where 0 indicates unsuitable habitat and 1 indicates optimum habitat, is a numerical index that represents the capacity of a given habitat to support a selected species. HSI model results represent the interactions of the habitat characteristics and how each habitat relates to a given species. The model can be constructed in a



variety of ways, such as a word model, a mechanistic model, a multivariate statistical model, or a combination of these methods. The value is to serve as a basis for improved decision making and increased understanding of species-habitat relationships (Terrell, 1982).

With a relatively low demand for data, HSI models provide flexible cost-effective decision support tools for natural resource management and ecosystem restoration (Burgman et al., 2001; Brooks, 1997). HSI models compute an HSI for flora or fauna species from one or more relevant habitat variables (Fish et al., 1980), and mainly have been used for assessment of reserve designs and potential impacts of management decisions on habitat quality (Burgman et al., 2001). With anticipated increasing climate and land-use change, HSI models may become increasingly important to address management objectives and to utilize the large and rapidly growing body of simulated climate and hydrology datasets.

### Concept of suitability index curve

The suitability index curve (Figure 2.3.1) shows the functional relationship between one habitat variable and suitability index. The curve can be obtained via the results of ecological experiments, ecologists' discussion, and etc.

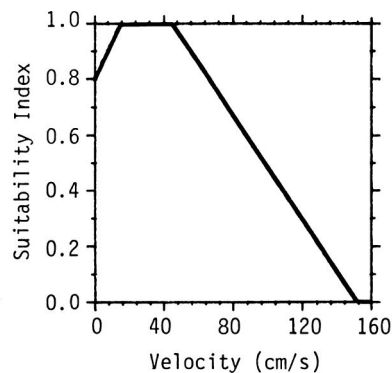


Figure 2.3.1: Example SI curve from HSI model of SHORTNOSE STURGEON (SUITABILITY, 1986)

### 2.3.2 Procedures of model set-up

Mechanistic HSI models are constructed as a hierarchical set of hypotheses about species-habitat relationships based on the documented opinion of model author(s). The hypotheses are developed in four stages during the process of model construction. First, variables are chosen that represent key habitat features known to affect the growth, survival, abundance, standing crop, distribution, or other measure of habitat quality for a species. Second, the relationship between each habitat

variable and carrying capacity (= habitat suitability) for the species is translated into a graphic hypothesis (= suitability index graph). Third, habitat variables are aggregated via mathematical equations into the model components of Food, Cover, Water Quality, and Reproduction. Last, the model components are aggregated into a species HSI equation that yields a single numerical description of habitat suitability. Because specific data on variable interactions are often lacking, model builders May have to develop assumptions on how the variables combine to determine habitat suitability. These assumptions are translated into simple mathematical language. The use of mathematical language results in a model that can produce an index with several decimal places. The number of decimal places does necessarily imply a certain level of accuracy.

Method to simplify a mechanistic HSI model is to define an evaluation species in such a manner that only the model component that appears to have the greatest influence on habitat suitability is used. The combination of life stage (e.g. fry and juvenile) or life requisite (e.g., food and water quality) components into an overall rating of habitat suitability is based primarily on the experience and intuition of the authors, not experimental data. These models are useful for exploring relationships between variables related to life stage habitat quality, but may not be useful for meeting some planning needs. Use of a single component for the total species HSI avoids the problem of making erroneous quantitative assumptions about the relationship between model components and requires only a decision about which component is most important for determining the suitability of the conditions being analyzed. The selected component may be the one that will be affected the most by the land use alternatives or the one that is assumed to have the most influence on population levels.

The figure 2.3.2 indicates the procedures for establishing HSI model and an example diagram of model structure(Figure 2.3.3) shows how model variables combine to determine an HSI.

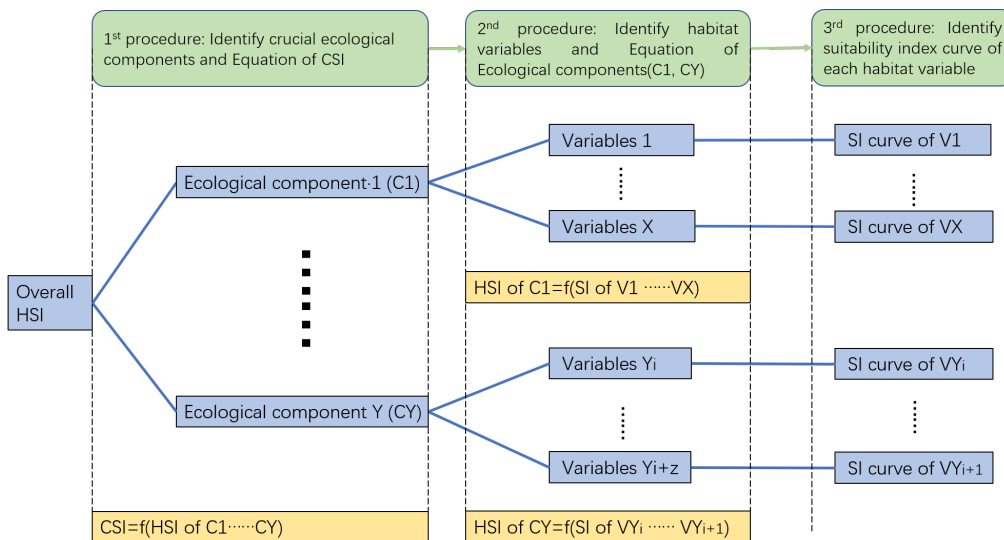


Figure 2.3.2: Flowchart of procedures for establishing HSI model

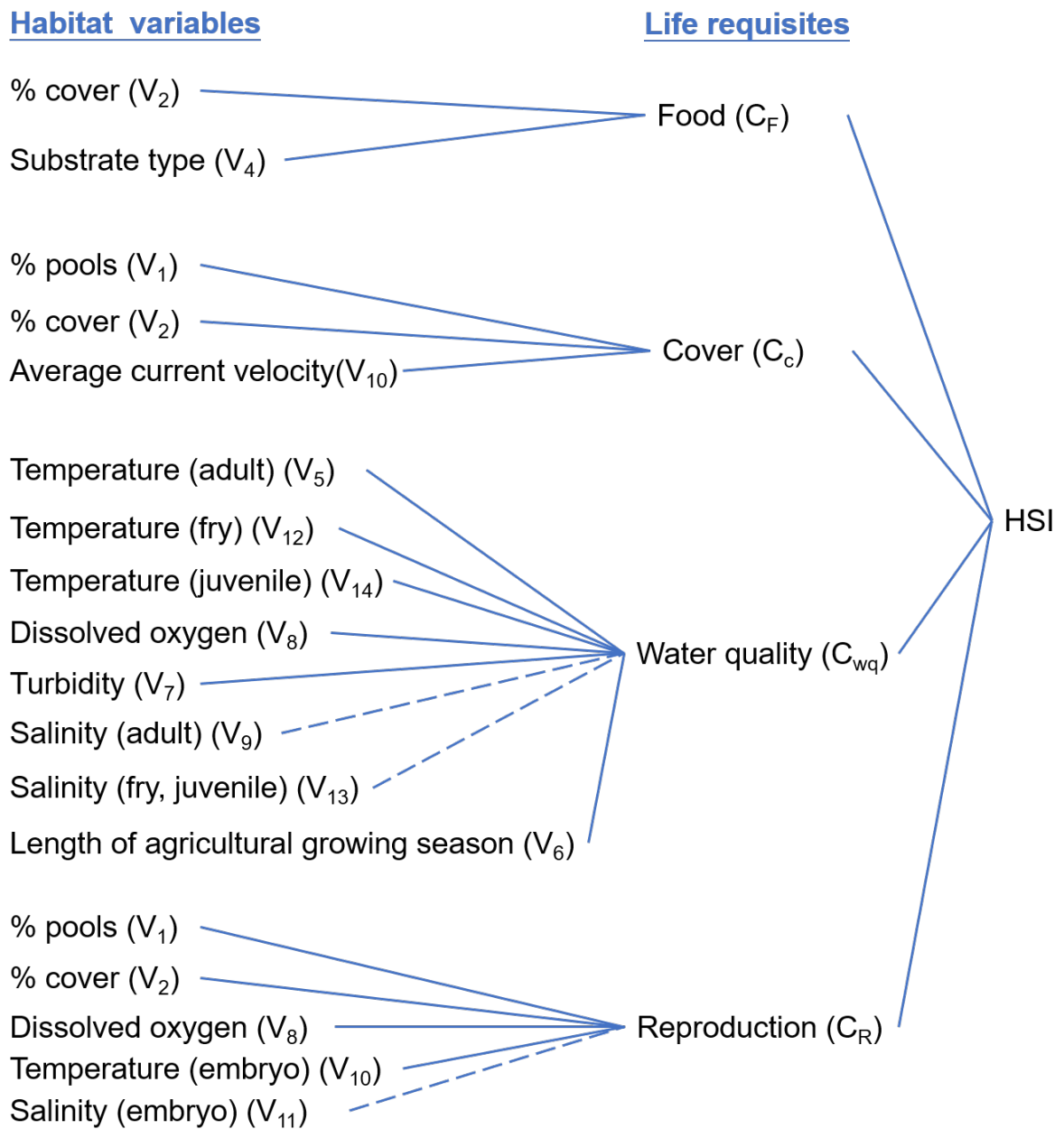


Figure 2.3.3: Example diagram of model structure showing how model variables combine to determine an HSI. Dashed lines indicate optional variables. (Terrell, 1982)

# Chapter 3 Study area

## 3.1 General

Hechangzhou reach, of which the left bank is Yangzhou City and the right bank is Zhenjiang City, is located in the lower reaches of the Yangtze River in Jiangsu Province, 250km upstream from the Yangtze river estuary(Shanghai). The study area, extending from Guazhou to Yuanji-agang, covers the whole Hechangzhou waterway and the upper part of Kouanzhi waterway(See Figure.3.1.1), with the total length about 70 km. HCZR is divided into 5 parts: Liuwei bending part, Hechangzhou branching part and Dagang bending part belong to Hechangzhou waterway scope, Luochengzhou branching part and Gaogang straight part belong to Kouanzhi waterway scope(See Figure.3.1.2). Liuwei bending part, is about 13.5km, of which the narrowest section is the start “Guazhou” of about 1480m and the end “Shatou” of about 1300m while the widest section is about 2350m in the middle near “Liuwei”. Hechangzhou branching part, divided by Hechangzhou dune into 2 branches. The north branch is 10.91km long and 1294m wide in average while the south branch is 10.2km long and 1053m wide in average. Dagang bending part, starting from Dagang and ending in Wufengshan Hill, is 8.3km long and 1500m wide in average. Luochengzhou branching part, divided by Luochengzhou dune into 2 branches, is 23km long and its widest section is about 3.5km wide(including the dune) in the middle and its narrowest section is at the start “Wufengshan Hill” about 1.1km wide. Gaogang straight part, starting from Gaogang and ending in Yuanjiagang, is about 13.5km long and 2.2km wide in average.

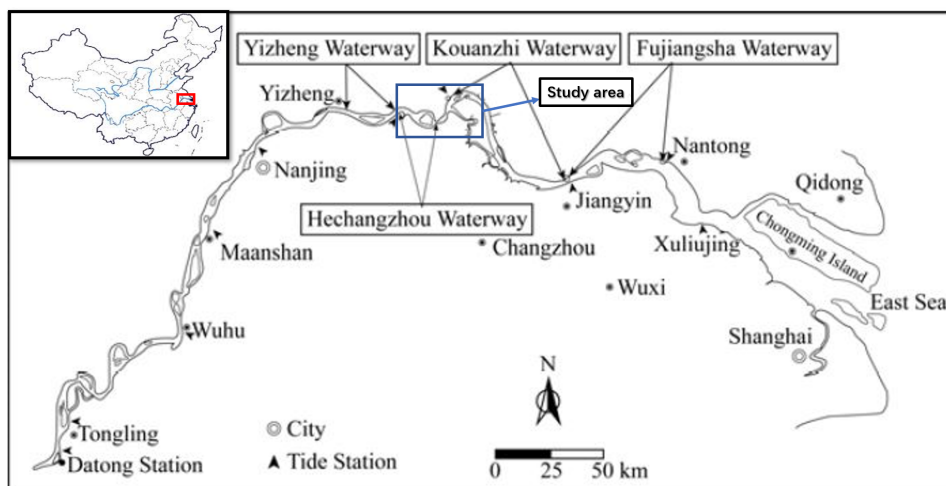


Figure 3.1.1: Schematic diagram of the Yangtze River from Datong to the estuary.

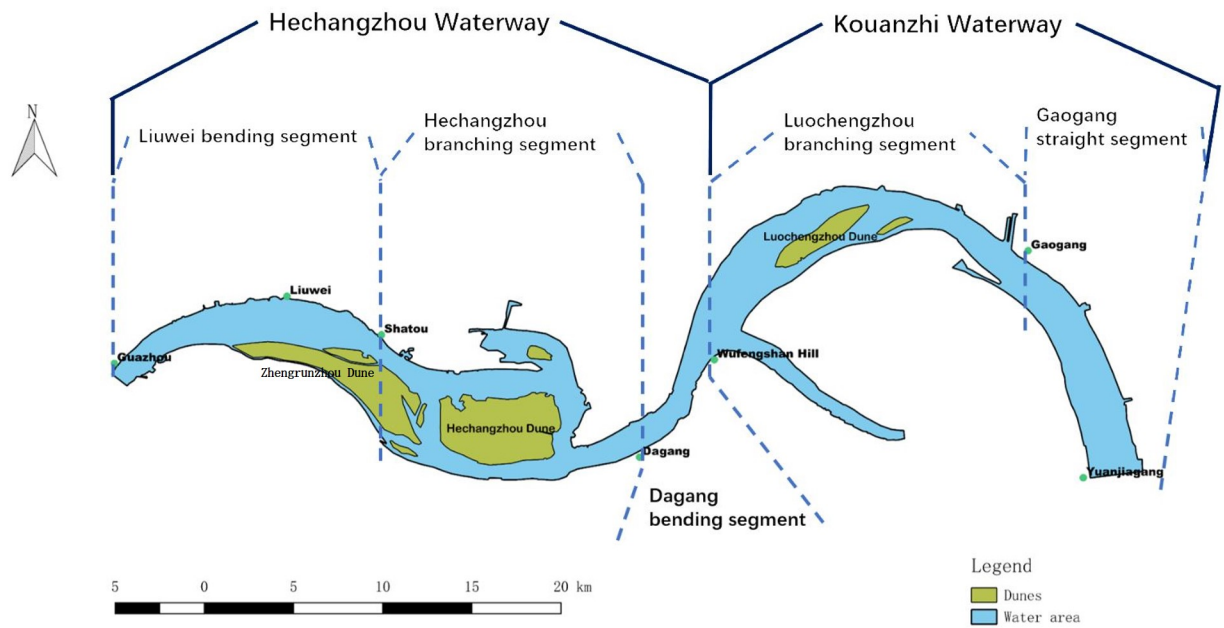


Figure 3.1.2: Schematic diagram of Hechangzhou reach.

## 3.2 Hydrodynamic characteristics

### 3.2.1 Upstream discharge

Datong gauge, 240km upstream of HCZR, controls the discharge of the lower Yangtze river. The annual discharge of tributaries is approximate 3-5% of the annual discharge of the trunk of the Yangtze river, thus the runoff input of HCZR can be referred to the data from Datong gauge station, which is the main gauge station measuring the hydrological data of the lower Yangtze river. Details are shown in Figure 3.2.1. According to statistical analysis of data of Datong gauge station from 1950 to 2007, several important indices are shown in Table 3.1.

Table 3.1: Several important hydrological indices measured measured at Datong gauge station from 1950 to 2007

Index name	Value	Time
Mean annual volume	$8973 \times 10^8 \text{m}^3$	-
Largest annual discharge	$92600 \text{m}^3/\text{s}$	1954.08.01
Smallest annual discharge	$4620 \text{m}^3/\text{s}$	1979.01.31
Mean discharge	$28400 \text{m}^3/\text{s}$	-
Mean discharge during the dry season	$16500 \text{m}^3/\text{s}$	-
Mean discharge during the monsoon season	$56800 \text{m}^3/\text{s}$	-

The monsoon season is from May to October while the dry season is from November to April in the next year. In recent years, several extreme flood occurred. The largest discharge of flood is  $75500 \text{m}^3/\text{s}$ ,  $75100 \text{m}^3/\text{s}$ ,  $82300 \text{m}^3/\text{s}$ ,  $83900 \text{m}^3/\text{s}$  in 1996, 1996, 1998 and 1999 respectively.

Due to the implement of Three gorges dam(TGD), both the water and sediment discharge were substantially changed. The average annual discharge in Datong almost remained the same. However, the largest annual discharge was declined from  $59478 \text{m}^3/\text{s}$  to  $52437 \text{m}^3/\text{s}$  while the smallest annual discharge climbed from  $8185 \text{m}^3/\text{s}$  to  $9977 \text{m}^3/\text{s}$  (See Figure 3.2.2). In addition, due to the impounding function of TGD, the monthly variation was also different from that before impounding water. The discharge in the monsoon season was declined 10.4% while it increased 29.4% in the dry season (See Figure 3.2.3).

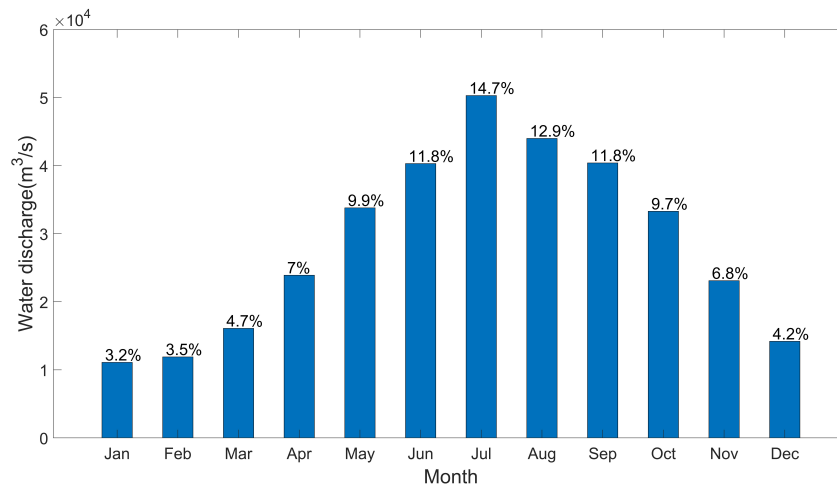


Figure 3.2.1: Monthly distribution of yearly mean discharge measured measured at Datong gauge station(percentage above column indicating monthly distribution).

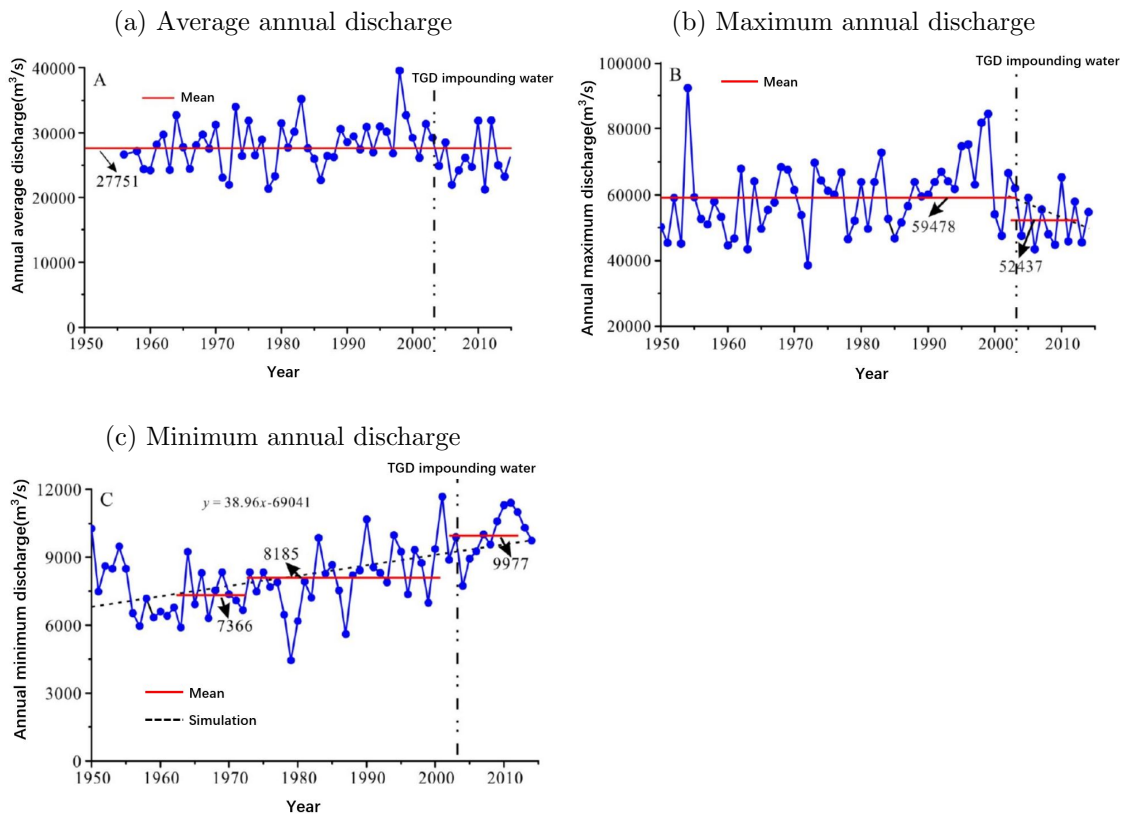


Figure 3.2.2: The annual (a) average (b) maximum and (c) minimum discharge measured at Datong gauge station (Ai, 2018)

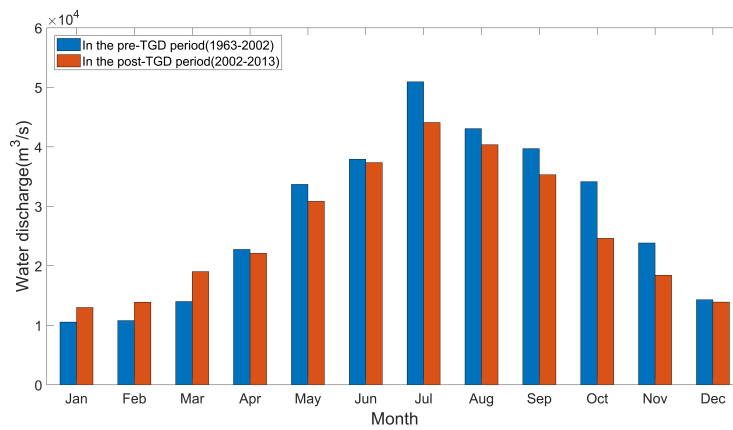


Figure 3.2.3: Variations of monthly discharge measured at Datong gauge station in the pre- and post- dam periods (Ai, 2018)

### 3.2.2 Tide and currents

The Yangtze River estuary is a medium-energy tidal estuary with tidal amplitude around 2-4m. The tide in this reach is an irregular semi-diurnal shallow tide, with two floods and two ebbs each day. The tidal limit in the lower reaches of the Yangtze River is located near Datong Station, while the tidal current limit lies near Jiangyin and its specific location varies with runoff intensity, tidal range and other factors. Under the obstruction of runoff and river bed boundary conditions, the tidal wave deforms a lot. Due to tidal asymmetry, the flood period is shorter than the ebb period. When the tidal currents come into the lower Yangtze River, the tidal range and flood duration decrease gradually along the way. Because Yizheng Reach and Hechangzhou Reach are far away from the estuary, the tidal effect is relatively weak, the average tidal range is 0.96 m for years and the tidal current is basically unidirectional. Kouanzhi Reach, under the combined impact of runoff and tide, has an average tidal range of about 1.60 m for years, and the spring tide currents in the dry season show obvious bidirectional current characteristics, but the flood current is small, around 0.2-0.5 m/s on average, and the average ebb current is 0.37-0.82 m/s. When the runoff is higher than 40000 m<sup>3</sup>/s, there is no flood current, and unidirectional flow is dominant. Some tidal characteristic values from 2 tide stations in HCZR are shown in Table 3.2.

The highest water level usually occurs when typhoon, astronomical tide, and large upstream discharge coincide at the same time or two of them coincide and typhoon plays the most important role. On August 1st in 1996, No.8 typhoon coincided with extremely large astronomical tide and extremely large flood (the discharge is 72000m<sup>3</sup>/s measured in Datong gauge), the highest water level in history occurred in Zhenjiang station and Sanjiangying station, which are located in HCZR.

Table 3.2: Tidal characteristic values from 2 tide stations in HCZR

Index	Zhenjiang Station	Sanjiangying Station
Highest water level(m)	6.70	6.14
Lowest water level(m)	-0.65	-1.10
Average flood water level(m)	3.43	-
Average ebb water level(m)	2.76	-
Average tidal range(m)	0.96	1.19
Maximum tidal range(m)	2.32	2.92
Minimum tidal range(m)	0	0



### 3.2.3 Suspended sediment and transport

According to statistics data of Datong gauge, in the pre-TGD period, the sediment input volume in the monsoon season accounts for 87.3% of the annual volume while the average sediment concentration in the monsoon season is  $0.542\text{kg}/\text{m}^3$ . Average monthly sediment transport rate as well as distribution are listed in Figure 3.2.4 and sediment characteristic values are listed in Table 3.3. After TGD was built the average monthly sediment input volume decreased(See Figure 3.2.5 and Table 3.4). Specifically, the average sediment input volume during the dry season before the dam construction was 21 million tons; after the dam construction, it reduced to 16 million tons which is 76.2% of the original one; the average sediment input volume during the monsoon season before the dam construction was 393 million tons; After the dam was built, it decreased to 109 million tons which is 27.7% of the original one(See Figure 3.2.6).

The sediment concentration was also reduced to approximately  $0.09\text{kg}/\text{m}^3$  and  $0.2\text{kg}/\text{m}^3$  in the dry season and monsoon season respectively(See Figure 3.2.7 and Table 3.4).

The median grain diameter of suspended sediment in Datong Station was 0.031 mm in 1960-1986, 0.009mm in 1987-2002 and 0.010mm in 2003-2009. The average median diameter of suspended sediment remained almost unchanged in the pre- and post-TGD period at Datong Station. In the dry season, the sediment is mainly composed of silt, which accounts for an average of 57.8-81.9% while sand and clay components are about 10 -20%. During the monsoon period, the sediment particle is relatively fine, mainly composed of clayey silt, of which silt accounts for about 60 -70%, clay accounts for about 30% and sand accounts for less than 10%.

Table 3.3: Several sediment characteristic values at Datong gauge station from 1950 to 2007

Index name	Value	Time
Maximum annual input volume	$6.78 \times 10^8 \text{t}$	1964
Minimum annual input volume	$0.848 \times 10^8 \text{t}$	2006
Average annual input volume	$4.04 \times 10^8 \text{t}$	-
Maximum concentration in history	$3.24 \text{kg}/\text{m}^3$	1959.08.06
Yearly average concentration	$0.452 \text{kg}/\text{m}^3$	-

Table 3.4: Annual sediment input volume and concentration in the post-TGD period at Datong gauge station

Index	Average before 2003	2003	2004	2005	2006	2007
Input volume( $\times 10^8 \text{t}$ )	4.33	2.06	1.47	2.16	0.85	1.38
Concentration ( $\text{kg}/\text{m}^3$ )	0.486	0.223	0.186	0.239	0.123	0.179

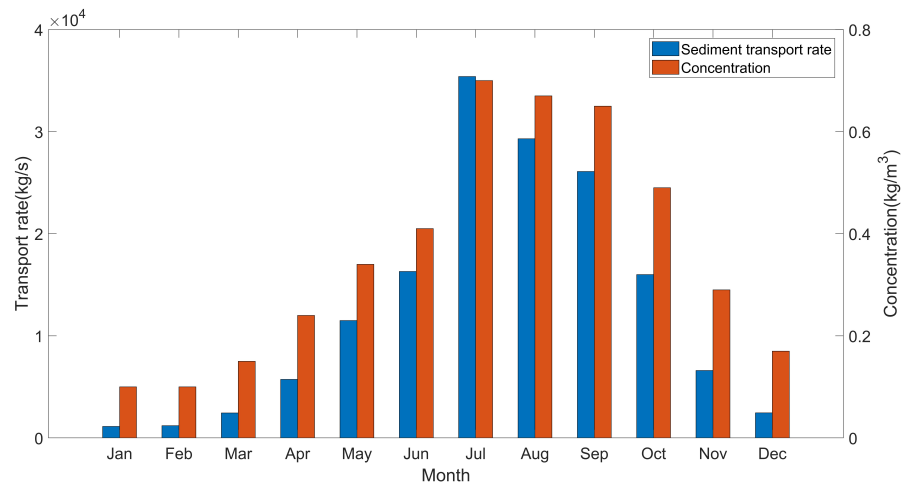


Figure 3.2.4: Average monthly sediment transport rate and concentration at Datong gauge station.

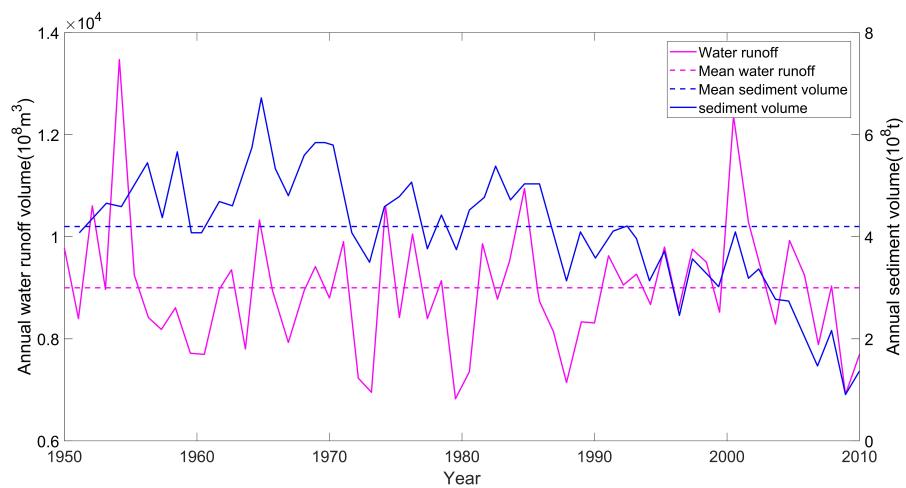


Figure 3.2.5: Annual runoff volume and sediment input volume measured at Datong gauge station in 1950-2007.

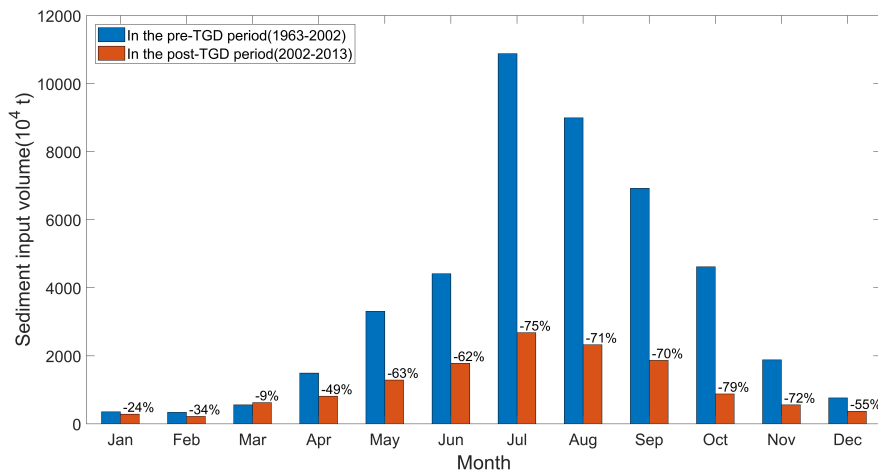


Figure 3.2.6: Variations of monthly sediment discharge of Datong station in the pre- and post-dam periods, percentage above column indicating decreasing proportion. (Ai, 2018)

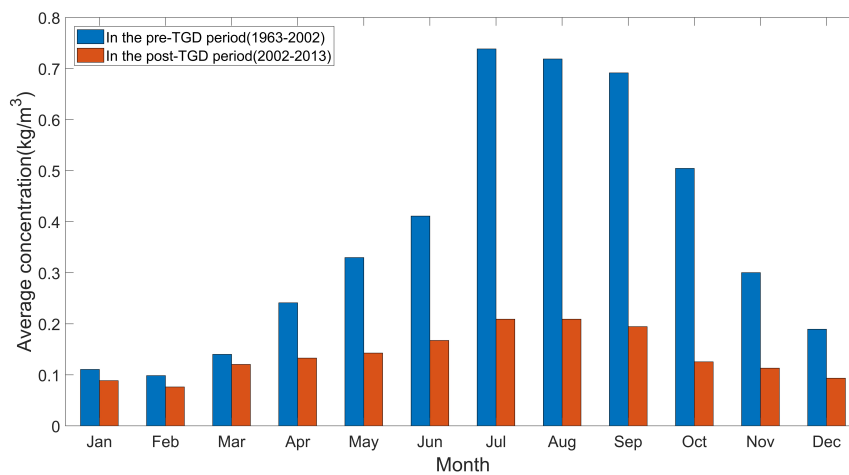


Figure 3.2.7: Variations of monthly sediment concentration of Datong station in the pre- and post-dam periods.

### 3.3 Bed material

Overall, the grain size of the riverbed surface sediments in the tidal reach of the Yangtze River becomes finer towards the section downstream of Datong. A mud layer with a thickness of 1–3 cm covers the riverbed surface sediments (Here, the sampled thick of sediment is about 5–8 cm) in the Yizheng and Kouanzhi waterway segments, with grain sizes of the mud layer of 11.2 $\mu$ m

and  $13.2 \mu\text{m}$  and grain sizes of the sediments beneath the mud layer of  $253.7 \mu\text{m}$  and  $269.9 \mu\text{m}$ , respectively (See Figure.3.3.1).

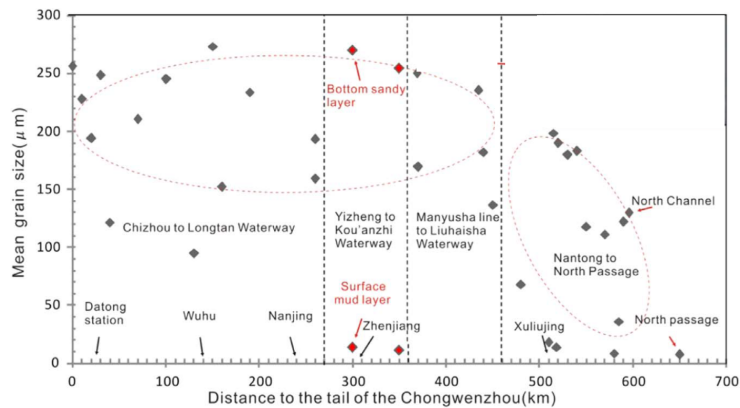


Figure 3.3.1: Riverbed surface sediment grain size for the tidal reach of the Yangtze River. (Shuwei et al., 2017)

### 3.4 Historical morphological changes

From 1954 to 1984, the concave bank was constantly eroded and retreated; Constant sedimentation took place in Zhengrunzhou dune north to the convex bank. After 1984, the concave bank was almost stable while Zhengrunzhou was slightly eroded.

From 1954 to 1984, the bifurcation area located upstream Hechangzhou dune and its north branch were dramatically eroded while the eastern part of Hechangzhou dune expanded due to sedimentation. After 1984, Zhengrunzhou dune expanded eastward, causing the entrance of the south branch of HCZ being narrowed regardless of the western part of Hechangzhou dune being eroded. The north branch was continuously being eroded about 15m in depth while Hechangzhou dune was continuously expanding eastward about 250m in width. The south bank of Hechangzhou dune expanded about 1km during this period. After the previous submerged sill was built in 2003 in the north branch entrance, the north branch was no more eroded while Zhenrunzhou dune kept extending gradually to the east and the south branch was slightly silted. According to statistics data, in the Hechangzhou branching part, the erosion area is 43% of the total while the sedimentation area is 42%. The largest erosion in depth is 50.49m while the largest sedimentation in depth is 30.81m. The average erosion depth is 1.06m.

Dagang bending part has remained almost unchanged overall till now.

Figure3.4.1 indicates the morphology changes of Hechangzhou waterway from 1954-2006.

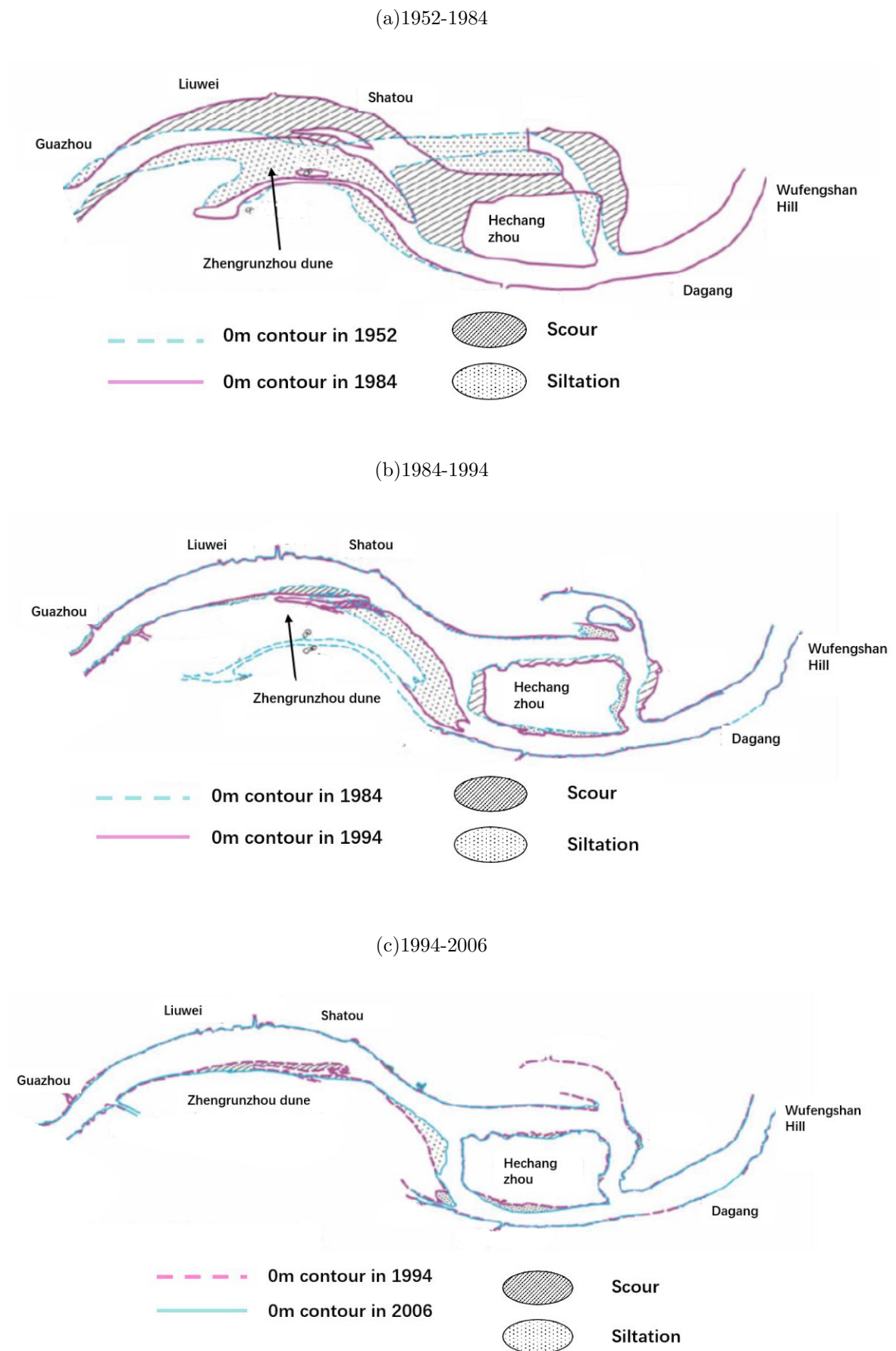


Figure 3.4.1: Changes of the river plane morphology of the reach downstream Nanjing in the last 50 years. (LIU et al., 2011)

### 3.5 Submerged sills

In order to limit the expansion of the north branch of HCZR and increase the discharge in the south branch, a previous submerged sill was built in 2003 and 2 following submerged sills were built in the end of 2017. The sketch of layout of the 3 submerged sills are shown in Figure 3.0(a) 3.0(b) while the sections of the 2 following sills are shown in Figure.3.0(c).

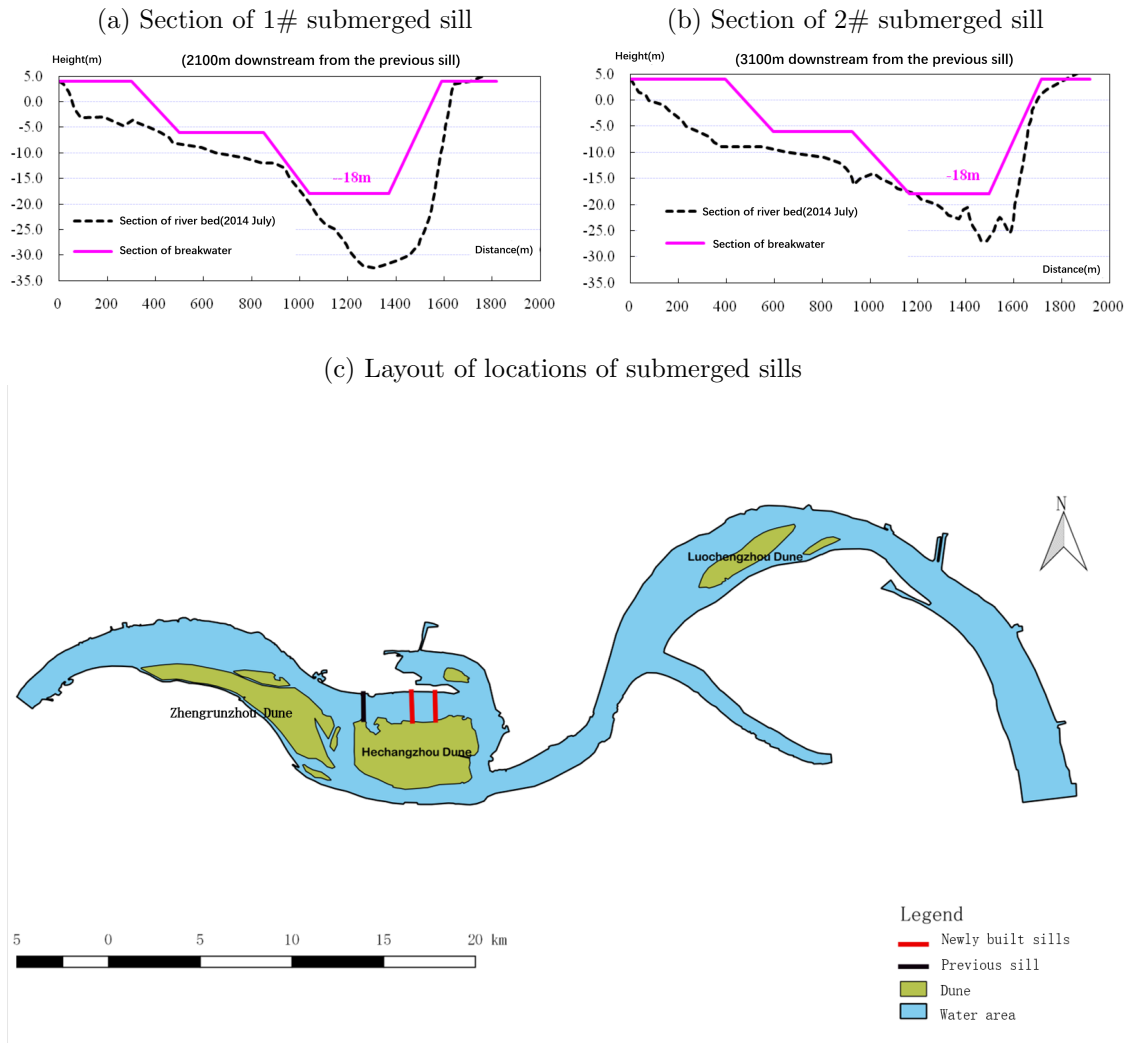


Figure 3.5.1: Section of the two newly-built submerged sills and layout of the submerged sills.

# Chapter 4 Method

In order to quantitatively investigate the preference of YFP towards its habitat and the changes of morphology and local hydrodynamics in the study area, a habitat suitability index model of YFP and a numerical model of the HCZR are established. In this chapter, the set-up method of the HSI model and its application to YFP are described as well as the set-up and validation methods of the numerical model are described.

## 4.1 Habitat suitability index model application

### 4.1.1 Ecological components

Normally, there are two main methods to determine aquatics' ecological components for HSI model. One determines the ecological components by taking the life stage of specie into consideration. For example, in the HSI model of brown trout, USFWS selected Adult, Embryo, Fry, Juvenile as the model's ecological components (Figure.4.1.1)(Raleigh et al., 1984). The other method identifies the ecological components from the view of the specie's life requisites. For example, food, water quality and reproduction are selected as model components in the HSI model of common carps (Figure.4.1.2)(Edwards and Twomey, 1982).

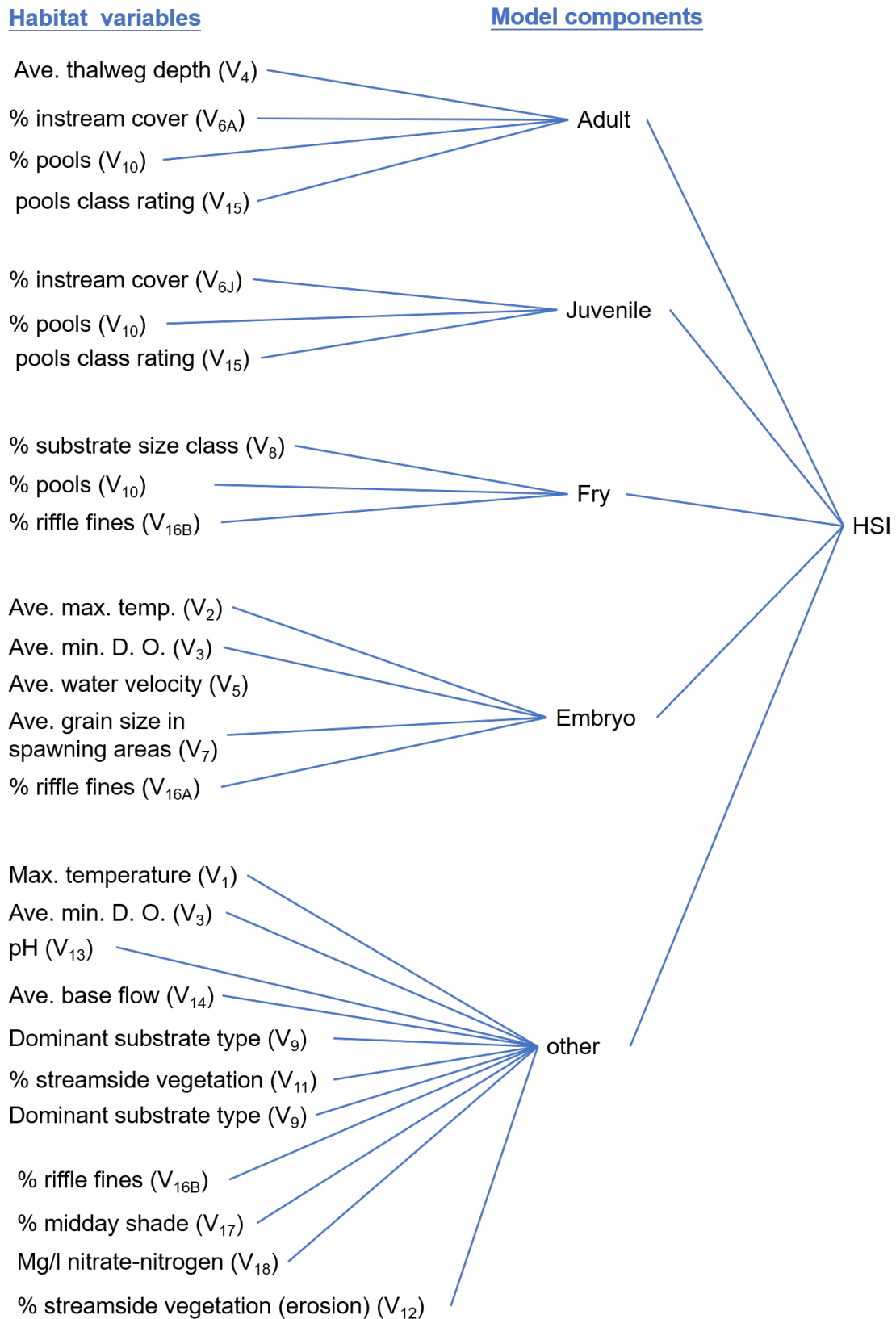


Figure 4.1.1: Diagram illustrating the relationship among model variables, components, and HSI in the model for the brown trout.(Raleigh et al., 1984)



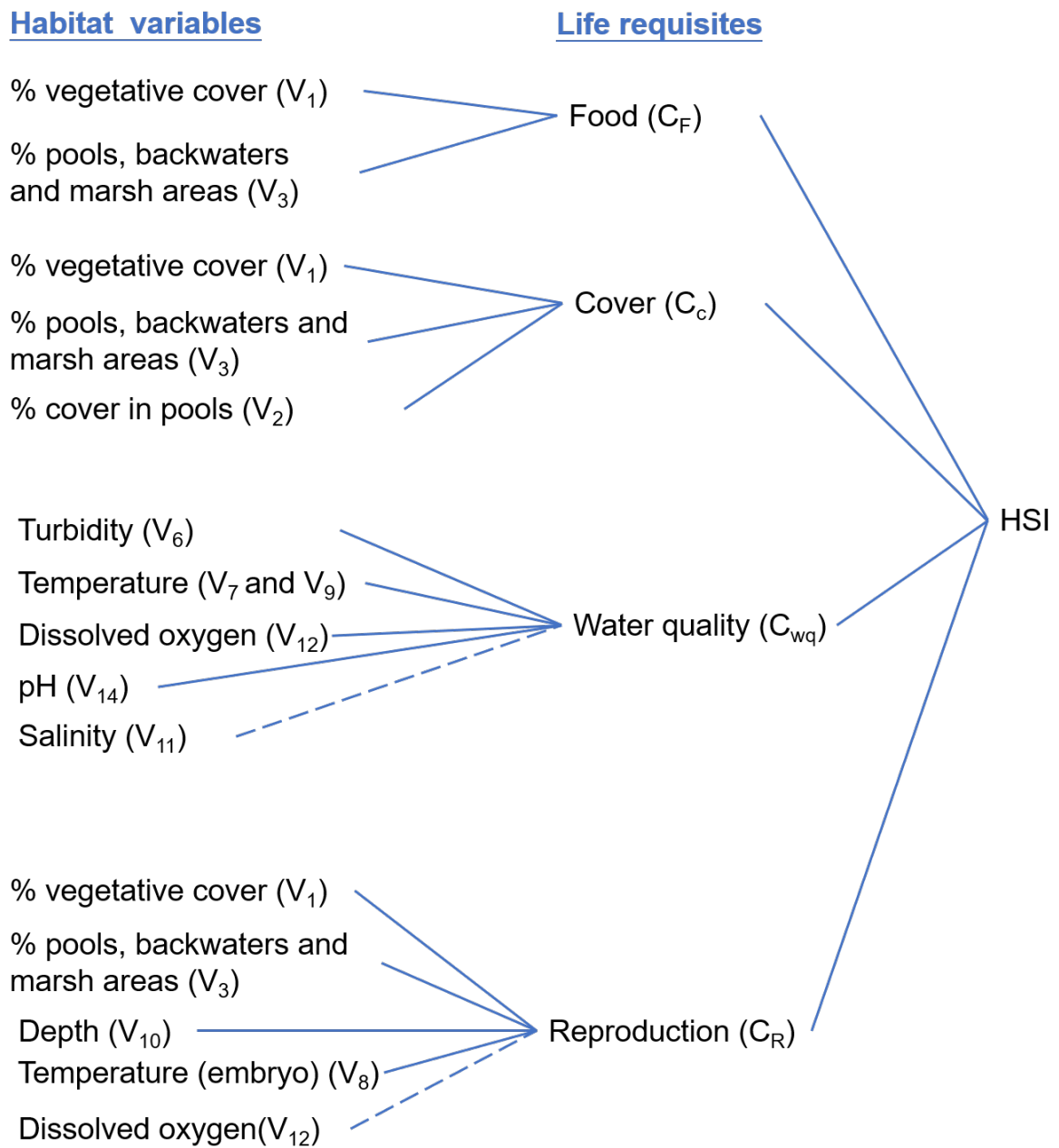


Figure 4.1.2: Tree diagram illustrating relationships of habitat variables and life requisites in the riverine model for the carp. Dashed line indicates optional variable in the model. (Edwards and Twomey, 1982)

Results from literature reviewing indicate that there is nearly none study on the differences of the preference of YFP towards habitat characteristics in its different life stages. Therefore, the

method depending on specie's life requisites is taken in YFP's HSI model. In Chapter 2.1.3, the hazard factors of YFP and the main ecological behavior of YFP are introduced and generalized in detail. In general, movement, food, water quality and reproduction are the main ecological components when establishing YFP's HSI model. Reproduction and water quality are not taken into account in the HSI model of YFP due to the reasons below:

#### Reproduction

The studies on YFP's reproduction habit are all qualitative rather than quantitative—YFP tend to choose quiet, low-velocity shallow water areas to mate and give birth (Wei et al., 2002). In addition, as YFP is the only freshwater subspecies of the narrow-ridged finless porpoise, it is not reasonable to refer to other narrow-ridged finless porpoise's reproduction HSI. In conclusion, there is very little reliable data to investigate HSI of YFP's reproduction quantitatively, the HSI of YFP's reproduction will not be taken into consideration in its HSI model in this thesis.

#### Water quality

According to water quality report of HCZR, the water quality is regarded to ensure YFP's healthy living. Although Water quality which consists of temperature, dissolved oxygen, pH value and etc. attaches great importance to aquatics' habitat, this thesis focuses on YFP's physical habitat and water quality will not be added in the HSI model.

In summary, YFP's HSI model consists of two components: food or feeding habitat (CF), and movement habitat (CM). Tree diagram (Figure 4.1.3) illustrates relationships of habitat variables and life requisites in the riverine model for Yangtze finless porpoise.

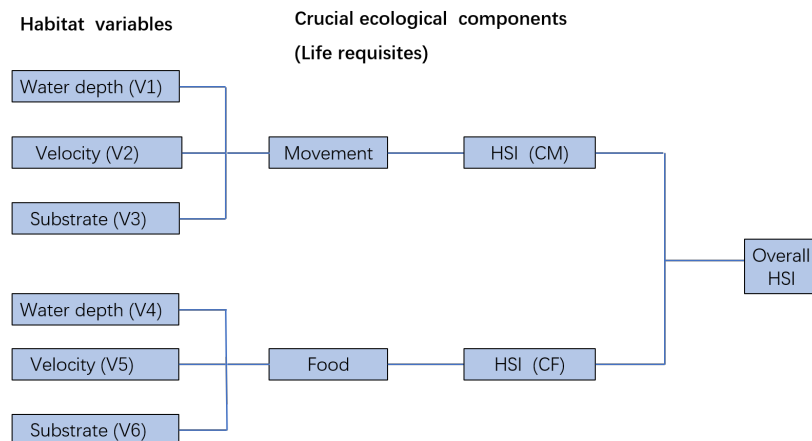


Figure 4.1.3: Tree diagram illustrating relationships of habitat variables and life requisites in the riverine model for Yangtze finless porpoise.

### 4.1.2 Habitat variables of each ecological components

Each component contains habitat variables specifically related to that component. Each habitat variable is considered to be capable of being measured in the field, but significant effort may be required to measure some variables. The assumed relationship of the habitat variable included in the HSI model to life requisites of the species in riverine habitat is illustrated in Figure 1. Some habitat-related variables that can potentially affect YFP populations (e.g. toxic wastes, competitors) are not included in the model because of insufficient information on the relationship of the variables to habitat suitability or the difficulty in measuring the variables in the field.

#### **Movement component**

water depth (V1) and flow velocity (V2) are normally regarded as the main variables which limits aquatics movement. Dominate substrate type(V3) is also selected because it is reported that large size of soil such as cobble or boulder may increase the risk for YFP being bruised (Yu et al., 2002). It is worth mentioning that since YFP's positioning capability is based on its sonar system, the influence of turbidity on YFP's movement is much less than that on other aquatics which target objects by sight, thus turbidity is not selected as a variable for its "Movement" component (Wei et al., 2003).

#### **Food component**

USFWS tended to select the areas of different covers such as vegetation or marsh as habitat variables for the "Food" components in the HSI model of herbivorous aquatics such as common carps. Since YFP is a carnivorous specie which is regarded as "opportunistic" feeder in biology, its feeding pattern is different from that of herbivorous aquatics, thus selecting the areas of different cover as its model's habitat variable is neither suitable nor reasonable for YFP's "Food" component.

Since there is no specialized study indicating which habitat variables are crucial for YFP's "Food" component, it is normally suggested that for selecting the variables scientifically, studies on YFP's main food source—bait fish's habitat variables are regarded as good reference. Many experts studied YFP's feeding habit and draw the same conclusion that YFP's "restaurant"—their feeding habitat, is very similar to its bait fish's habitat. According to studies on YFP's food choice from Literature review, it can be generalized that fish of Cyprinidae family can be set as the referring bait when selecting habitat variables of YFP's feeding habitat.

In summary, the habitat variables of YFP's "Food" component are directly replaced by the variables of Cyprinidae's HSI model: Water depth (V4), velocity (V5), and predominate substrate type (V6).

### 4.1.3 Suitability index curve of each habitat variable

In this part, after combining and generalizing different literature, SI curves of each habitat variable and the data sources are shown(Figure 4.1.4). The description of different data source can be seen in Table 4.1. The general method to derive the SI curve in this thesis is based on the number of pieces of literature. If more literature confirms that in a certain range of velocity of water depth is suitable, the index will be higher.

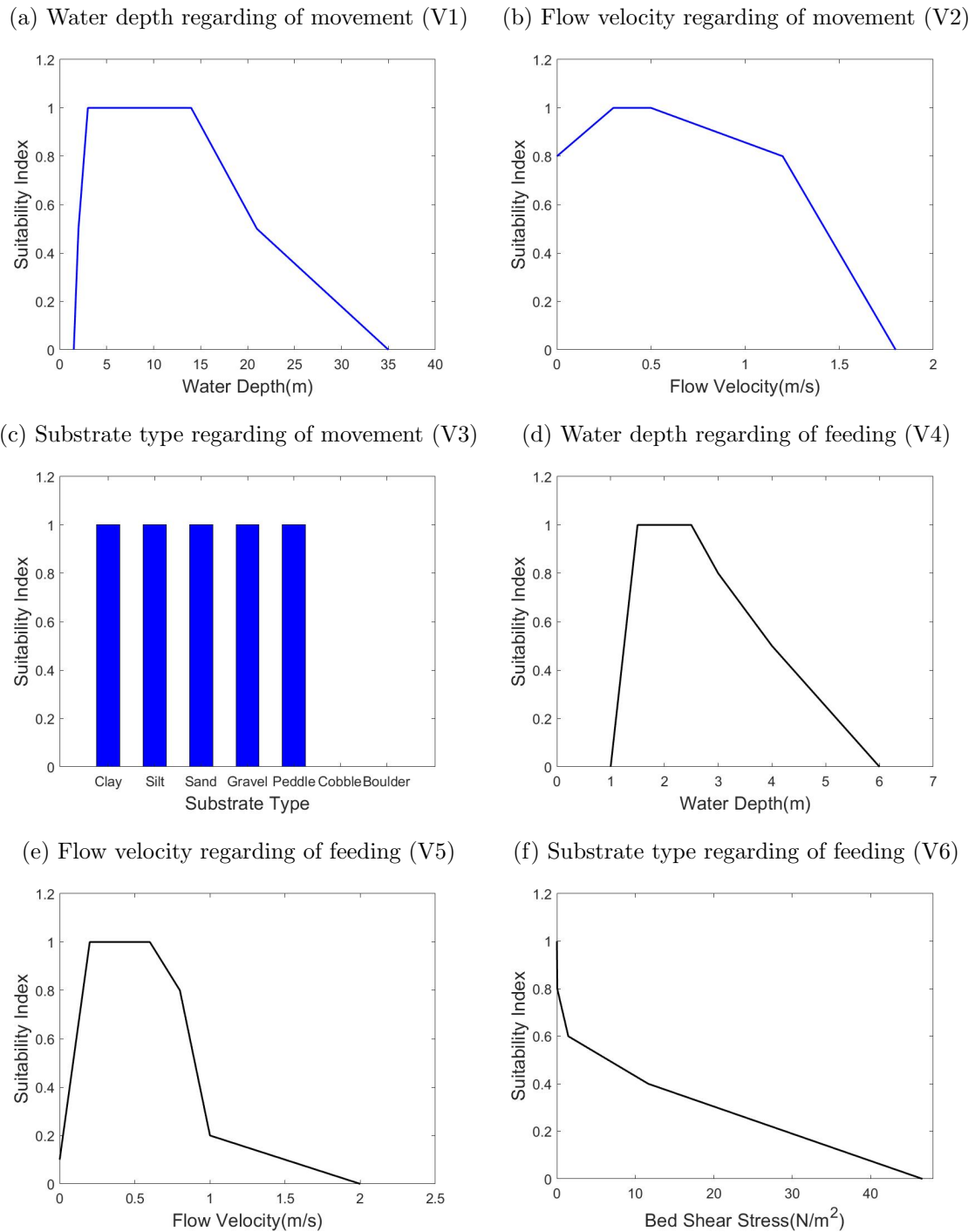


Figure 4.1.4: Illustration of the derived SI curves for (a) Water depth regarding of movement (V1); (b) Flow velocity regarding of movement (V2); (c) Substrate type regarding of movement (V3); (d) Water depth regarding of feeding (V4); (e) Flow velocity regarding of feeding (V5); (f) Substrate type regarding of feeding (V6)

Table 4.1: Data sources for Yangtze finless porpoise suitability indices

Variable	Source and Description
V1	<p>Wei et al. (2003): None of YFP was found in the water depth more than 21m or less than 3m.</p> <p>Zhao and Wang (2011): YFP are not found in the area with water depth less than 1.5m.</p> <p>Dong (2009): In Hukou, water depth of the area where YFP were found is between 2m 14m.</p> <p>Summary: It can be generalized that when the water depth is less than 1.5m, the risk for YFP being stranded is extremely high, and YFP can be regarded to move safely with the water depth more than 3m and less than 14m. Since there is no YFP found in the water with depth more than 21m in Balijiang reach, it can be presumed that the water depth more than 21m is much less suitable for YFP's movement.</p>
V2	<p>Wei et al. (2003):In Bailijiang reach, YFP moves in the area with flow velocity between 0.3-1.2m/s.</p> <p>Yu et al. (2005): YFP prefers the low-velocity area with flow velocity less than 0.5m/s, and has no obvious preference on the velocity between 0.5m/s 1m/s.</p> <p>Zhao and Wang (2011): In Tian'ezhou old waterway, which is a semi-nature reserve for YFP, the velocity there is nearly 0 m/s, and YFP can healthily live, which indicates that the minimum velocity for YFP's movement can be around 0 m/s.</p> <p>Summary: Since the reserves of YFP are in middle and lower Yangtze river, the velocity range in middle and lower Yangtze river is 0.1-1.8 m/s, it can be generalized that the velocity does not affect YFP's movement between 0-1.2m/s, and gradually plays a role between 1.2-1.8m/s, when velocity is more than 1.8m/s, it can be presumed that YFP's movement is almost limited.</p>
V3	<p>Yu et al. (2002): The soil with large size and sharp shape such as cobble or boulder increases the risk for YFP being bruised.</p>
V4	<p>Summary of the work of Chou and Chuang (2011); Yang et al. (2010); WANG and YAN (2008); WANG et al. (2009) is shown in Figure.4.1.5.</p> <p>Tan et al. (2011): Schizothoracinae 0.5-4.5m.</p> <p>Im et al. (2011): Zacco platypus 0.2-0.6m/s.</p>
V5	<p>Summary of the work from Chou and Chuang (2011); Yang et al. (2010); WANG and YAN (2008); WANG et al. (2009) is shown in Figure.4.1.5.</p> <p>Tan et al. (2011): Schizothoracinae 0.3-3m/s.</p> <p>Im et al. (2011): Zacco platypus 0.2-0.6m/s.</p>
V6	<p>Edwards and Twomey (1982): In both riverine and lacustrine habitats, carps prefer enriched, relatively shallow, warm, sluggish, and well-vegetated waters with a mud or silt substrate. The suitability index for clay, silt, sand, gravel and pebble are 1.0, 0.8, 0.6, 0.4 and 0 respectively. The detailed description of the approach to derive the SI curve of V6 can be read in Chapter.4.1.4.</p>

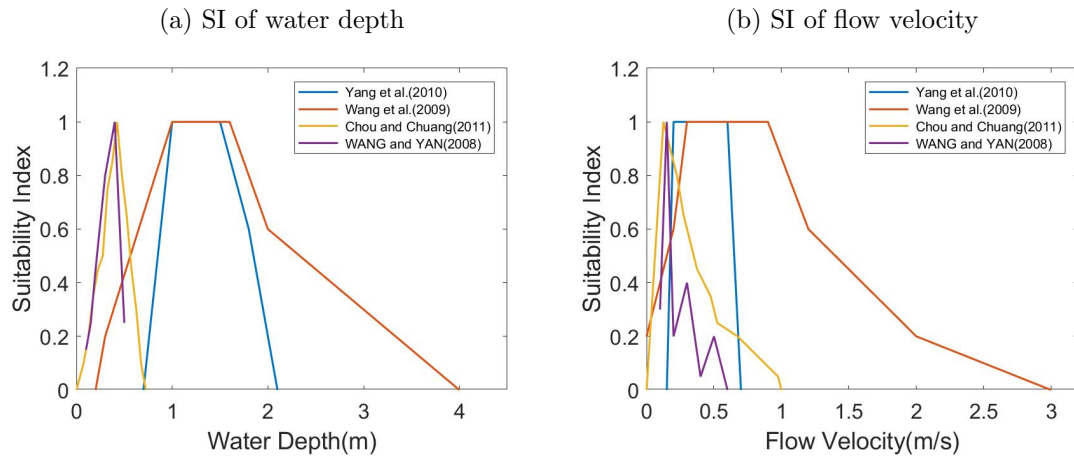


Figure 4.1.5: Suitability index graphs for (a) water depth and (b) flow velocity of Cyprinidae's HSI model from literature (Chou and Chuang, 2011; WANG and YAN, 2008; WANG et al., 2009; Tan et al., 2011; Yang et al., 2010; Im et al., 2011)

#### 4.1.4 Approach to derive the SI curve of V6

Shields parameter is such common and effective parameter used to adjust sediment movement in ecological hydrology which can be obtained by calculating from the shear stress of the river bed:

$$\psi_c = \frac{\tau_b}{(\rho_s - \rho_w)gd_{50}} \quad (4.1)$$

Where,  $\psi_c$  is Shields parameter,  $\tau_b$  is the shear stress of the river bed,  $\rho_s$  and  $\rho_w$  are the density of sediment and water,  $g$  is the gravity constant and  $d_{50}$  is median diameter of the sediment.

If Shields parameter—a value for the critical movement of sediment, is identified, the critical shear stress for erosion of different sediment with different grain sizes can be calculated. By comparing with the local bed shear stress, the area of different fractions of sediment which is able to be retained can be identified.

$$\tau_c = \psi_c(\rho_s - \rho_w)gd_c \quad (4.2)$$

Where,  $\psi_c$  normally ranges between 0.03-0.045. Sawyer et al. (2010) have conducted a lot of comparative studies on the two-dimensional numerical model of gravel-bed or sandy-bed rivers with measured motions, and believe that 0.045 is more appropriate. By using Equation.4.1.4,

the critical shear stress for different fractions of sediment can be calculated. Combined with the suitability index from Table.4.1 "V6" column, the results are summarized and shown in Table.4.2 and the SI curve of V6 can be identified and shown in Figure.4.1.4.

Table 4.2: Critical shear stress and suitability index of different fractions of sediment

Index name	Clay	Silt	Sand	Gravel	Pebble
Median grain size(mm)	<0.004	0.004-0.062	0.062-2	2-16	16-64
Critical shear stress(N/m <sup>2</sup> )	<0.0029	0.0029-0.0452	0.0452-1.46	1.46-11.65	11.65-46.62
Suitability index	1	1-0.8	0.8-0.6	0.6-0.4	0.4-0

#### 4.1.5 Equations in the HSI model

The composite suitability index(CSI) is the overall suitability index, which is obtained by mathematically calculating the individual suitability indices of the selected habitat components to give an overall HSI value (also from 0 to 1). Ahmadi-Nedushan et al. (2006) suggested that some methods may be used for aggregating with habitat components into a CSI, such as limiting factor, cumulative, arithmetic mean value, geometric mean value, and weighted mean value methods.

For deriving the SI of YFP's movement, limiting factor method is taken due to the "bucket effect". It is well-known and acknowledged that YPF's movement is limited by the worst habitat variable.

For deriving the SI of YFP's feeding, weighted mean value method, which is common in the habitat study of Cyprinidae family fish, is taken here because different habitat variables have different degrees of effect on Cyprinidae family fish's habitat. The weights of each habitat variable are referred to the HSI model of common carps in US and many pieces of Chinese literature (Edwards and Twomey, 1982; Chou and Chuang, 2011; WANG and YAN, 2008; WANG et al., 2009; Tan et al., 2011; Yang et al., 2010; Im et al., 2011).

For deriving CSI, geometric mean value method and imiting factor method are combined. Since the movement component is prior to feeding component , when  $HSI_{CM}$  is less than  $HSI_{CF}$ , CSI equals to  $HSI_{CM}$ ; when  $HSI_{CM}$  is larger than  $HSI_{CF}$ , CSI equals to the geometric mean value of



$HSI_{CM}$  and  $HSI_{CF}$  considering the availability of food source and the suitability of movement.

$$HSI_{CM} = \min(SI_{V1}; SI_{V2}; SI_{V3}) \quad (4.3)$$

$$HSI_{CF} = 0.2 \times SI_{V4} + 0.45 \times SI_{V5} + 0.35 \times SI_{V6} \quad (4.4)$$

$$CSI = \begin{cases} HSI_{CM} & HSI_{CM} \leq HSI_{CF} \\ \sqrt{HSI_{CM} \times HSI_{CF}} & HSI_{CM} > HSI_{CF} \end{cases} \quad (4.5)$$

where  $HSI_{CM}$  and  $HSI_{CF}$  are the habitat suitability index of YFP's movement and feeding;  $SI_{V1}$ - $SI_{V6}$  are the suitability index corresponding with the six habitat variables;  $CSI$  is the composite suitability index.

## 4.2 Numerical model configuration

In order to test several hydro,- and morphodynamic processes in HCZR and simulate the effect of the submerged sills in different scenarios, use will be made of the open-source numerical model Delft3D, developed by Deltares (Deltares, 2018). In order to simulate the flow and transport with a higher resolution in HCZR, a smaller finer domain was outline-nested within Dr.Qinghua and Dr.Sien Liu's model with use of the Domain Decomposition (DD) approach (Deltares, 2018). which covers the lower section of Yangtze river.

### 4.2.1 Basic Lower Yangtze River model

Lower Yangtze River model(LYRM) is developed by Dr.Qinghua Ye from Deltares and Dr.Sien Liu from TU Delft, which extends upstream from Xinchengwei Reach in Nanjing and downstream to Tiansheng port in Nantong, using a computational grid of 14445 grid cells with a resolution varying from 500m to 1km in flow direction and 50m to 100m perpendicular to flow direction. The length of the model domain is 200km.

The upstream boundary condition of LYRM is discharges-time series derived from Datong hydrological station while downstream boundary condition is waterlevel-time series measured in Tiansheng port, Nantong city.



Figure 4.2.1: Domain map of Lower Yangtze River Model

### 4.2.2 Domain and computational grids

Hechangzhou reach model(HCZRM) is extracted from Lower Yangtze river model, using a computational grid of 62 by 283 grid cells with a higher resolution varying from 50m to 200m in flow direction and 20m to 50m perpendicular to flow direction. The length of the model domain is 50km.

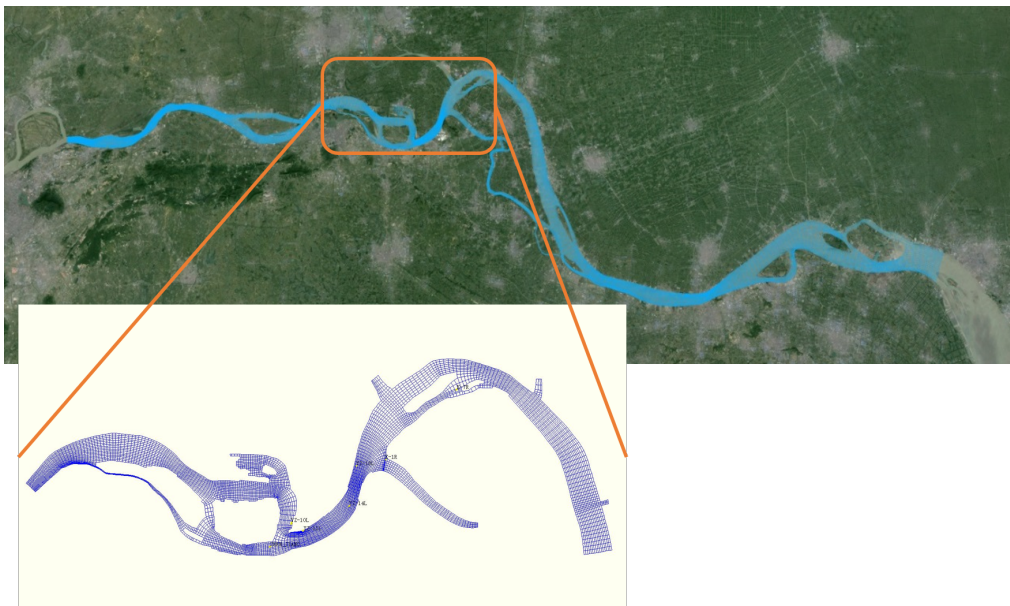


Figure 4.2.2: Domain map of Hechangzhou Reach Model

### 4.2.3 Boundary conditions

The upstream boundary condition and downstream boundary condition of HCZRM are all waterlevel-time series derived from the nested results of Lower Yangtze river model.

### 4.2.4 Bathymetry

Bathymetry data is based on that from the lower Yangtze river model(measurements conducted around 2013). During the calibration phase, due to higher resolution, the bathymetry was updated mainly via interpolation calculation and was modified in some areas without samplings, by slightly deepening the channels and correcting the data of shoals around the sand bars.

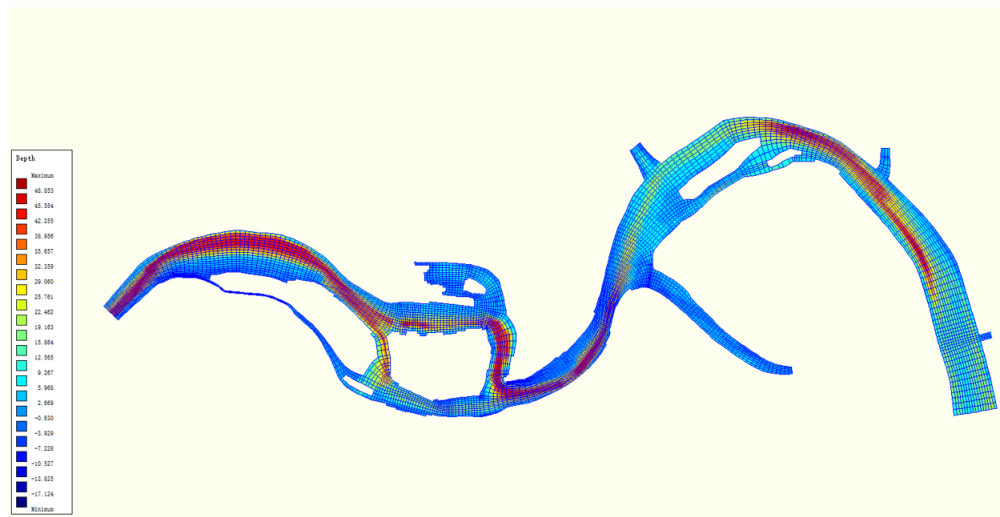


Figure 4.2.3: Bathymetry map of Hechangzhou Reach Model

### 4.2.5 Scenario description

Since the upstream discharge or flow is substantial to morphology of lower Yangtze river, hereby three scenarios are set-up with different upstream discharges. The 3 scenarios are called the dry season, normal-water season and monsoon season.

For obtaining the boundary conditions in 3 scenarios, the approach is the same as that in Chapter.4.2.3. The boundary condition of Hechangzhou reach model are derived from the nested lower Yangtze river model. Via setting  $10000m^3/s$ ,  $25000m^3/s$  and  $40000m^3/s$  as constant discharge input at Datong station(upstream border of lower Yangtze river model) corresponding with the 3 scenarios respectively, water level-time series at the upstream and downstream boundary can

be obtained and were set as the upstream and downstream boundary condition of Hechangzhou reach model.

#### 4.2.6 Simulation time and morphological scale factor

The morphological change at each time step was multiplied by a morphological acceleration factor (Roelvink, 2006), to increase the morphology changes and thereby efficiently model long-term morphology. It is known that the 3 water seasons in lower Yangtze river normally last 4-5 months and 12 is taken as the morphological scale factor in order to simulate extremely critical scenarios. The hydrodynamic simulation time is one month. With morphological factor equal to 12, the morphodynamic simulation time is one year.

#### 4.2.7 Physical factor and median sediment diameter

Referring to literature and other previous numerical model in Hechangzhou reach (Wang et al., 2014), the roughness coefficient is taken as Manning parameter 0.023, the viscosity is taken as  $1 \text{ m}^2/\text{s}$  and the median sediment diameter is taken as 200 microns. The time-step in this numerical model is 0.5s.

#### 4.2.8 Calibration method

The performance of the model is calibrated through qualitative and quantitative assessments between the calculated and measured values at several monitoring locations at Hechangzhou Reach.

The quantitative assessment compares the calculated and measured values through statistical quantities. For the case of coupled hydrodynamic-ecosystem models, Allen et al. (2007) suggest the use of the Nash-Sutcliffe Model Efficiency coefficient, ME (Nash and Sutcliffe, 1970) and the bias expressed in percentages, PB. The model efficiency coefficient is the ratio of the variance in the calculated values and the measured ones. It quantifies if the modeled values vary more or less with the measured values and is a measure how accurate the model predictions are relative to the mean of the observed data. Including the effect of a possible error in the measurements, the definition is as follows:

$$ME = 1 - \frac{\sum (|m - p| - \Delta m)^2}{\sum (m - \bar{m})^2} \quad (4.6)$$

where  $m$  is the measured value;  $p$  is the predicted or calculated value by the model;  $\bar{m}$  is the mean measured value;  $\delta m$  is the error in the measurements. The absolute value between the

measured and calculated value minus the error in the measured value, cannot be negative. In that case, the whole term becomes zero. The value of ME are classified based on the performance the model represent. This classes ranges from: excellent ( $ME > 0.65$ ), very good ( $0.5 > ME > 0.65$ ), good ( $0.2 > ME > 0.5$ ) and poor ( $ME < 0.2$ ). The bias of the model is an overall error relative to the expected values and is expressed in percentages. Including the error margin, the definition is as follows:

$$PB = \frac{\sum [(m - p) \pm \Delta m]}{\sum m} \times 100 \quad (4.7)$$

The absolute value of the percentage bias are also classified in four classes: excellent ( $|PB| < 10\%$ ), very good ( $10\% < |PB| < 20\%$ ), good ( $20\% < |PB| < 40\%$ ) and poor ( $|PB| > 40\%$ ).

# Chapter 5 Results

## 5.1 Numerical model performance

In order to obtain confidence in the ability of the model to represent the flow and transport characteristics in Hechangzhou Reach, the model results are visually and statistically calibrated. Locations of the 7 waterlevel measuring stations are shown in Figure 5.1.1.

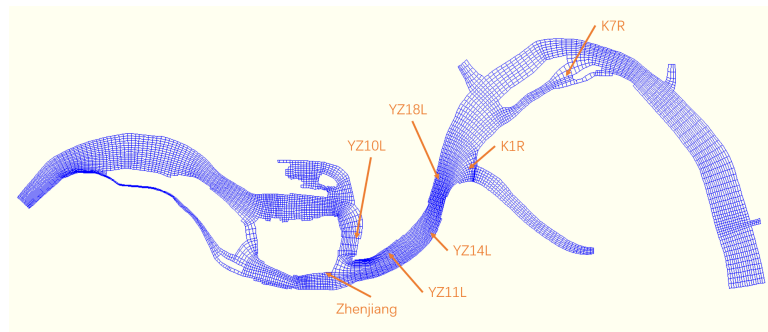


Figure 5.1.1: Sketch of locations of 7 waterlevel measuring stations

### 5.1.1 Visual calibration

Figure 5.1.2 shows the predicted and measured water levels at seven waterlevel gauges, namely Zhenjiang, YZ10L, YZ11L, YZ14L, YZ18L, K1R and K7R. The water levels were measured from June 17th/2014 to July 17th/2014 every hour at Zhenjiang station. At YZ10L, YZ11L, YZ14L, YZ18L station, the water level measuring started from June 20th/2014 to June 26th/2014 every hour. At K1R and K7R station, the water level measuring started from June 27th/2014 to July 13th/2014 every hour. Predicted water levels show a good agreement with measured values, with a slight under prediction at YZ10L, YZ11L, YZ14L and YZ18L gauges. This disagreement could be caused by inaccuracy in the bathymetry. Also grid resolution could play a role.

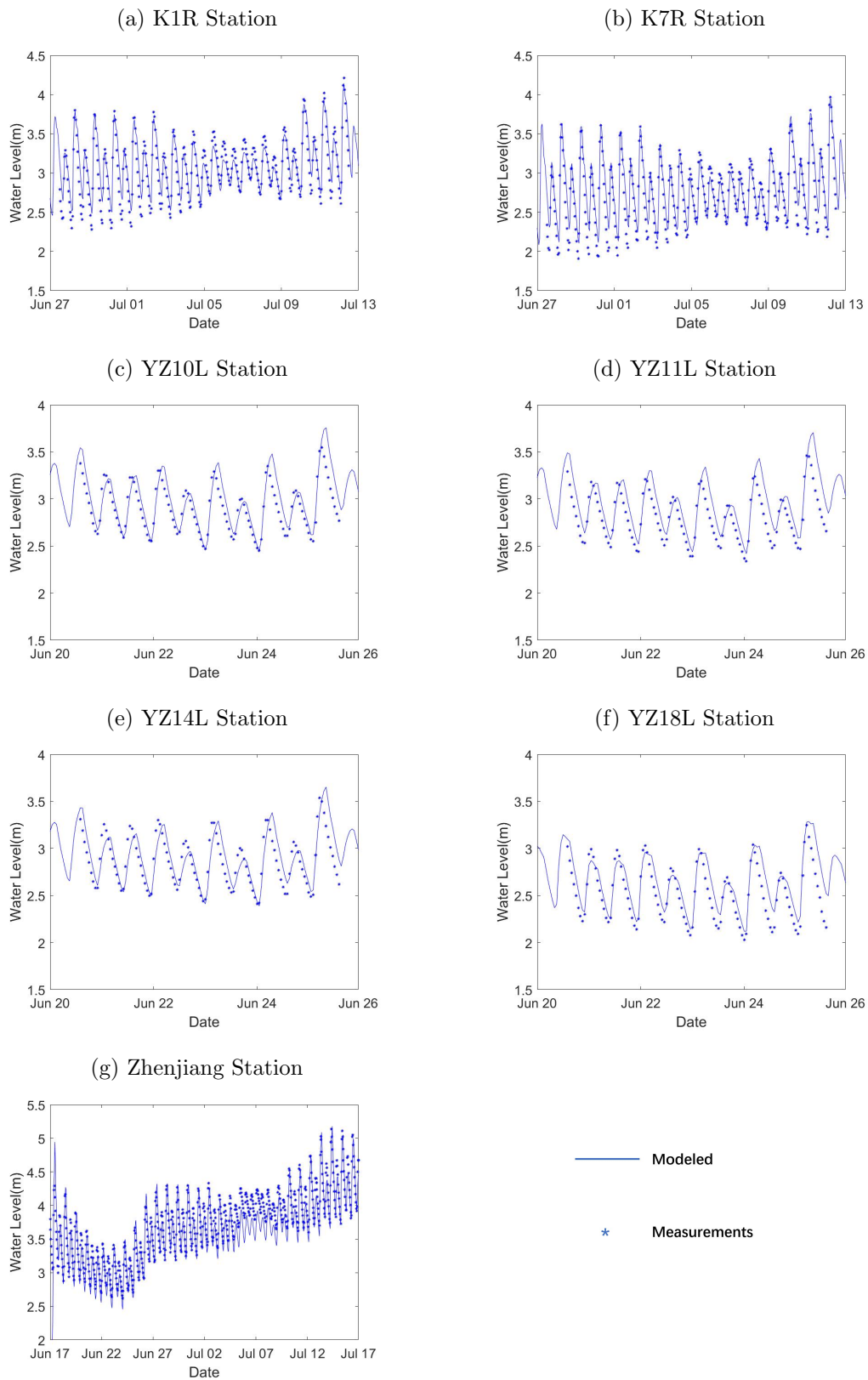


Figure 5.1.2: Calculated and measured waterlevels at (a) K1R Station, (b) K7R Station, (c) YZ10L Station, (d) YZ11L Station, (e) YZ14L Station, (f) YZ18L Station and (g) Zhenjiang Station

### 5.1.2 Statistical calibration

After the visual calibration, the model results are evaluated by two statistical parameters, namely the Model Efficiency ME coefficient and the overall bias PB. Figure 5.1.3 and Figure 5.1.4 show the ME and PB for the calculated water levels at the 7 measuring stations. With an efficiency of  $ME > 0.65$  the model shows an excellent performance on calculating water levels. YZ11L station shows a slightly less accurate performance. This could be due to bathymetry inconsistencies. The model shows similar results for the percentage bias, scoring excellent for all the stations.

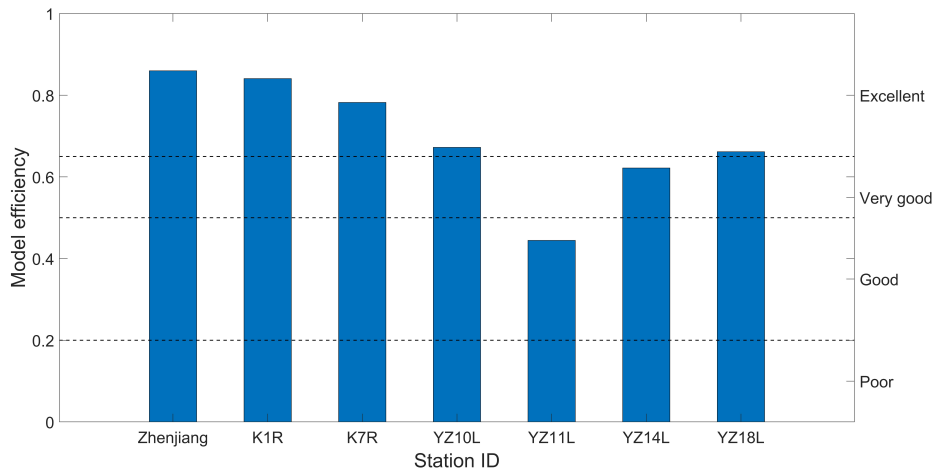


Figure 5.1.3: Model Efficiency for the calculated waterlevels at the 7 measuring stations

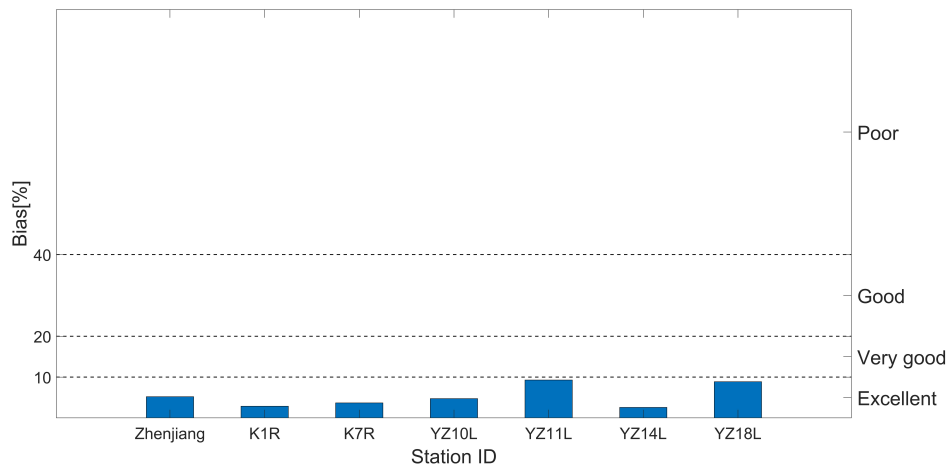


Figure 5.1.4: Percentage Bias for the calculated waterlevels at the 7 measuring stations



## 5.2 Numerical model results

The numerical model results are divided into two parts: morphology changes and local hydrodynamics changes. The part of "morphology changes" is introduced and analyzed first and the part of "local hydrodynamics changes" follows because the water depth changes(Chapter 5.2.2) highly depend on the morphology changes. The morphology changes do not show difference during a tidal cycle since the reach has reached the morphological equilibrium. The changes of local hydrodynamics are collected during the tidal flooding period. After comparing with the changes of the local hydrodynamics during the tidal ebbing period, the differences induced by the tidal effect are treated in Chapter 5.5.

### 5.2.1 Changes of morphology

The changes of bed level caused by submerged sills are relatively small in the dry season. Compared with the bed level change without the submerged sills, the additional erosion and sedimentation are less than 0.5m in the situation with the sills. In the normal-water season(see Figure 5.2.1(a)), the sills affect the morphology to a considerable extent. Compared with the bed level change without the submerged sills, the sills reduce the erosion occurring in front of the sills about 3m while the sills reduce the sedimentation occurring behind the sills about 3m. In the adjacent area of the confluence 2 km upstream Dagang, due to the sills' blocking, less water discharge comes downstream, leading the bed shear stress there to decline(see Figure A.1.1(i)), which induces less erosion there as well. All the phenomenon or changes are enhanced in the monsoon season(see Figure 5.2.1(b)). The sills reduce the erosion about 8m in the adjacent area of the confluence 2 km upstream Dagang. The channel near the upstream boundary is moved a little to the south. In the south branch, additional erosion occurs, which is caused by additional inward flux of water from upstream through the south branch. The sills reduce the sedimentation occurring very close to the sills about 4m, which can be explained by that the discharge input is reduced by the 2 sills, thus the sediment input is also reduced at the same time. The distribution maps of bed level changes of the three scenarios with- or without- submerged sills are shown in Figure 5.2.2.

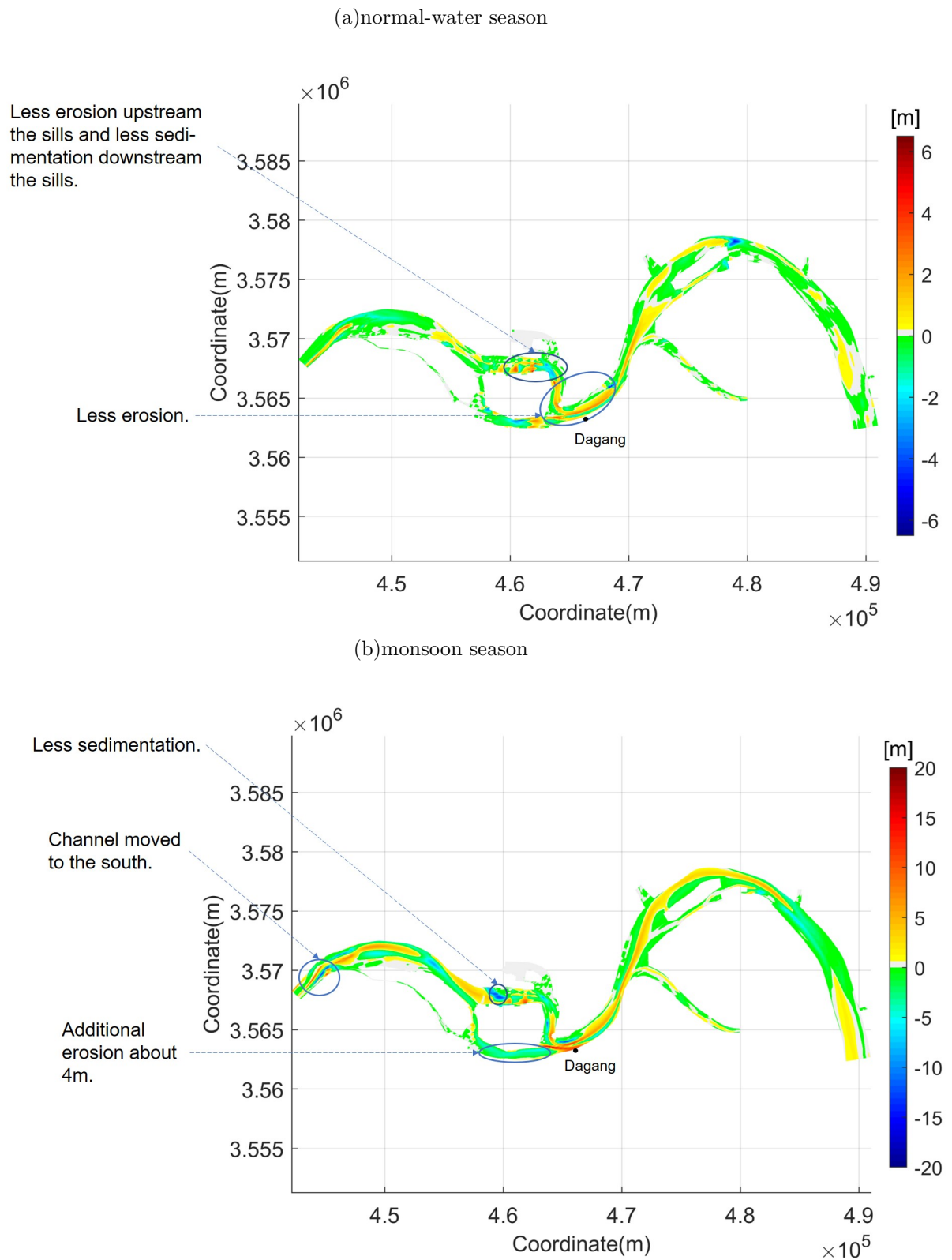


Figure 5.2.1: Differences of bed level change caused by the submerged sills in the (a) normal-water season and (b) monsoon season

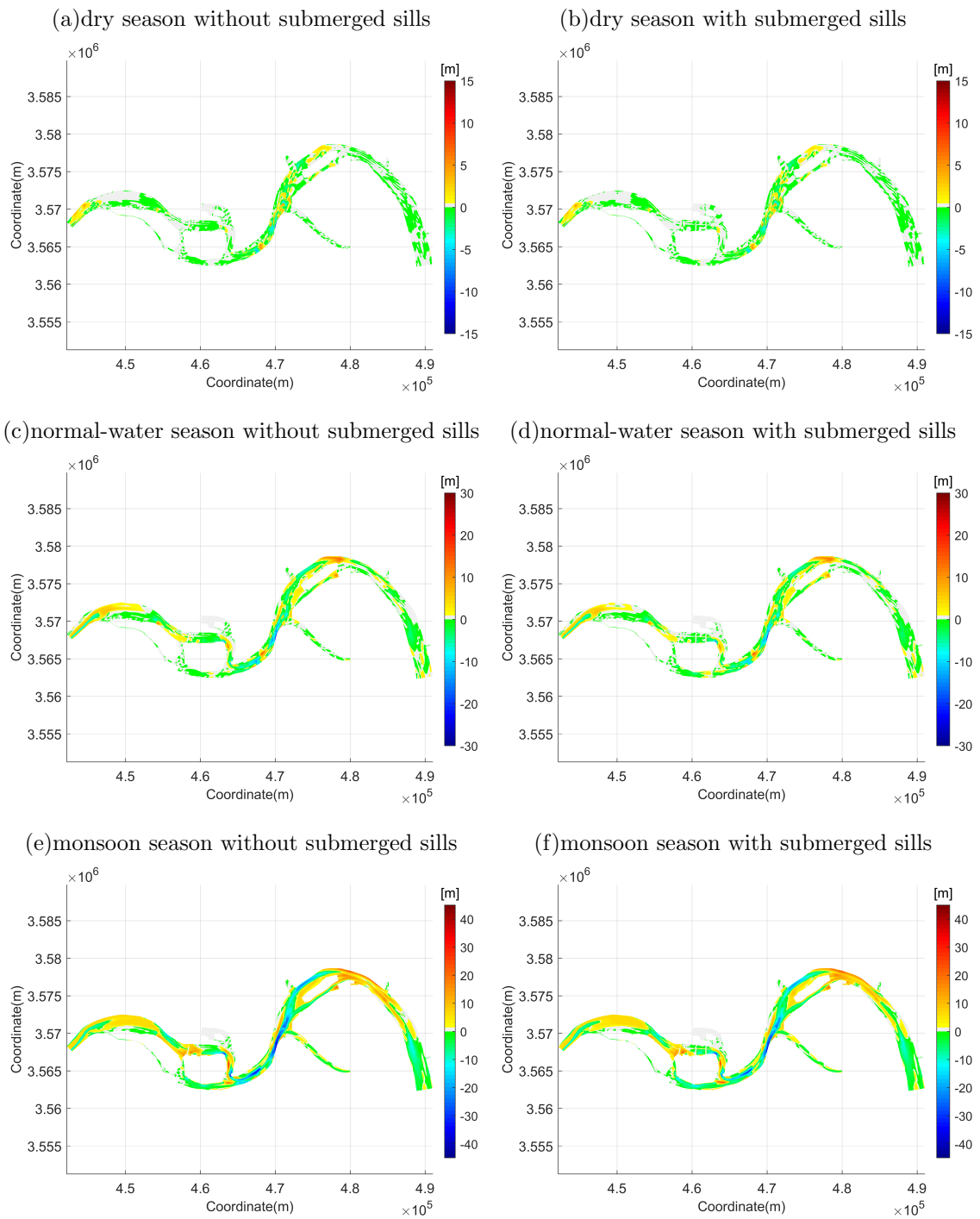


Figure 5.2.2: Distribution map of bed level changes of the three scenarios with- or without-submerged sills.

## 5.2.2 Changes of hydrodynamic condition

### Flow velocity

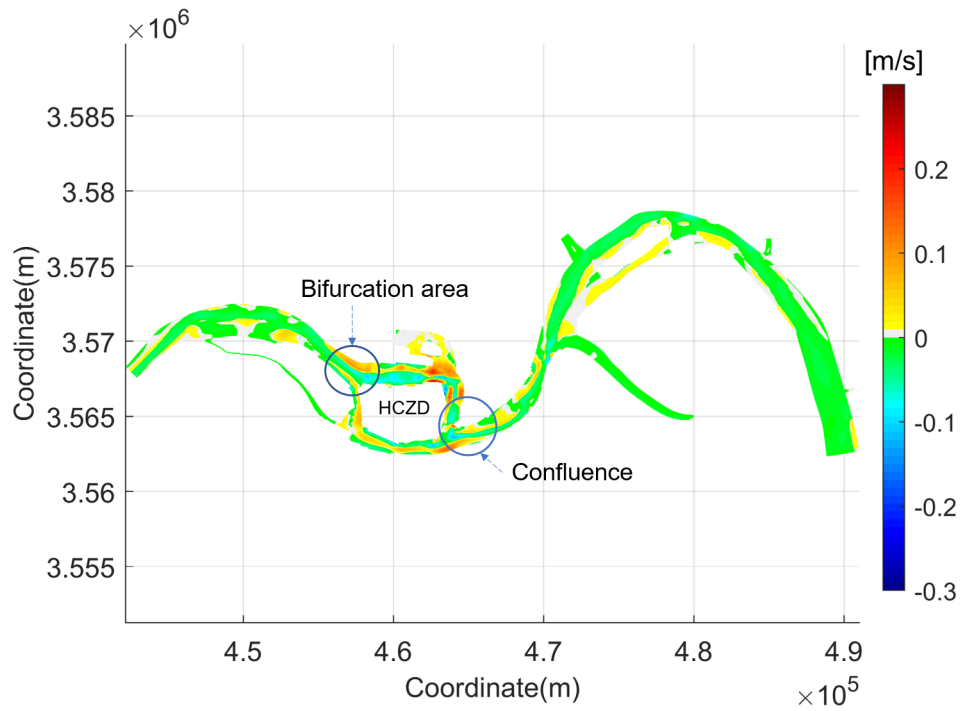
From the view of the whole reach, the reduction of velocity caused by the sills in the channel is more than that in the floodplain. The velocity change highly depends on different upstream discharge in different scenarios (see Figure 5.2.4).

In the dry season(see Figure 5.2.3(a)), the reduction caused by the submerged sills on flow velocity is limited. The velocity in most area of channel decreases less than 0.05m/s while it increases less than 0.05m/s in the most floodplain area. The velocity change is more substantial when approaching to the submerged sills. In the bifurcation area west to the sills and the north branch of HCZD, the velocity in the channel declines about 0.1m/s while it grows about 0.08m/s in the floodplain. Downstream of 2 submerged sill, the velocity increases about 0.15m/s because the upstream discharge is blocked by the sill and the blocking creates large circulation with combined effect of the tidal current from downstream. In the south branch of HCZD, the velocity increases more than 0.08m/s in the channel and reduces very little in the floodplain, which reveals that the engineering aim of submerged sills is now preliminarily realized—improving the south channel’s navigation condition. In the confluence area, the velocity growth occurs in the southern floodplain, which means the main stream flowing direction changes a little due to the faster flow coming from the north branch.

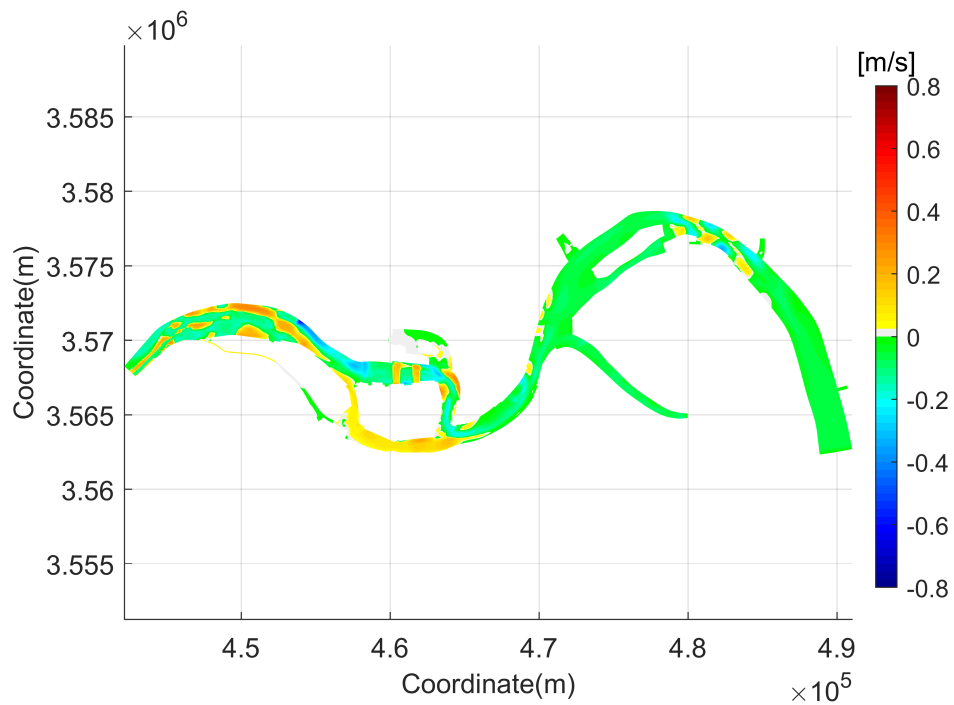
In the normal-water season(see Figure 5.2.3(b)), all the velocity changes mentioned above are about 4 times of those in the dry season. It is noteworthy that the velocity in the bifurcation area decreases both in the channel and the floodplain, which reveals that the backwater effect dominates now. The flow substantially accelerates in the south branch, meaning the effectiveness of sills is now further enhanced.

In the monsoon season(see Figure 5.2.3(c)), velocity changes dramatically in the whole reach. At the entrance of the reach, the velocity changes are obvious because the channel is now moved south, which can also be verified in Chapter 5.2.1. In Liuwei bending segment, the velocity declines about 0.65m/s in the channel and increases about 0.55m/s in the floodplain. In the south branch of HCZD, the velocity keeps increasing and its growth is about 0.2-0.3m/s now while the flow decelerates in the north branch except the over-sills area, which reveals that the engineering aim of submerged sills is now fully realized.

(a) dry season



(b) normal water season



(c) monsoon season

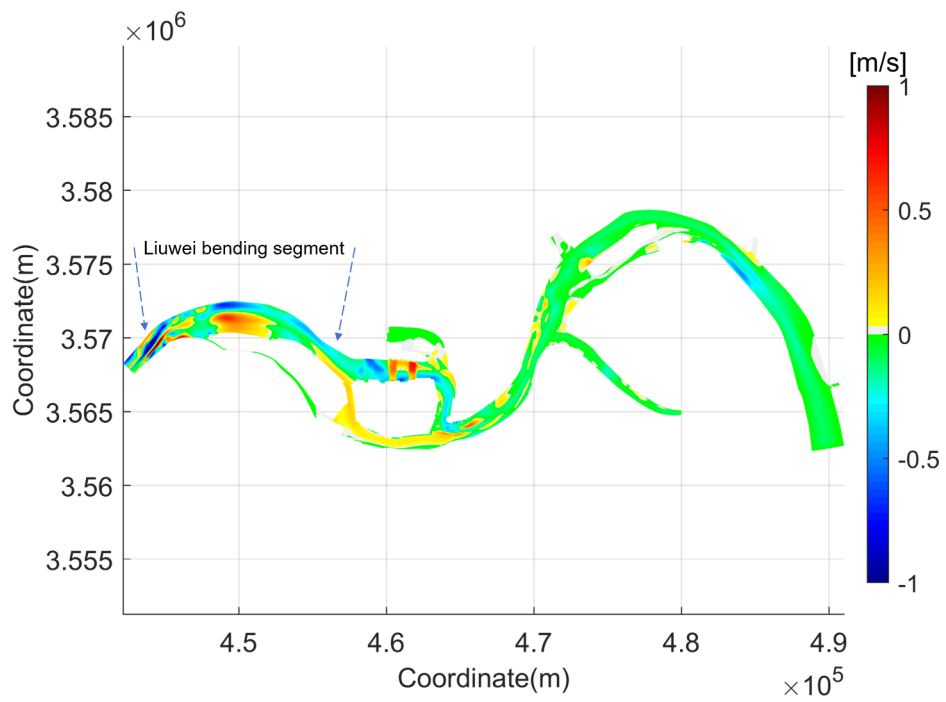


Figure 5.2.3: Differences of flow velocity caused by the submerged sills in the (a) dry season (b) normal water season and (c) monsoon season.

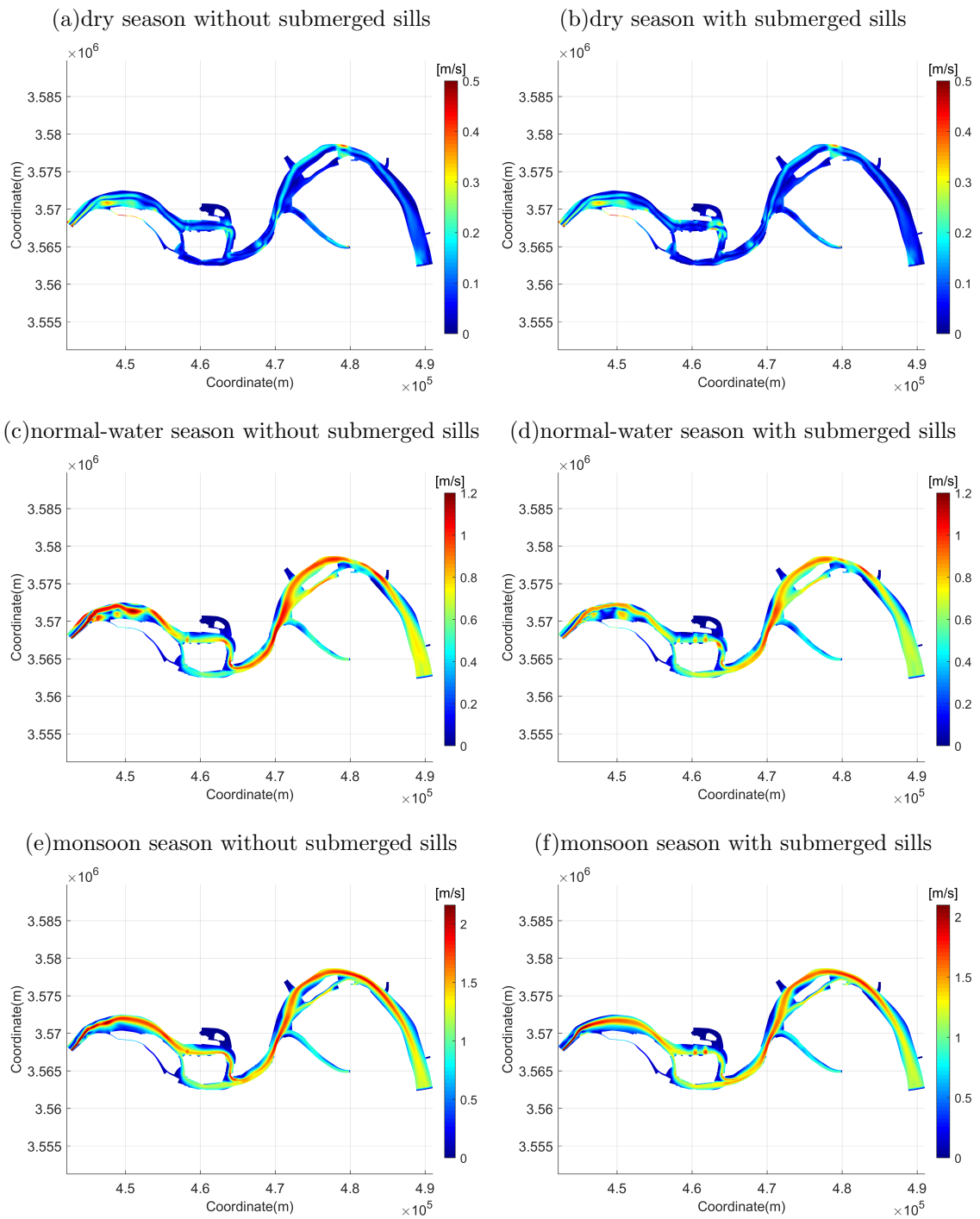


Figure 5.2.4: Distribution map of flow velocity of the three scenarios with- or without- submerged sills.

### **Water depth**

The changes of water depth(See Figure 5.2.6) are mainly caused by bed level change and backwater effect. In the dry season(See Figure 5.2.5(a)), both effects are weak. In the normal water season(See Figure 5.2.5(b)), the effects are relatively obvious leading to about 3m growth of water depth downstream the sills. In front of the sills, the water depth does not change much, which can be explained by the balance of the sedimentation and the backwater effect. In the monsoon season(See Figure 5.2.5(c)), the water depth increases about 10m in front of the sills due to less sedimentation there. In the bifurcation area of HCZD, the water depth in the southern part of channel grows while it declines in the northern part. It is due to the sill-induced discharge comes into the south branch of HCZD, which is enhanced by the reduced bed elevation in the southern part of channel. The water depth increases much in the south branch of HCZD and the area downstream of sills which means the additional erosion is dominant in both area.



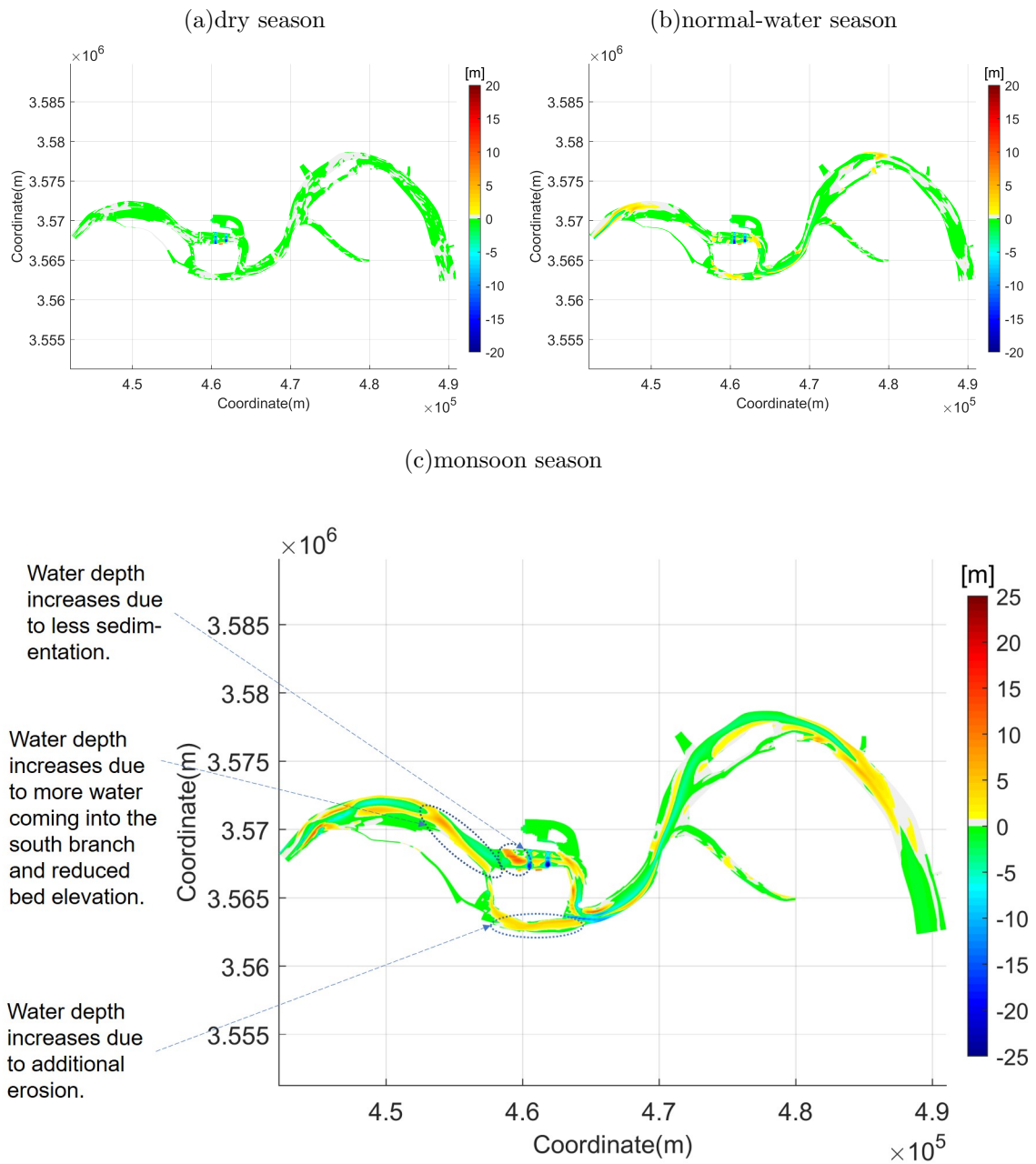


Figure 5.2.5: Differences of water depth caused by the submerged sills in the (a)dry season (b)normal-water season (c)monsoon season

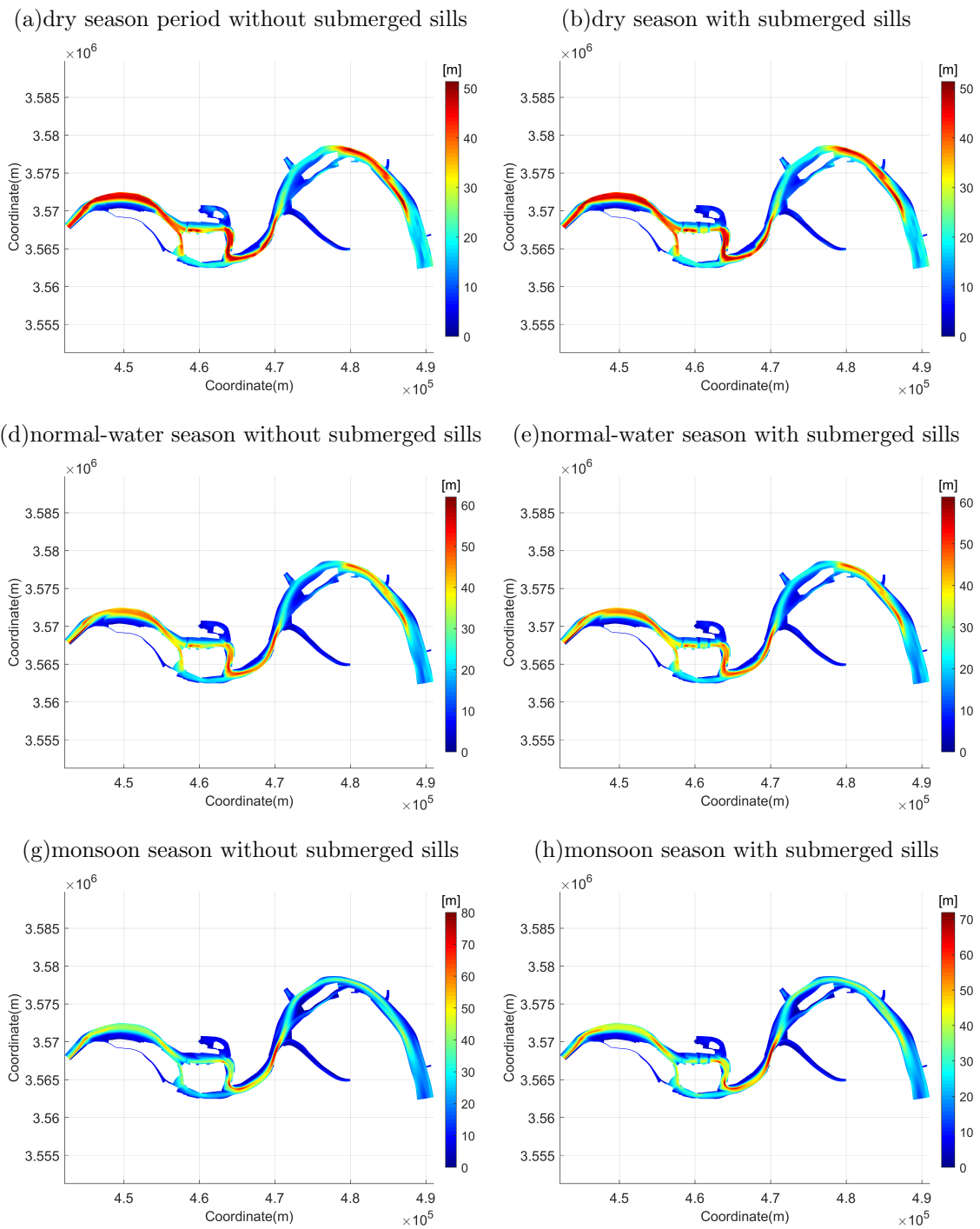


Figure 5.2.6: Distribution map of water depth of the three scenarios with- or without- submerged sills.

**Tidal range**

The tidal range is ranging between 1.2-1.4m, 0.7-1.1m and 0.3-0.8m in the 3 scenarios(See Figure 5.2.7). The tidal range decreases gradually from the downstream boundary to the upstream boundary. The sills change the tidal range very little with the difference of tidal range less than 0.2m in all water seasons.

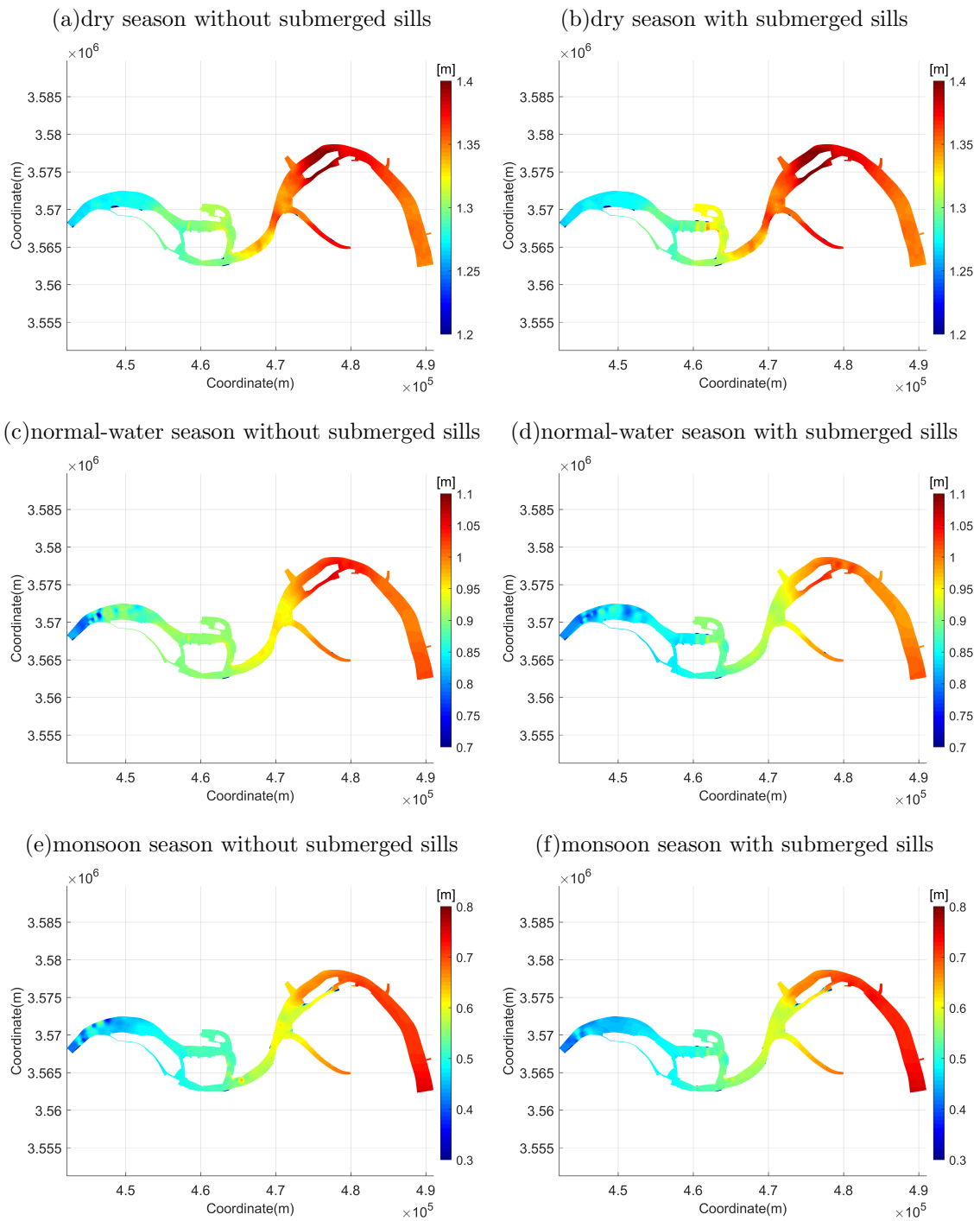


Figure 5.2.7: Distribution map of tidal range of the three scenarios with- or without- submerged sills.

## 5.3 HSI model performance

### 5.3.1 Visual validation

After obtaining the results of the local hydrodynamics and morphology, the habitat suitability index model can be validated combined with the distribution map of YFP's occurrence. Chinese fishing service roughly conducted the survey on the population and abundance of Yangtze finless porpoise by boat sight-seeing in HCZR during the normal-water season from 2006-2013 (Jianjun, 2016). By combining the distribution map of YFP's occurrence and the distribution map of composite suitability index in the normal-water season (See Figure 5.3.1), a close match of YFP's occurrence can be observed in high-index areas which reflects the HSI model of YFP is relatively reliable.

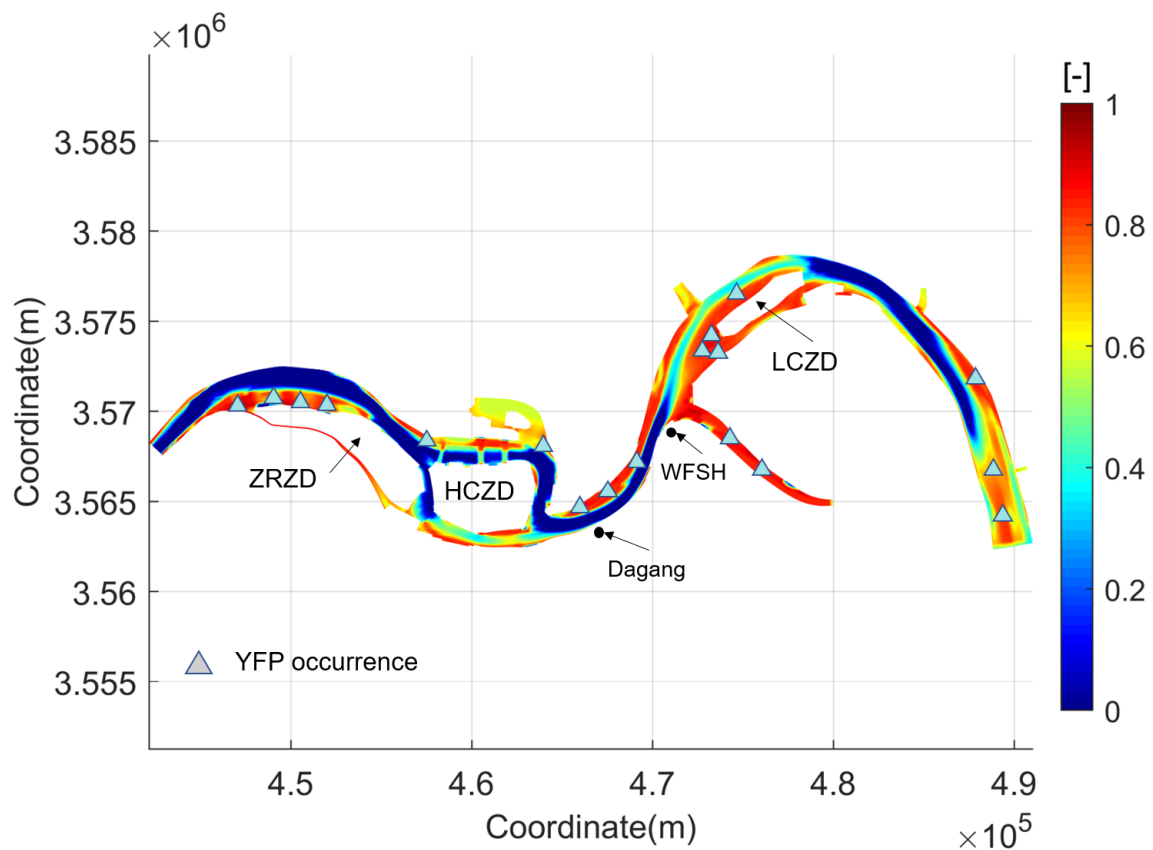


Figure 5.3.1: Distribution map of YFP's occurrence and composite suitability index in the normal-water season

## 5.4 Results of hydraulic-habitat model

Hydraulic-habitat model model is the combination of the numerical model and the habitat suitability index model, which can show the distribution of suitability index of each habitat variable and composite suitability index. Differences of habitat variable caused by the 2 submerged sills lead to the changes of suitability index of habitat variable, which can also be demonstrated in this part.

### 5.4.1 Water depth impact

Suitability index of V1 and V4 reveal the relation between water depth and habitat suitability index for YFP corresponding with its movement and feeding component.

In all 3 scenarios, no matter with or without submerged sills, SI of V1 indicates that floodplain is perfect area for YFP to swim while the movement of YFP in channel areas is extremely limited(See Figure 5.4.2). The influence of the sills on V1 index is next to nothing for the whole reach except the area over the sills during the dry and normal season(See Figure 5.4.1(b)(c)). In the monsoon season(See Figure 5.4.1(c)), in the bifurcation area upstream the sills, V1 index grows by 0.2 with the local water depth declining while the index decreases from 1.0 to 0.8 when closer to the sills. The south branch of HCZD is less suitable for YFP's movement due to the increasing water depth.

For V4 index(See Figure 5.4.3(a)(c)(e)), since only very shallow water is suitable for YFP's main food source, the areas with high index of V4 is very rare, thus the sills do not change V4 index much in all 3 scenarios(See Figure 5.4.3(b)(d)(f)). Although it seems that the water depth of the whole reach is not suitable for YFP's feeding component, it should be kept in mind that the influence of water depth is just one of the factors affecting YFP's food source, in other words, very low index of V4 does not mean the area is totally not suitable for YFP's food source growth.

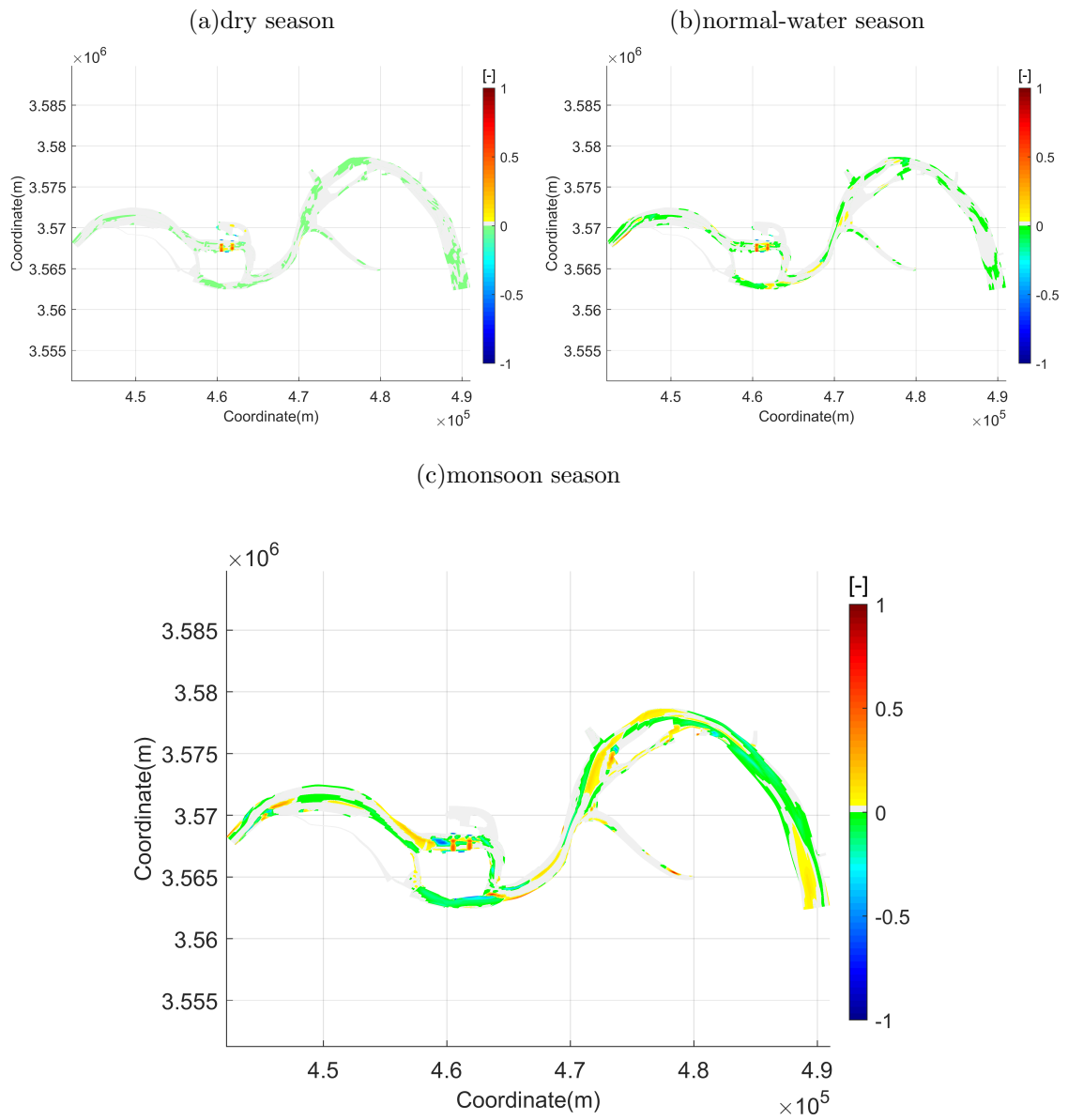


Figure 5.4.1: Differences of SI of V1 caused by the submerged sills in the (a) dry season (b) normal-water season and (c) monsoon season

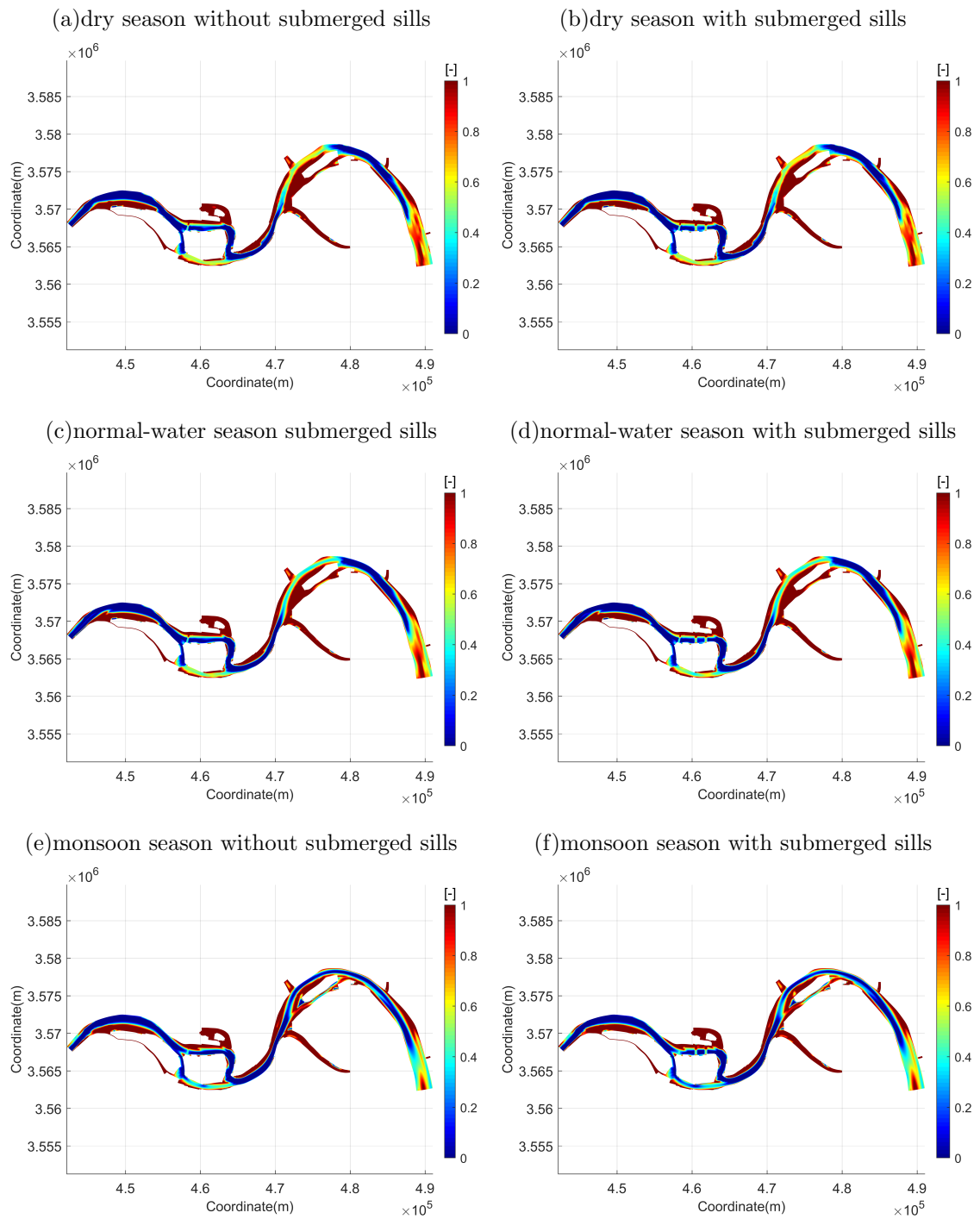


Figure 5.4.2: Distribution map of SI of V1 of the three scenarios with- or without- submerged sills.



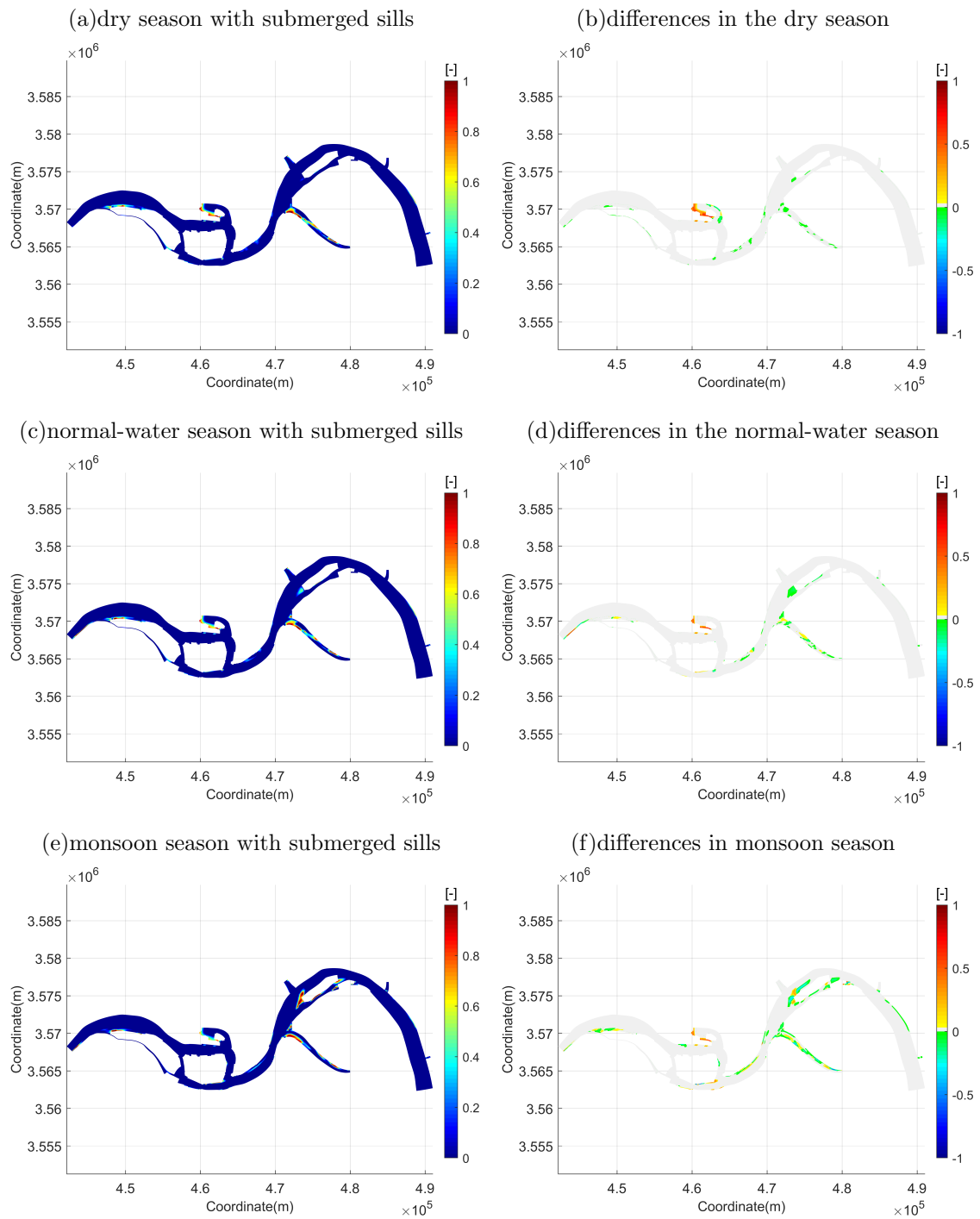


Figure 5.4.3: Distribution map of SI of V4 with submerged sills and differences of SI of V4 caused by the submerged sills in the three scenarios.

## 5.4.2 Flow velocity impact

Suitability index of V2 and V5 reveal the relation between flow velocity and habitat suitability for YFP corresponding with its movement and feeding component.

It can be seen that the whole reach offers considerably suitable velocity to YFP's for its movement in the dry season and the velocity is even more suitable in the normal-water season with suitability index about 0.95 in the whole reach(See Figure 5.4.5). The sills do not change the positive result in the dry season while in the normal water season, the index of V2 is also above 0.9 under the influence of the sills, with very limited area being a little worse—adjacent area of ZRZD, upstream and downstream area adjacent to the sills and the whole south branch of HCZD(See Figure 5.4.4(a)). In the monsoon season, the channel is no longer suitable in terms of flow velocity for YFP's movement(See Figure 5.4.5(e)). Decreased velocity caused by the sills effectively improve this phenomenon with the index of V2 growing above 0.4(See Figure 5.4.4(b)).

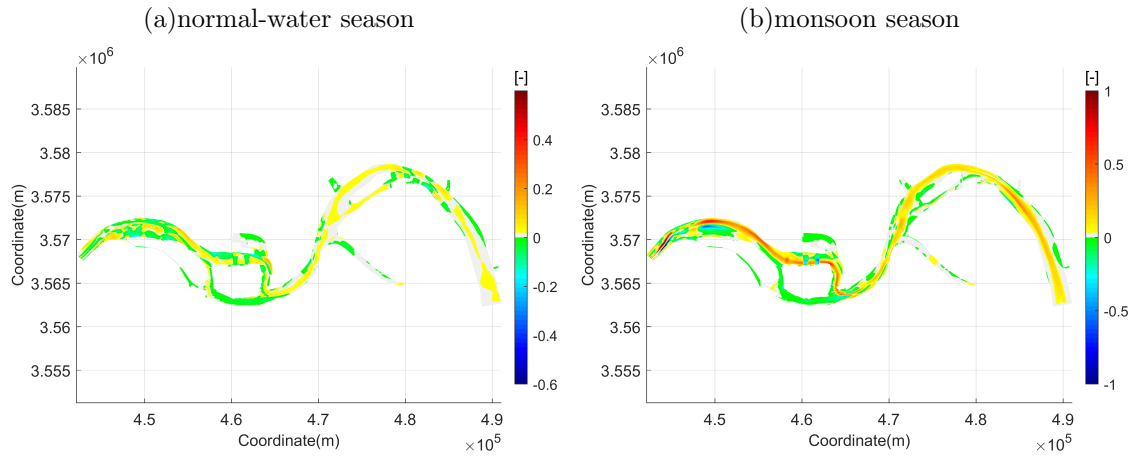


Figure 5.4.4: Differences of SI of V2 caused by the submerged sills in the (a) normal-water season and (b) monsoon season

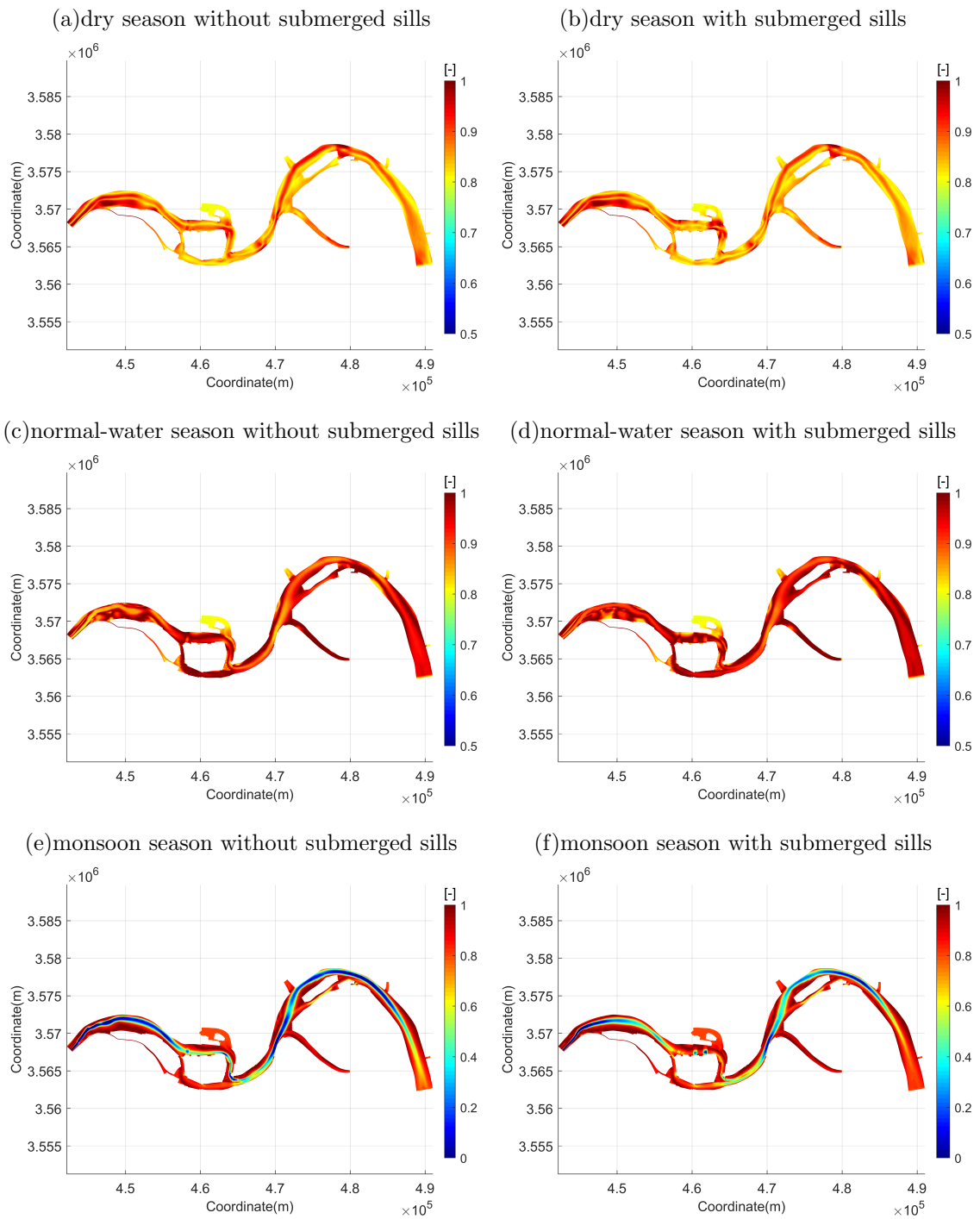


Figure 5.4.5: Distribution map of SI of V2 of the three scenarios with- or without- submerged sills.

For SI of V5, in the dry season, ZRZD, and downstream area of the sill as well as the channel next to LCZD are the areas with the most suitable velocity for YFP's food source(See Figure 5.4.6(a)). The sills improve a lot in the south branch of HCZD, the entrance of the pool north to the sill and the bifurcation area upstream the old sill. However, the sills also bring negative changes in the deep areas in north branch of HCZD(See Figure 5.4.6(b)).

In the normal-water season, the suitability index of velocity is above 0.9 in the most areas(See Figure 5.4.6(c)). The influence of submerged sills, from 2-13km away from the upstream boundary, is mainly manifested as position adjustment of the suitable area –pushing the suitable area a little upstream. Both the area which is within 3km upstream of the bifurcation area and most areas downstream the confluence area are improved considerably with the index increasing from 0.2 to 0.5(See Figure 5.4.6(d)).

In the monsoon season, the channels are all no longer suitable for YFP's food source in terms of velocity(See Figure 5.4.6(e)). The sills upgrade the channel which situates upstream of the confluence area of HCZD except in the south branch. The velocity suitability in side channel next to WFSH is also improved by the sills influence(See Figure 5.4.6(f)).

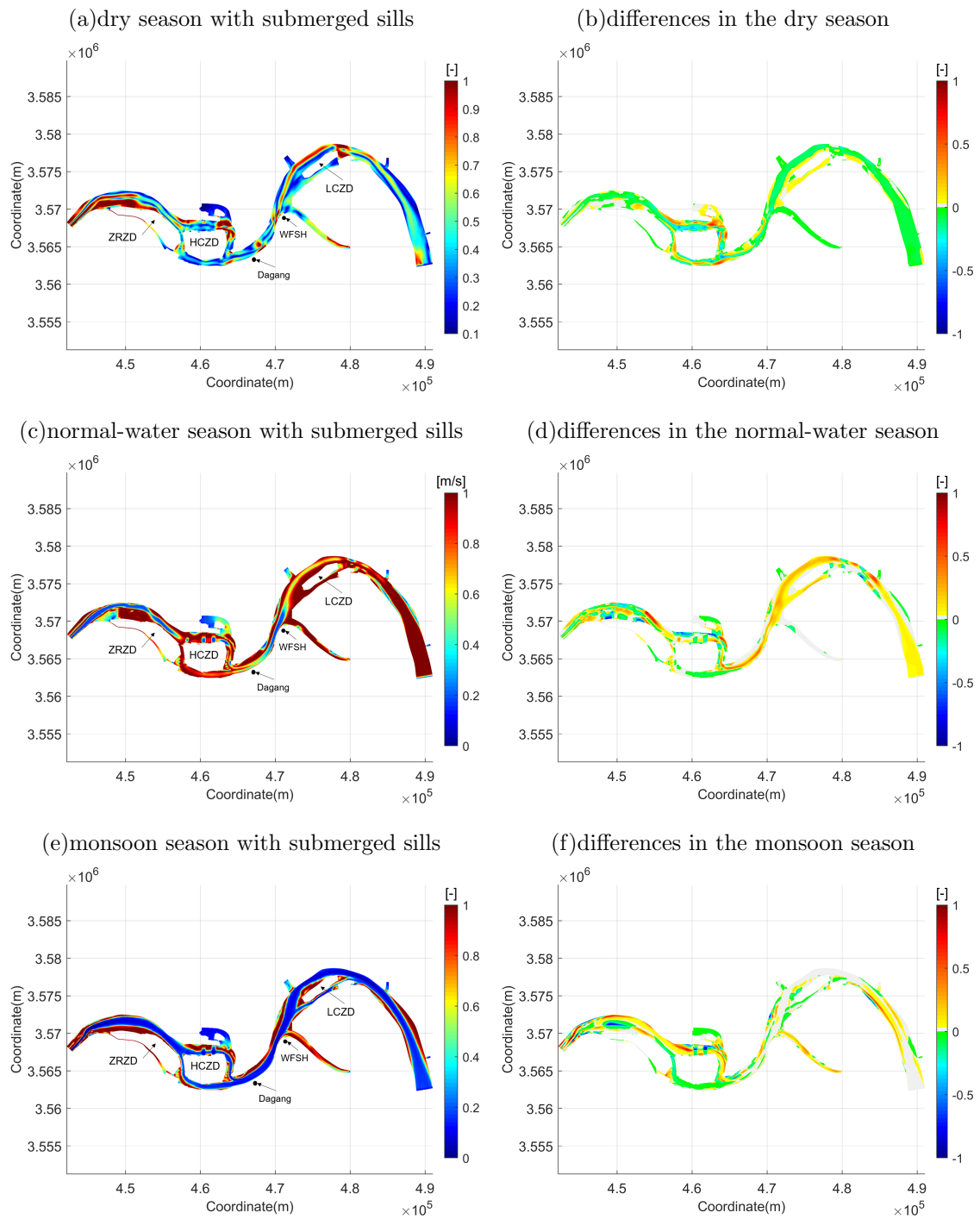


Figure 5.4.6: Distribution map of SI of V5 with submerged sills and differences of SI of V5 caused by the submerged sills in the three scenarios.

### 5.4.3 Substrate type impact

Suitability index of V3 and V6 reveal the relation between substrate type and habitat suitability for YFP corresponding with its movement and feeding component. In all 3 scenarios, no matter with or without the sills, the maximum bed shear stress (less than  $8\text{N/m}^2$ ) is much less than the critical shear stress of cobble (around  $47\text{N/m}^2$ ), which means the soil composition of the river bed does not include these large-sized particles such as cobble or boulder. In other words, the SI of V3 will not be changed and keep as 1.0 after the sills are built. Thus, the distribution map of SI of V3 is not shown here.

For the SI of V6, from the bed shear stress map (see Figure A.1.1), it is clear that in all 3 scenarios, the bed shear stress is always less than  $10\text{ N/m}^2$ , as a result, all the soil larger than gravel can be retained in the whole reach, thus, the SI of V6 in all scenarios is larger than 0.4 (see Figure 5.4.7(a)(c)(e)). In the floodplain or the adjacent areas of the dunes, relatively fine sediment such as clay or silt can be kept while these particles are easily to be flushed away in channels.

In the dry season, the sills do not change the SI of V6 much, only some adjustment of substrate type occurs a little downstream of the sills (see Figure 5.4.7(b)). Both in the normal-water season and the monsoon season (see Figure 5.4.7(d)(f)), the SI of V6 increases around 0.15 in most area of channels due to the bed shear stress is reduced in these areas.

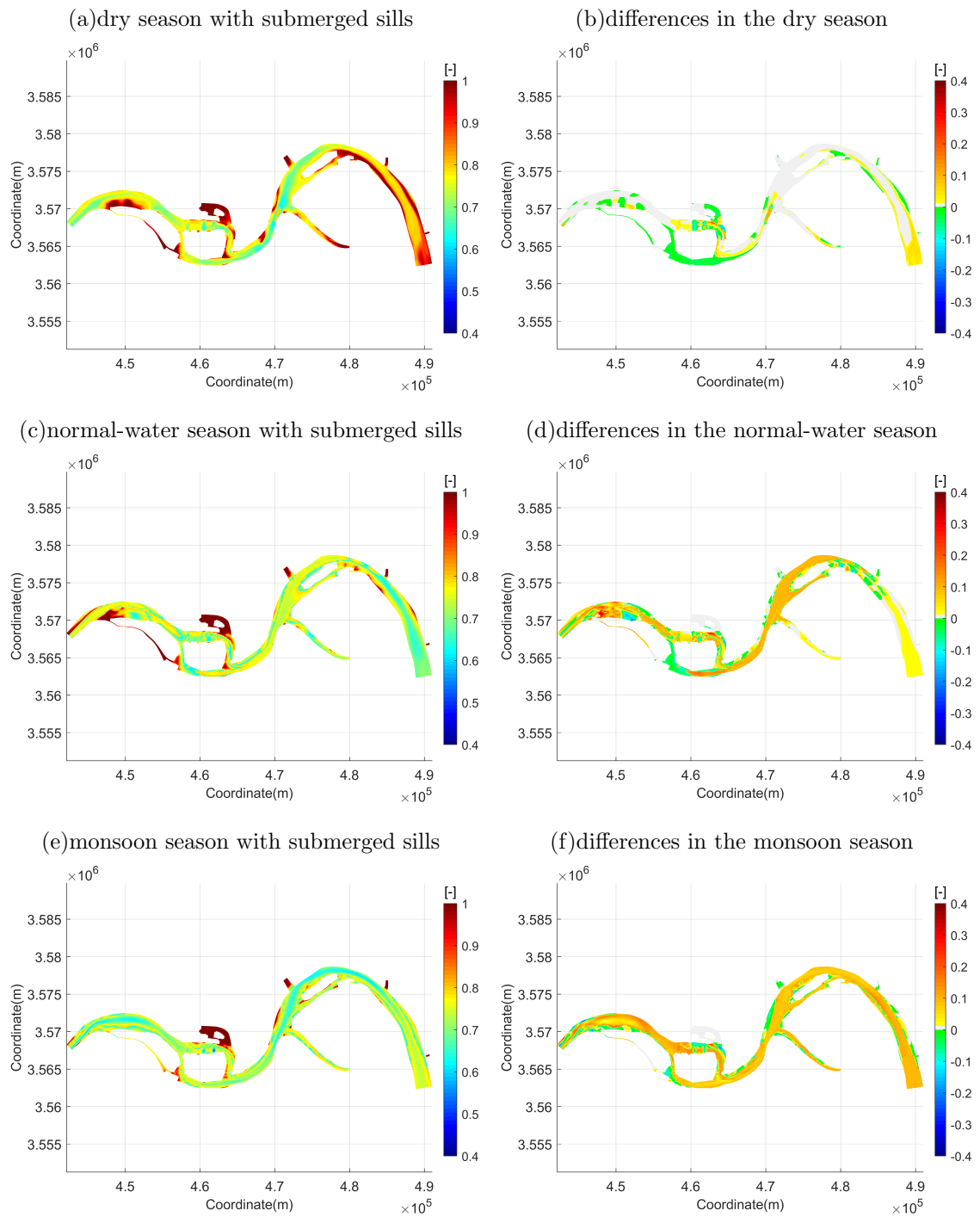


Figure 5.4.7: Distribution map of SI of V6 with submerged sills and differences of SI of V6 caused by the submerged sills in the three scenarios.

#### 5.4.4 Changes of composited suitability index(CSI)

Composited suitability index(CSI) reflects the overall evaluation of YFP's habitat quality. In all 3 scenarios, ZRZD, floodplains of HCZ north branch, floodplains of the section from Dagang to the tail of LCZD, and the side channel next to WFSH are the most suitable habitats for YFP(see Figure 5.4.9). The sills in the dry season slightly change the SI in both branches of HCZD(see Figure 5.4.8(a)). Part of the bifurcation area and the entrance of the pool north to the 2 sill are upgraded while the floodplain of south branch of HCZD is deteriorated. In the normal-water season(see Figure 5.4.8(b)), adjacent areas of LCZD are improved by the sills with the CSI rising about 0.1, especially the upstream areas. Both the 2 branches of HCZD are downgraded under the influence of the sills. In the monsoon season(see Figure 5.4.8(c)), the significant improvement of the sills occurs in the bifurcation area of HCZD while both the 2 branches of HCZD are undermined. Other improvements caused by the sills occur in the side channel next to WFSH as well as in the upstream area of LCZD.



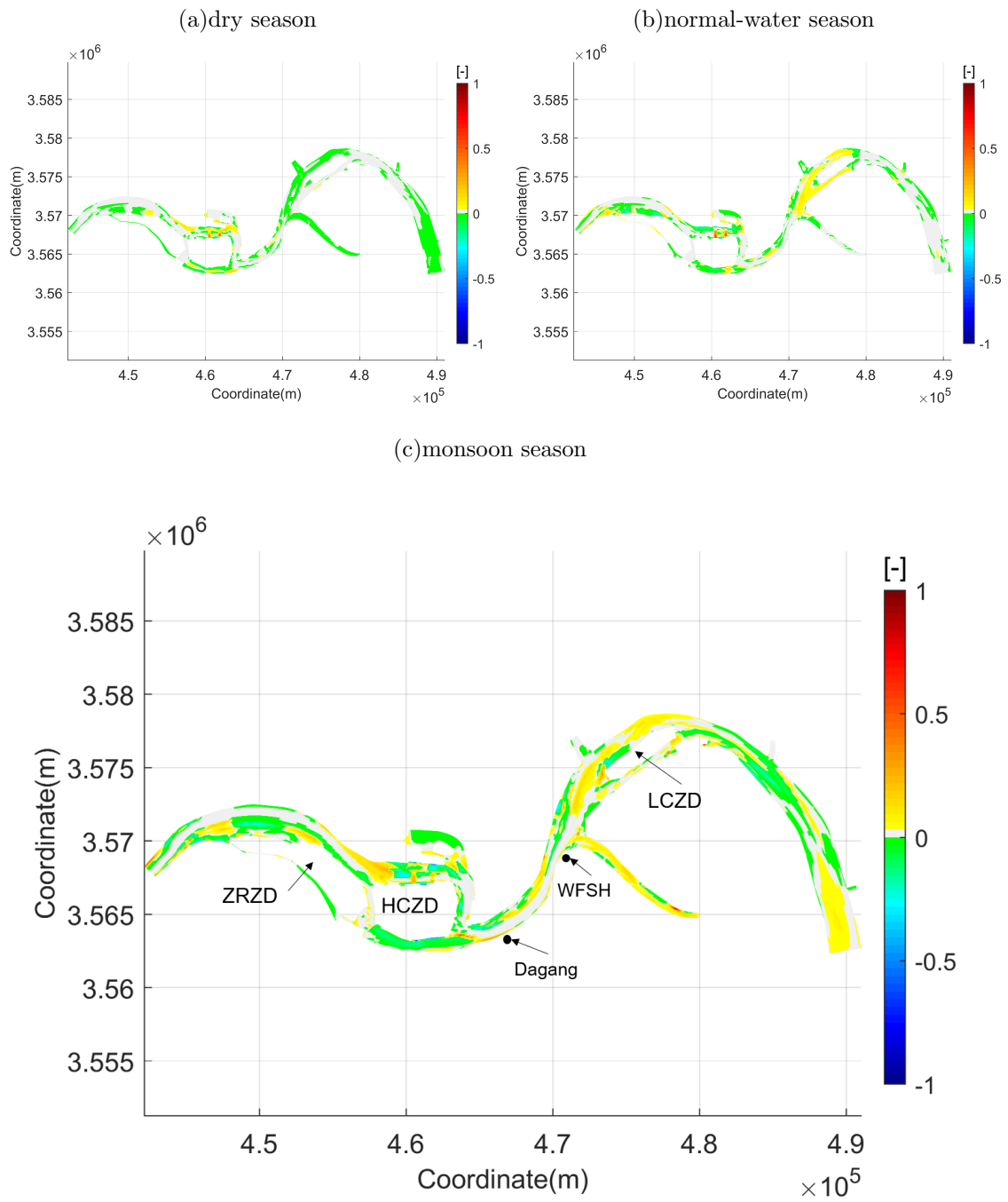


Figure 5.4.8: Differences of CSI caused by the submerged sills in the (a) dry season, (b) normal-water season and (c) monsoon season.

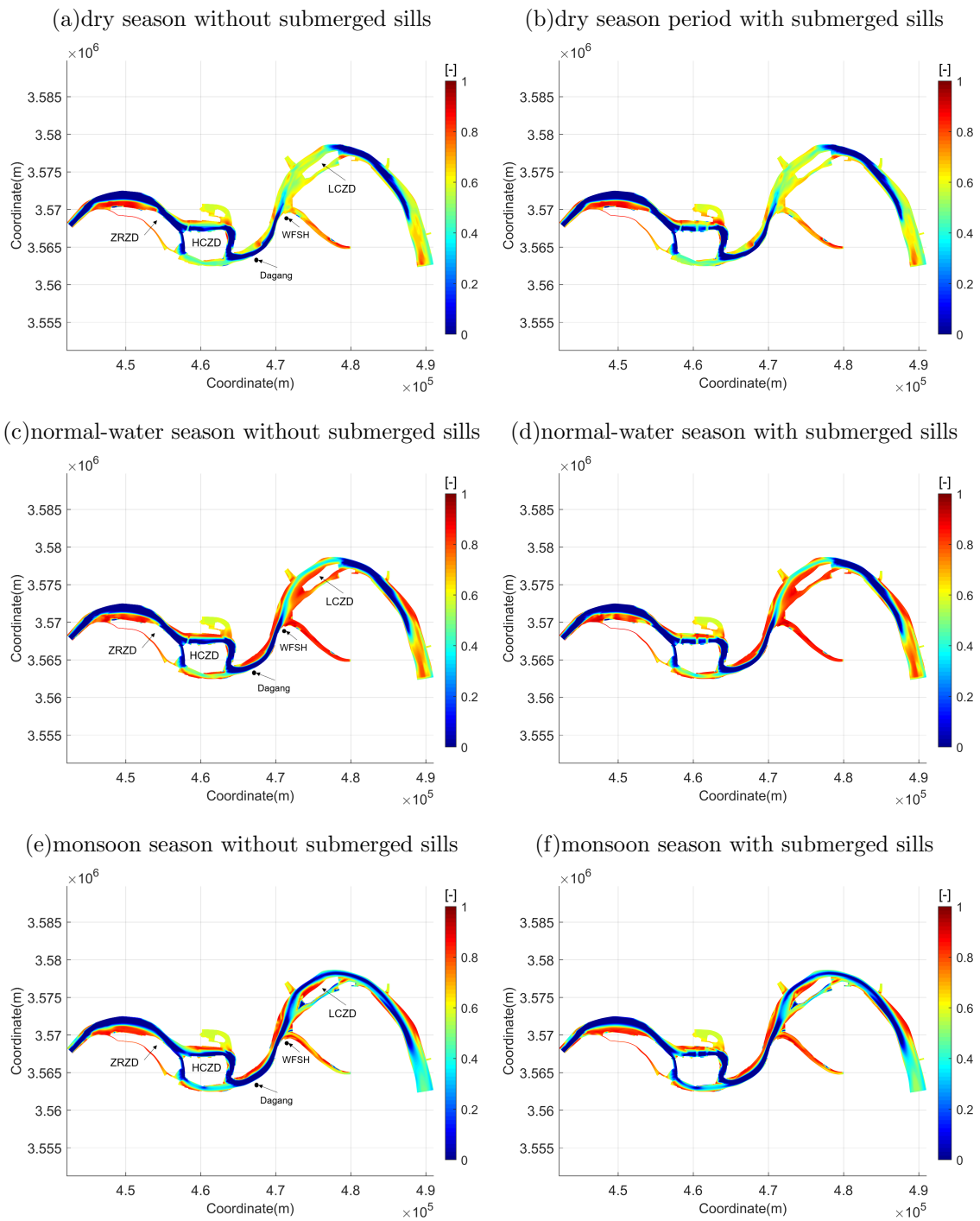


Figure 5.4.9: Distribution map of CSI of the three scenarios with- or without- submerged sills.

### 5.4.5 Changes of habitat area and quality

Habitat area is defined as the area of a river with a composited habitat suitability index more than 0, and effective habitat area is defined as a weighted usable area(WUA), that is, the area of a river area unit multiplied by the unit's composited suitability index, which is more representative of YFP's tendency of demand. The average suitability index of the whole reach is defined as the ratio of effective habitat area to habitat area.

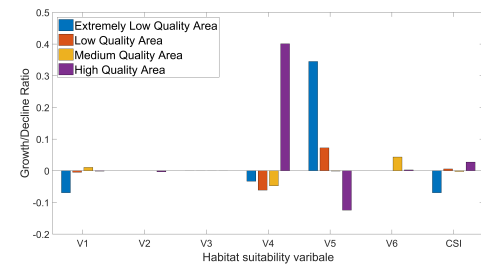
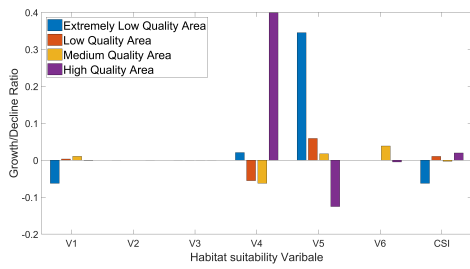
From Table.5.1, it can be seen that the area and the quality of YFP's habitat are improved by the 2 submerged sills. The habitat area, the effective habitat area and the averaged suitability index of the whole reach all slightly increase due to the sills, which means the sills bring positive changes to YFP's habitat in HCZR.

Leclerc et al. (1995) divided the quality of physical habitats into different levels according to the suitability index:  $0 < \text{CSI} < 0.1$  is very low quality,  $0.1 < \text{CSI} < 0.4$  is low quality,  $0.4 < \text{CSI} < 0.7$  is medium quality, and  $0.7 < \text{CSI} < 1.0$  is high quality. From Figure 5.4.10, it can be concluded that suitability of YFP's movement does not change much and suitability of YFP's feeding is improved in all three scenarios. Although the positive changes brought by the submerged sills on the overall reach are limited, the sills attach more importance on those high quality habitat area. According to the last column of Table.5.1, the growth ratios of WUA of high quality habitat area are 2.73%, 4.80%, 5.47% in 3 periods. The growth/decline ratios of habitat areas or weighted areas(product of CSI multiplied by area) distributed according to CSI in all three scenarios with submerged sills are shown in Figure 5.4.11, which give detailed information of changes to the habitat area classified according to CSI.

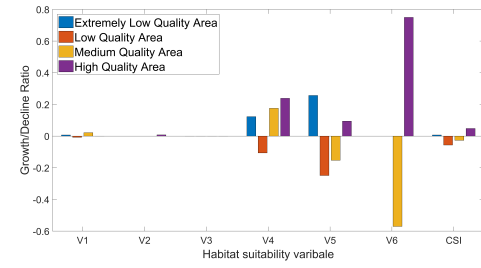
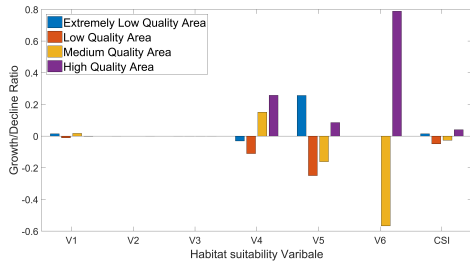
Table 5.1: Changes of habitat area and quality

Index name	Dry season	Normal-water season	Monsoon season
Habitat area without sills ( $km^2$ )	120.7680	120.1650	124.0860
Habitat area with sills ( $km^2$ )	120.7917	120.4391	124.9293
Difference of habitat area ( $10^4m^2$ )	2.3724	27.4123	84.3320
Weighted usable area without sills ( $km^2$ )	66.3763	73.9151	64.3998
Weighted usable area with sills ( $km^2$ )	66.4966	75.0911	65.7891
Difference of weighted usable area ( $km^2$ )	0.1203	1.1759	1.3893
Average suitability index without sills	0.548	0.615	0.519
Average suitability index with sills	0.551	0.623	0.527
Difference of average suitability index	0.003	0.008	0.008
Growth ratio of WUA of high quality area(%)	2.73	4.80	5.47

(a) Growth/Decline ratio of habitat areas in the dry season (b) Growth/Decline ratio of effective habitat areas in the dry season



(c) Growth/Decline ratio of habitat areas in the normal-water season (d) Growth/Decline ratio of effective habitat areas in the normal-water season



(e) Growth/Decline ratio of habitat areas in the monsoon season (f) Growth/Decline ratio of effective habitat areas in the monsoon season

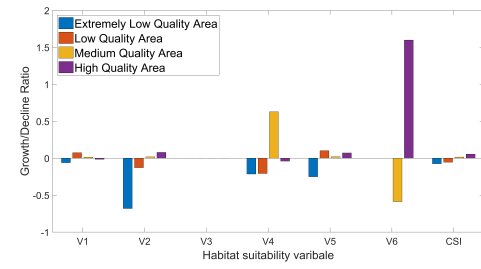
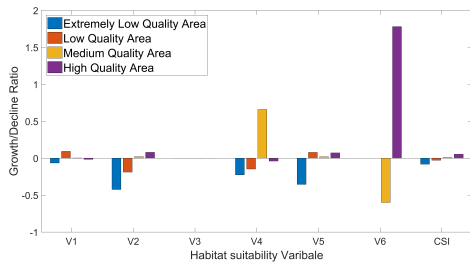
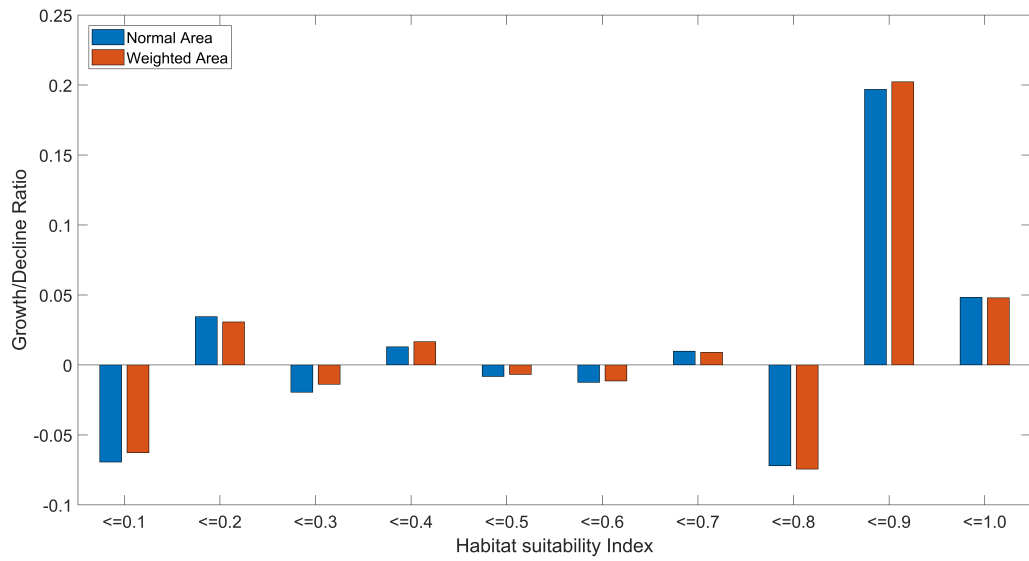
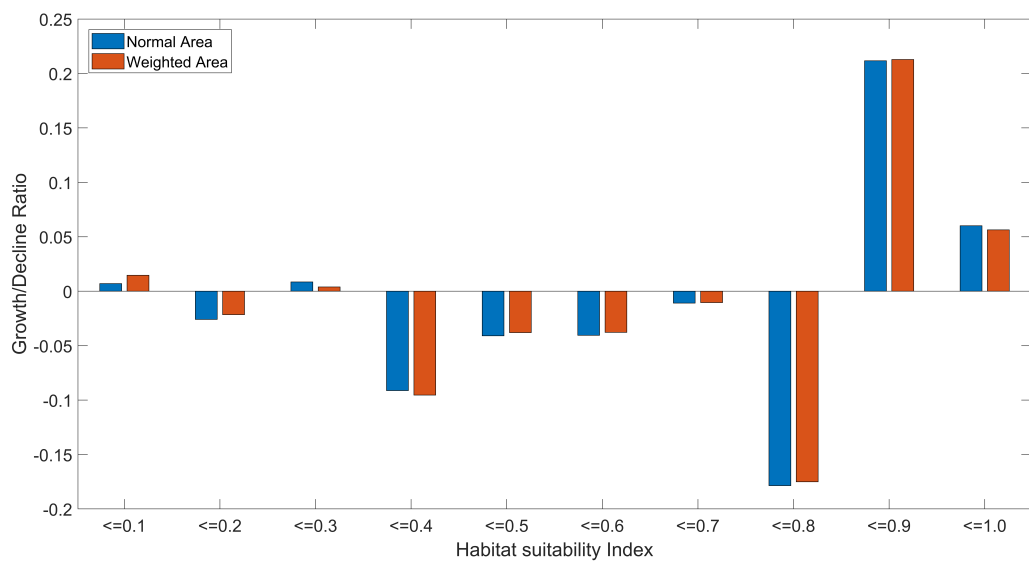


Figure 5.4.10: Growth/Decline ratio of habitat areas and effective habitat areas with the submerged sills in the three scenarios.

(a) dry season



(b) normal water season



(c) monsoon season

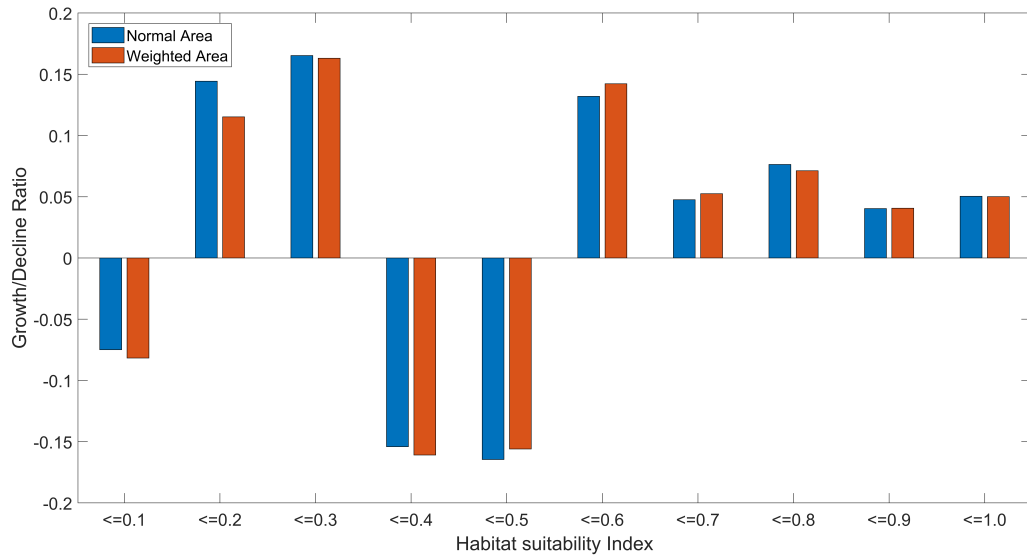


Figure 5.4.11: The growth/decline ratios of habitat areas or weighted areas (product of CSI multiplied by area) with the submerged sills in the (a) dry season (b) normal-water season and (c) monsoon season.

## 5.5 Tidal effects

According to Chapter 4.1.2, it is known that the habitat suitability index of YFP is affected by three habitat variables: water depth, flow velocity and substrate type. In Chapter 5.4, all the results in the tidal flooding period are collected. The tidal effect will not change the substrate type in a tidal cycle. Since in Chapter 5.2.2, it is known that the tidal range in HCZR is less than 1.2m. Compared with the local water depth (around 20m-30m), tidal effect does not change the water depth substantially, in other words, the water depth does not show great differences during a tidal cycle. Therefore, the distribution maps of water depth are not shown here. In conclusion, only flow velocity plays a role in the differences of HSI of YFP considering the tidal effect.

### 5.5.1 Flow velocity during tidal ebbing period

From Figure 5.5.1, it is obvious that the flow velocity during the tidal ebbing period increases about 1m/s, 0.8m/s and 0.5m/s in the dry, normal-water and monsoon season respectively

compared with that in the flooding period(See Figure 5.2.4). In the normal-water and monsoon season(See Figure 5.2.4), the differences of velocity caused by the sills are highly similar as that in tidal flooding period(See Figure 5.5.2(a)(b)) because the tidal prism is very small compared with the upstream discharge in the 2 scenarios. In the dry season(See Figure 5.5.2(c)), in the whole reach except the south branch of HCZD, the velocity decreases, which is different from that during tidal flooding period.

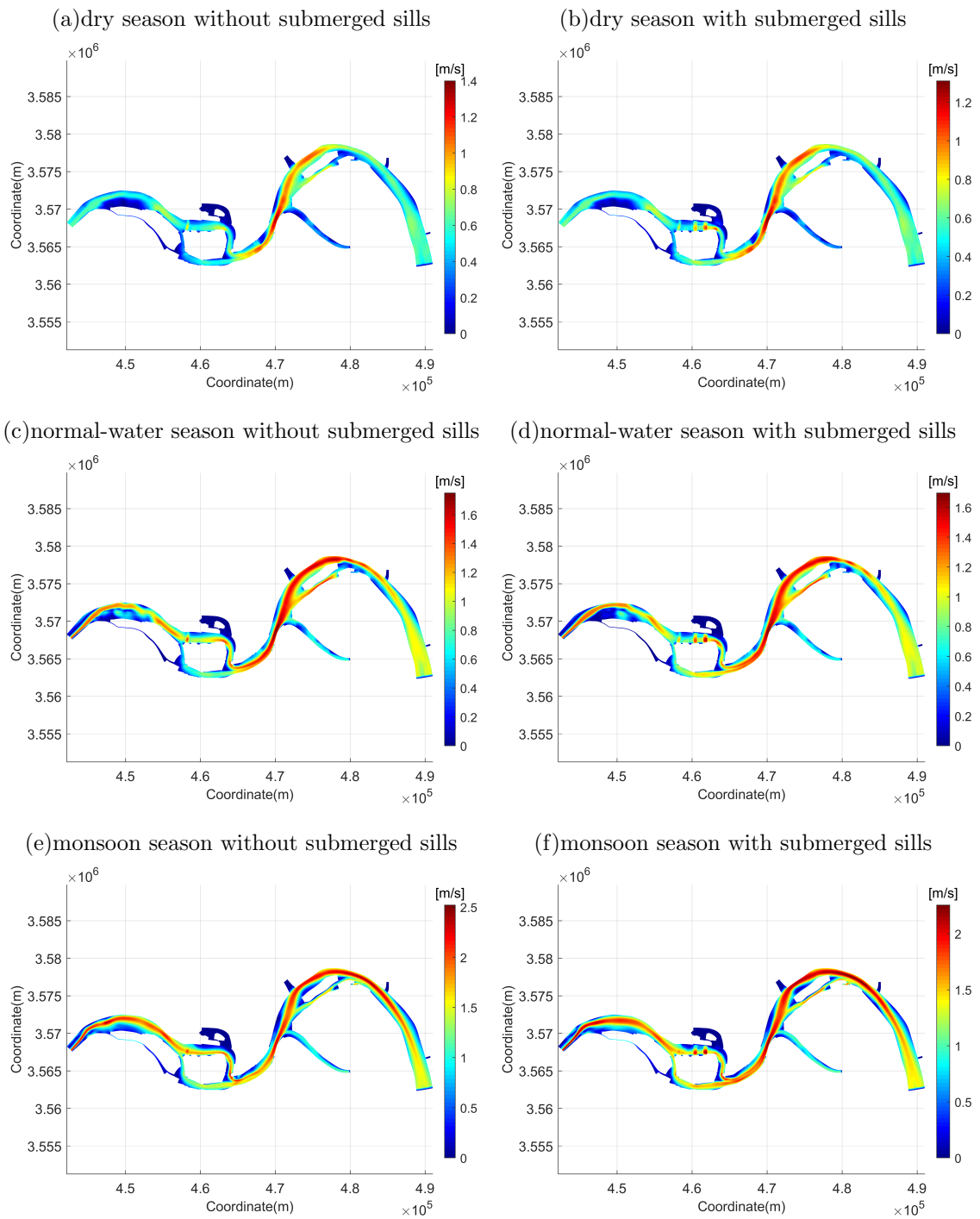


Figure 5.5.1: Distribution map of flow velocity of the three scenarios with- or without- submerged sills during tidal ebbing period.



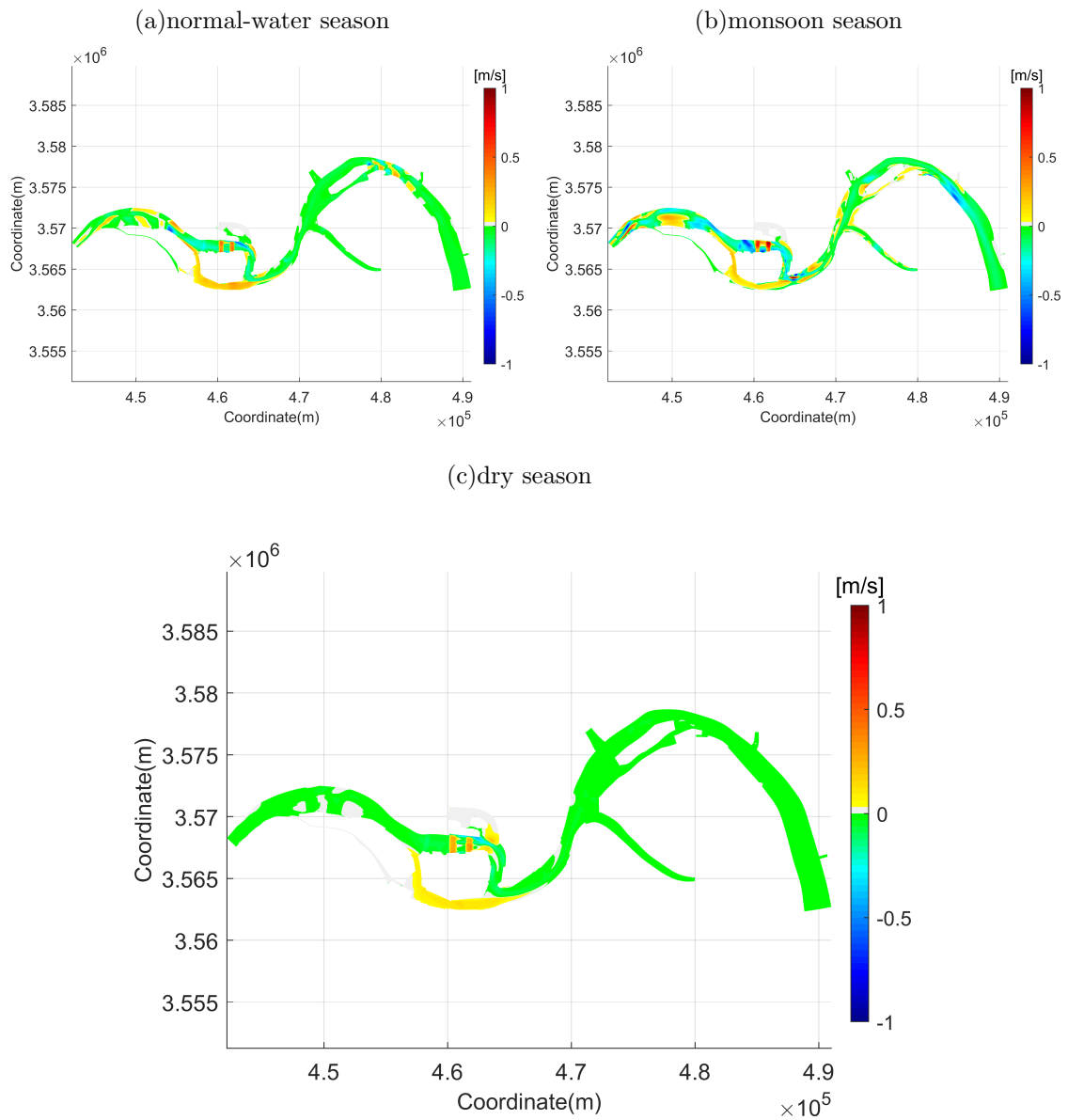


Figure 5.5.2: Differences of flow velocity caused by the submerged sills during the tidal ebbing period in the (a)normal-water (b)monsoon season and (c)dry season

## 5.5.2 Flow velocity impact

Suitability index of V2 and V5 reveal the relation between flow velocity and habitat suitability for YFP corresponding with its movement and feeding component.

It is obvious that the whole reach offers considerably suitable velocity to YFP's for its movement in the dry season while the velocity in the channel downstream the confluence area is less suitable in the normal-water season(See Figure 5.5.3(a) (c)). The sills reduce the suitability of V2 in the 2 branches of HCZD in the dry season(See Figure 5.5.3(b)). In the normal water season, the index of V2 grows in the north branch of HCZD, the bifurcation area upstream the sills and the channel downstream the confluence area under the impact of sills while the south branch of HCZD is downgraded by the sills(See Figure 5.5.3(d)). In the monsoon season, the channel is no longer suitable in terms of flow velocity for YFP's movement(See Figure 5.5.3(e)). The impact of the sills on the SI of V2 is similar as that in the normal-water season. The area of which the SI is effectively improved by the decreased velocity caused by the sills in the north branch extends more upstream. Compared with the changes in the normal water season, the sills improve the channel which close to the downstream boundary of HCZR instead of the channel downstream the confluence area(See Figure 5.5.3(f)).

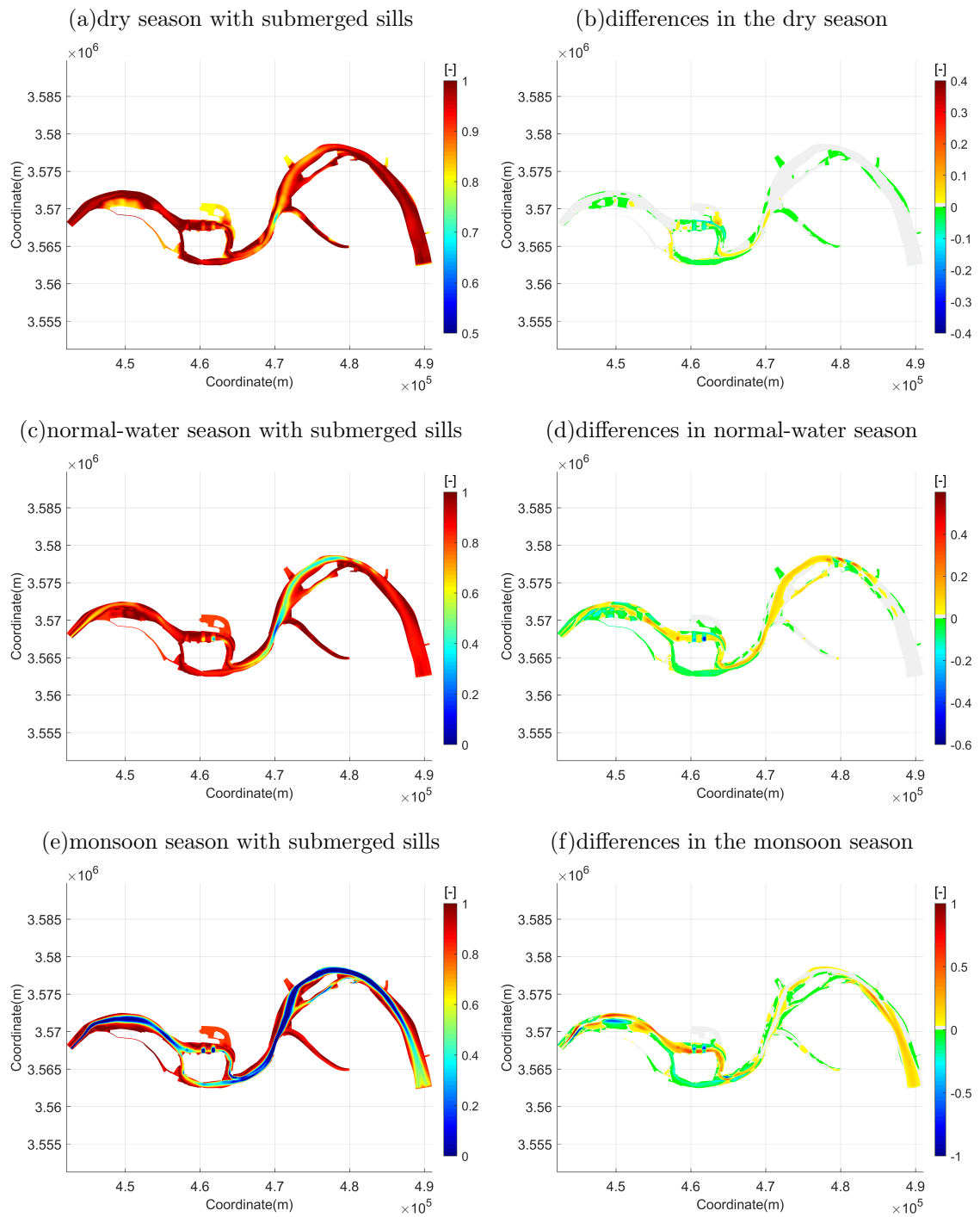


Figure 5.5.3: Distribution map of SI of V2 with submerged sills and differences of SI of V2 caused by the submerged sills in the three scenarios during tidal ebbing period.

For SI of V5, in the dry season, the whole reach except part of the channel downstream the confluence area is perfect considering the suitability of the velocity for YFP's food source. The sills improve the suitability a little in the channel which situates upstream LCZD and north to LCZD. The sills also bring negative changes in the south branch of HCZD.

In the normal-water season, the suitability of velocity is satisfying only in the upstream area of the sills, the side channel close to WFSH, the adjacent area of ZRZD and the floodplain area downstream LCZD. The submerged sills undermines the suitability in the south branch of HCZD a lot while improves that substantially in the upstream area of the sills. Some areas close to the downstream boundary of HCZR are improved by the sills.

In the monsoon season, the channels are almost no longer suitable for YFP's food source in terms of velocity. The sills still benefits the upstream area of the sills less and undermine the suitability in the south branch less compared with the situation in the normal-water season.

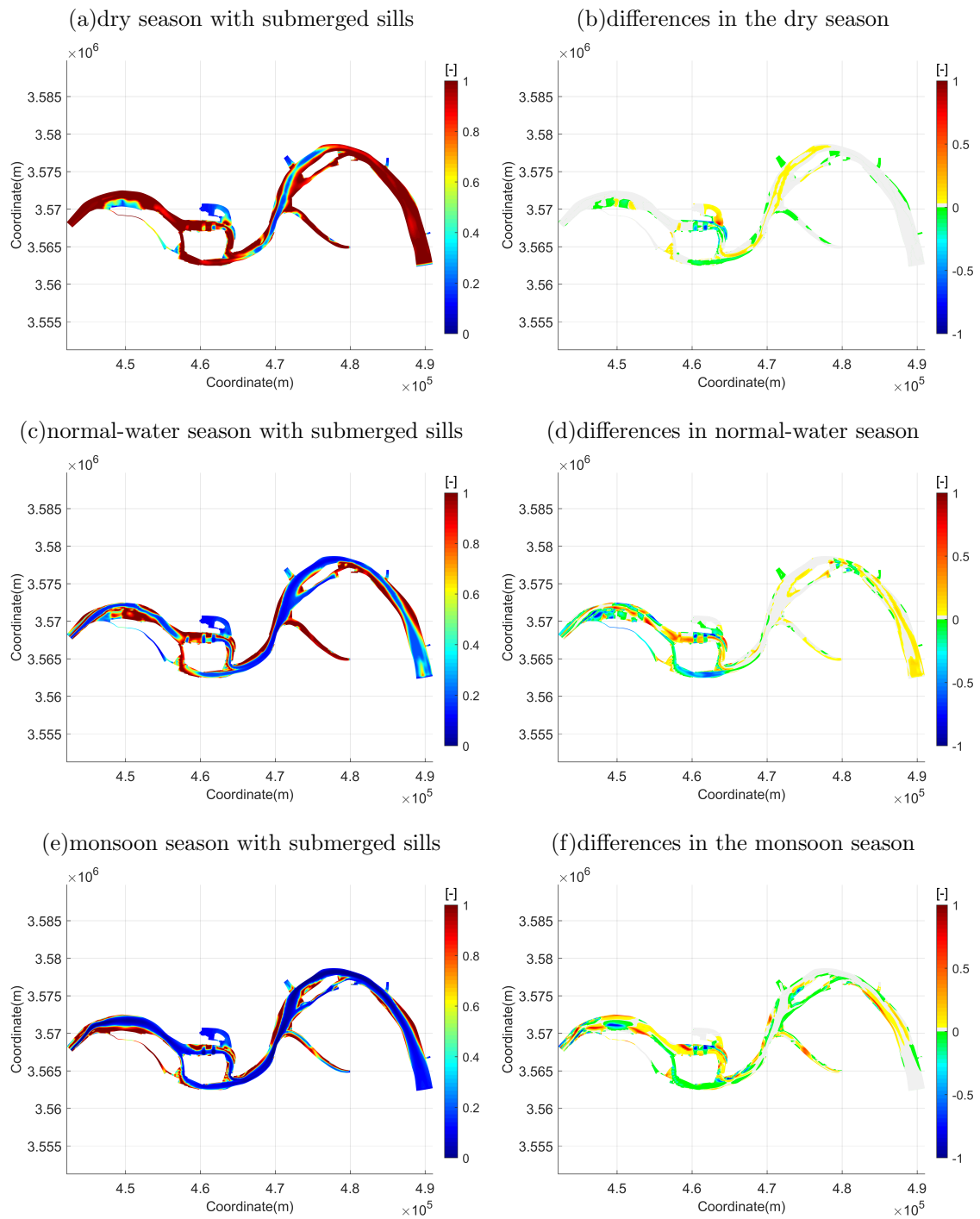


Figure 5.5.4: Distribution map of SI of V5 with submerged sills and differences of SI of V5 caused by the submerged sills in the three scenarios during tidal ebbing period.

### 5.5.3 Changes of habitat area and quality

From Figure 5.5.5, in the dry and normal-water season, the suitability index of YFP's movement considering flow velocity is changed substantially. In the dry season, about half of the medium quality area is converted into high quality area considering SI of V2. In the normal-water season, almost all the extremely low quality area and about half of the low quality area are transferred into higher quality area.

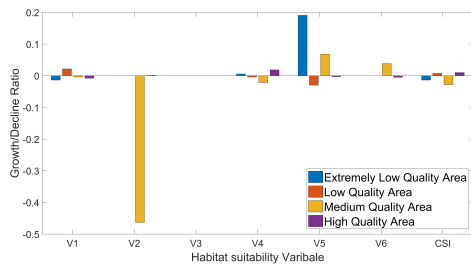
For SI of V5, in the dry season, very little high quality area is downgraded while all the other quality areas extends. In the normal-water season, half of the extremely low quality area and limited fraction of high quality area are converted into low and medium quality area.

From Table.5.2, it can be seen that the habitat area, the effective habitat area and the averaged suitability index of the whole reach all slightly increase after the sills are built in the normal-water and monsoon season, which means the sills bring positive changes on YFP's habitat in HCZR. Although the habitat area and the effective habitat area decrease a little in the dry season, the increasing average suitability index reveals the overall habitat quality of the whole reach is improved by the sills.

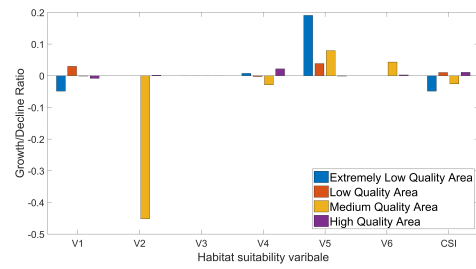
Table 5.2: Changes of habitat area and quality in the tidal ebbing period

Index name	Dry season	Normal-water season	Monsoon season
Habitat area without sills (km <sup>2</sup> )	122.6985	121.3062	113.4299
Habitat area with sills (km <sup>2</sup> )	122.1970	121.4749	116.1154
Difference of habitat area (10 <sup>4</sup> m <sup>2</sup> )	-50.1460	16.8698	268.5563
Weighted usable area without sills (°)	78.2435	68.1276	57.4593
Weighted usable area with sills (km <sup>2</sup> )	78.2000	68.9224	59.6141
Difference of weighted usable area (km <sup>2</sup> )	-0.044	0.795	2.1547
Average suitability index without sills	0.638	0.562	0.507
Average suitability index with sills	0.640	0.567	0.513
Difference of average suitability index	0.002	0.006	0.007
Growth ratio of WUA of high quality area(%)	1.07	-1.27	5.99

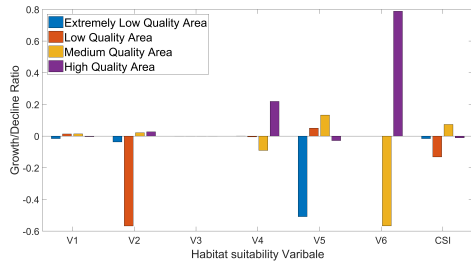
(a) Growth/Decline ratio of habitat areas in the dry season



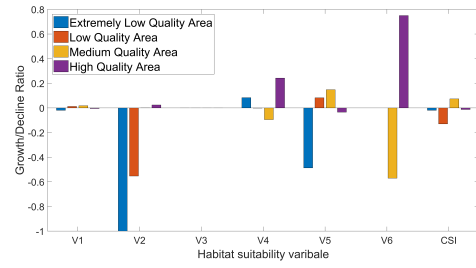
(b) Growth/Decline ratio of effective habitat areas in the dry season



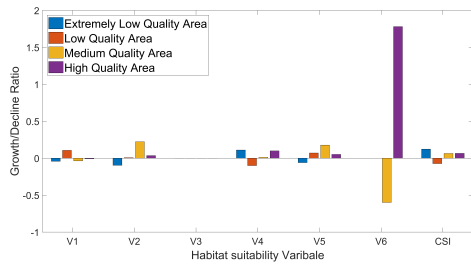
(c) Growth/Decline ratio of habitat areas in the normal-water season



(d) Growth/Decline ratio of effective habitat areas in the normal-water season



(e) Growth/Decline ratio of habitat areas in the monsoon season



(f) Growth/Decline ratio of effective habitat areas in the monsoon season

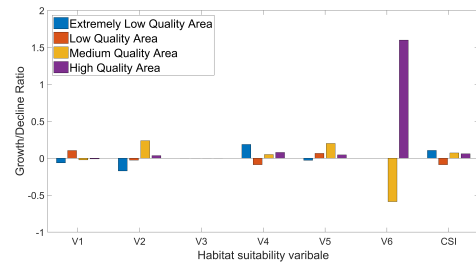


Figure 5.5.5: Growth/Decline ratio of habitat areas and effective habitat areas in the three scenarios caused by the submerged sills during the tidal ebbing period.

# Chapter 6 Discussions

## 6.1 Habitat suitability index model

### 6.1.1 Ecological component

According to Chapter 4.1.1, YFP's reproduction is not included in the HSI model due to lack of quantitative data. Referring to limited information about YFP's reproduction, it is acknowledged that YFP tend to mate, give birth and baby-care in the low-velocity areas. The high quality area of YFP's habitat in this thesis corresponds with this characteristic, which means that the HSI model of YFP can reflect the consideration of YFP's reproduction to a certain extent.

### 6.1.2 Habitat variable

Water depth, flow velocity and substrate type are chosen as habitat variables for YFP's HSI model. Since the 2D numerical model is applied in this thesis, the flow velocity is taken as depth averaged velocity. It is acknowledged that most fish such as common carps and grass carps may swim and feed in the middle layer of water or close to the river bed. Therefore, fish shows preference on the flow velocity close to the river bed rather than depth averaged velocity. Taking depth averaged velocity as the flow velocity in this thesis may cause some deviation of the suitability index of flow velocity.

The most suitable substrate for YFP and its bait fish is regarded as the soil with small grain size in this thesis because this small-grain soil are beneficial for nutrient retention and vegetation growth, which is favorable for bait fish's growth. It is acknowledged that most fish stings their eggs to the soil with large grain size such as gravel, which means this soil are suitable for bait fish's spawning. In the Yangtze river, the middle section rather than the lower section is the main reach for fish's spawning. Therefore, in this thesis, bait fish's spawning is not taken into consideration when establishing the SI curve of substrate type regarding of YFP's food source. Not considering fish's spawning at all will lead to a certain deviation in the results. How to trade off the weights of fish's spawning and growth when establishing the SI curve of substrate type in the lower Yangtze river needs more local ecological experiments.



# Chapter 7 Conclusions and Recommendation

## 7.1 Conclusions

In order to conclude on the findings of this thesis, the previous formulated research sub-questions and main question are stated again and will be answered accordingly.

*(1) What is the preference of Yangtze finless porpoise towards its habitat? (Which habitat variables are important and what is the suitable range of each variable for YFP?)*

Habitat suitability index model is such a effective and superior tool for solving the above research question. After investigating YFP's ecological habit, especially its main behaviors, feeding choice and characteristics of habitat, water level, flow velocity and substrate type are regarded as the most vital habitat variables for its physical habitat. Considering YFP's movement, combining with hydrological and hydrodynamics data of main reserves of YFP in middle and lower section of Yangtze river, 1.5-35m water depth, 0-1.8m/s flow velocity and substrate with small or medium grain size are favourable for YFP's movement. When considering YFP's feeding, Cyprinidae fish is chosen as YFP's main food source, and 1-6m water depth, 0-2m/s flow velocity and substrate with small grain size are suitable for YFP's food source growth. The suitability index curves of each habitat variable are derived from literature reviewing and inquiring biologists, which reveals YFP's more detailed preference towards its physical habitat variable.

*(2) What morphology and hydrodynamics which will affect the Yangtze finless porpoise's habitat will be changed by the two submerged sills? (How will the submerged sills change the habitat variables mentioned in 1st research question?)*

According to the answer of Research question 1, water depth and flow velocity are chosen to represent the changes of local hydrodynamics conditions while bed level change and substrate type change represent the morphology change. 3 scenarios based on upstream discharge are created in order to distinguish the changes caused by the sills in different water seasons.

**Water depth:** The changes of water depth are mainly caused by bed level change and backwater effect. In the dry season, both effects are weak which make the water depth almost remain the same. In the normal-water season, the effects are relatively enhanced, leading to about 3m

growth of water depth downstream the sills. In front of the sills, the water depth does not change much, which can be explained by the balance of the sedimentation and the backwater effect. In the monsoon season, the water depth increases about 10m in front of the sills due to less sedimentation there. In the bifurcation area of HCZD, the water depth in the southern part of channel grows while it declines in the northern part. It is due to the sills block the flow in the north branch while induce more water flux through the south branch of HCZD, which is enhanced by the reduced bed elevation in the southern part of channel. The water depth increases much in the south branch of HCZD and the area downstream of sills which means the bed elevation is reduced due to additional erosion occurring there.

The tidal range in HCZR is less than 1.2m. Compared with the local water depth(around 20m-30m), tidal effect does not change the water depth substantially, in other words, the water depth does not show great differences during a tidal cycle.

**Flow velocity:** From the view of the whole reach, the reduction of velocity caused by the sills in the channel is more than that in the floodplain. The velocity change highly depends on different upstream discharge in different scenarios.

In the dry season, the reduction caused by the submerged sills on flow velocity is limited. The velocity in most area of channel decreases less than 0.05m/s while it increases less than 0.05m/s in the most floodplain area. The velocity change is more substantial when approaching to the submerged sills. In the bifurcation area west to the sills and the north branch of HCZD, the velocity in the channel declines about 0.1m/s while it grows about 0.08m/s in the floodplain. Downstream of 2 submerged sill, the velocity increases about 0.15m/s because the upstream discharge is blocked by the sill and the blocking creates large circulation with combined effect of the tidal current from downstream. In the south branch of HCZD, the velocity increases more than 0.08m/s in the channel and reduces very little in the floodplain, which reveals that the engineering aim of submerged sills is now preliminarily realized—improving the south channel's navigation condition. In the confluence area, the velocity growth occurs in the southern floodplain, which means the main stream flowing direction changes a little due to the faster flow coming from the north branch.

In the normal-water season, all the velocity changes mentioned above are about 4 times of those in the dry season. It is noteworthy that the velocity in the bifurcation area decreases both in the channel and the floodplain, which reveals that the backwater effect dominates now. The flow substantially accelerates in the south branch, meaning the effectiveness of sills is now further enhanced.

In the monsoon season, velocity changes dramatically in the whole reach. At the entrance of the reach, the velocity changes are obvious because the channel is now moved south. In Liuwei bending segment, the velocity declines about 0.65m/s in the channel and increases about 0.55m/s in the floodplain. In the south branch of HCZD, the velocity keeps increasing and its growth is

about 0.2-0.3m/s now while the flow decelerates in the north branch except the over-sills area, which reveals that the engineering aim of submerged sills is now fully realized.

The flow velocity during the tidal ebbing period increases about 1m/s, 0.8m/s and 0.5m/s in the dry, normal-water and monsoon season respectively compared with that in the flooding period. In the normal-water and monsoon season the differences of velocity caused by the sills are highly similar as that in tidal flooding period because the tidal prism is very small compared with the upstream discharge in the 2 scenarios. In the dry season, in the whole reach except the south branch of HCZD, the velocity decreases, which is different from that during tidal flooding period.

**Substrate type:**In the dry season, the submerged sills do not change the substrate type in the whole reach. In the normal-water season, soil with smaller grain size are retained due to the declining bed shear stress in most areas of the reach except the western part of the south branch of HCZD. The domain where more soil with smaller grain size can be retained extends to the whole reach in the monsoon season. The substrate of the whole reach consists of the mixture of sand and silt in the situation without the submerged sills while the sills lead much more silt to be retained in the whole reach.

The tidal effect will not change the substrate type in a tidal cycle.

*(3) How the changed morphology and hydrodynamics affect the Yangtze finless porpoise's living? (How to evaluate the changes mentioned in 2nd research question?)*

Composited suitability index(CSI) reflects the overall evaluation of YFP's habitat quality. In all 3 scenarios, adjacent areas of ZRZD, floodplains of HCZ north branch, floodplains of the section from Dagang to the tail of LCZD, and the side channel next to WFSH are the most suitable habitats for YFP. The sills in the dry season slightly change CSI in both branches of HCZD. Part of the bifurcation area and the entrance of the pool north to the 2 sill are upgraded while the floodplain of south branch of HCZD is deteriorated. In the normal-water season, adjacent areas of LCZD are improved by the sills with the CSI rising about 0.1, especially the upstream areas. Both the 2 branches of HCZD are downgraded under the impact of the sills. In the monsoon season, the significant improvement of the sills occurs in the bifurcation area of HCZD while both the 2 branches of HCZD are undermined. Other improvements caused by the sills occur in the side channel next to WFSH as well as in the upstream area of LCZD.

In all 3 scenarios, the sills offer limited potential habitat area for YFP, slightly extend the high-quality habitat area and improve the existing habitat. In conclusion, the submerged sills bring limited but beneficial changes on the physical habitat of Yangtze fineless porpoises in Hechangzhou reach.

## 7.2 Recommendation

From the conclusions drawn in the previous section, several recommendations are made for future endeavors.

The numerical model only incorporates limited amount of processes that are present in Hechangzhou reach. For instance, processes that influence depositions, such as consolidation and vegetation's effects were also not included. As these are crucial for morphology changes, it has to be determined how large this effect is on long-term natural development.

Habitat suitability index model is applied in this thesis based on literature reviewing and expert's opinion. Conducting local ecological experiments is recommended in order to further develop and verify the HSI model of Yangtze finless porpoises. More ecological component such as reproduction and baby-caring, could be included in the model after obtaining data of suitable ranges of different variables from ecological experiments. More habitat variables such as turbidity, temperature can be judged whether they can be taken into account in the HSI model after collecting more data from ecological experiments concerning on the sensitivity of YFP to these habitat variables.

# Appendix A Related graphs

## A.1 Hydrodynamic conditions

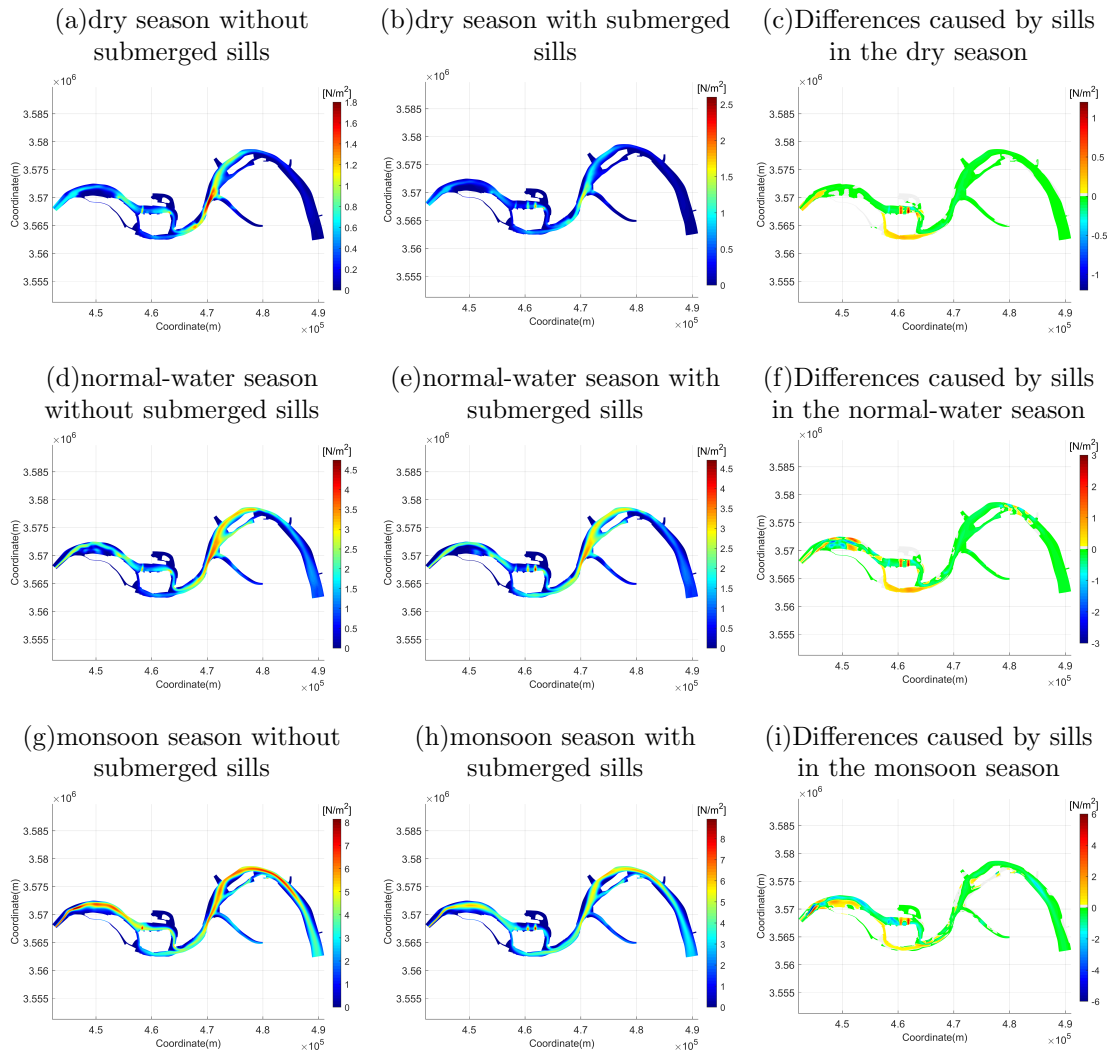


Figure A.1.1: Distribution map of bed shear stress in the three scenarios with- or without-submerged sills and the distribution difference caused by the submerged sills.

## A.2 Morphology

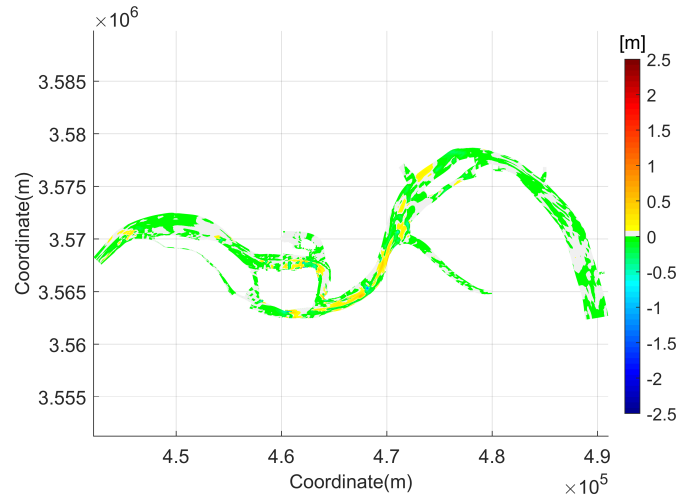


Figure A.2.1: Differences of bed level change caused by the submerged sills in the dry season.

## A.3 HSI model results

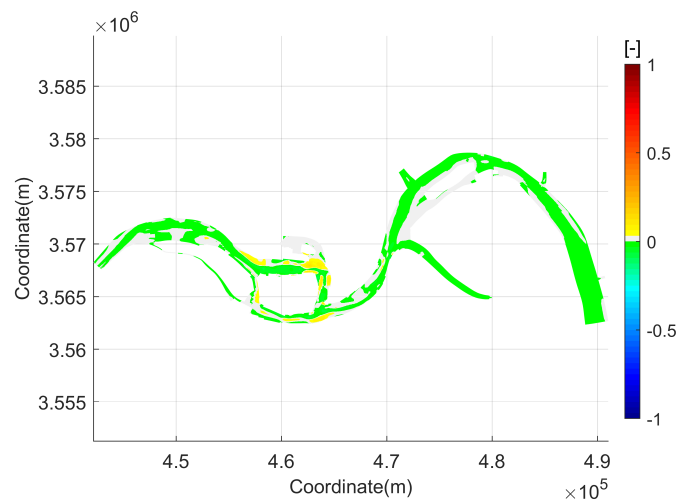


Figure A.3.1: Differences of SI of V2 caused by the submerged sills in the dry season.

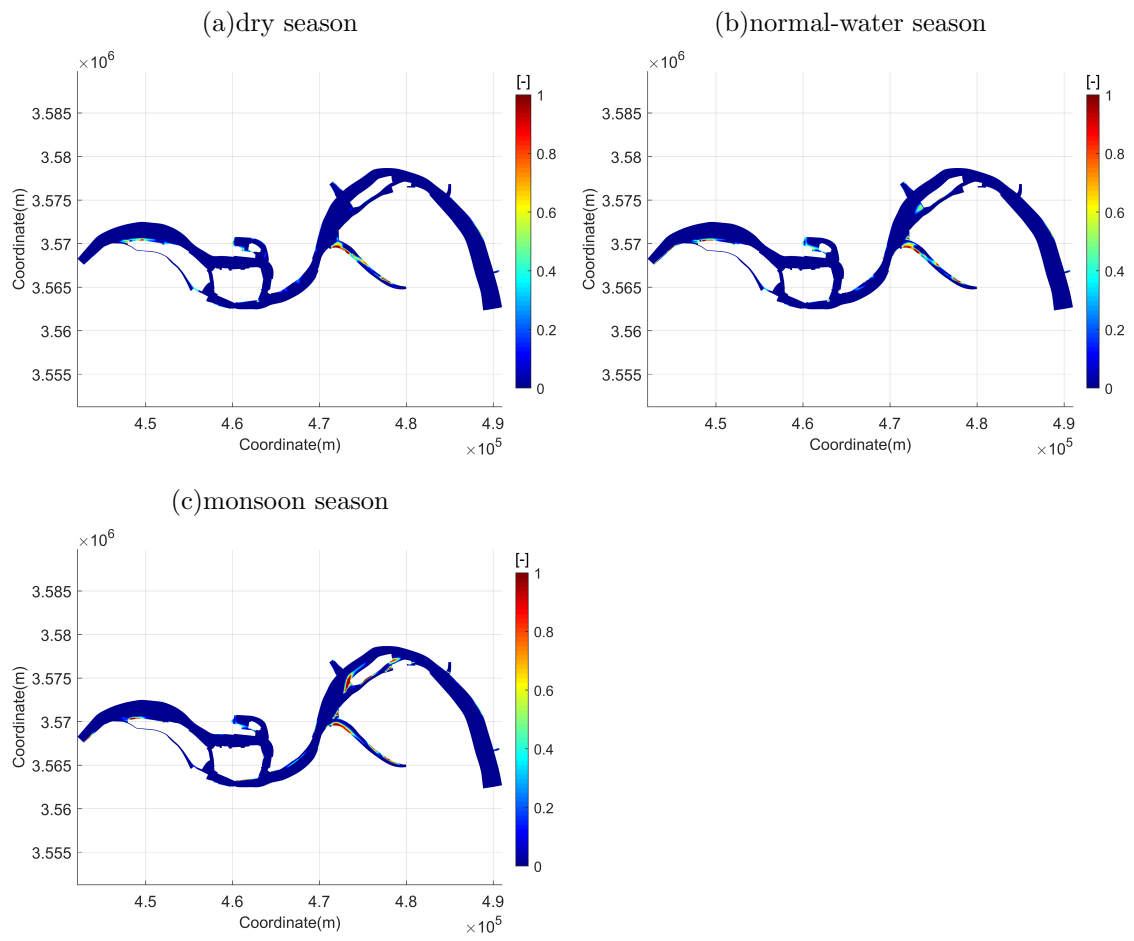


Figure A.3.2: Distribution map of SI of V4 without submerged sills in the three scenarios.

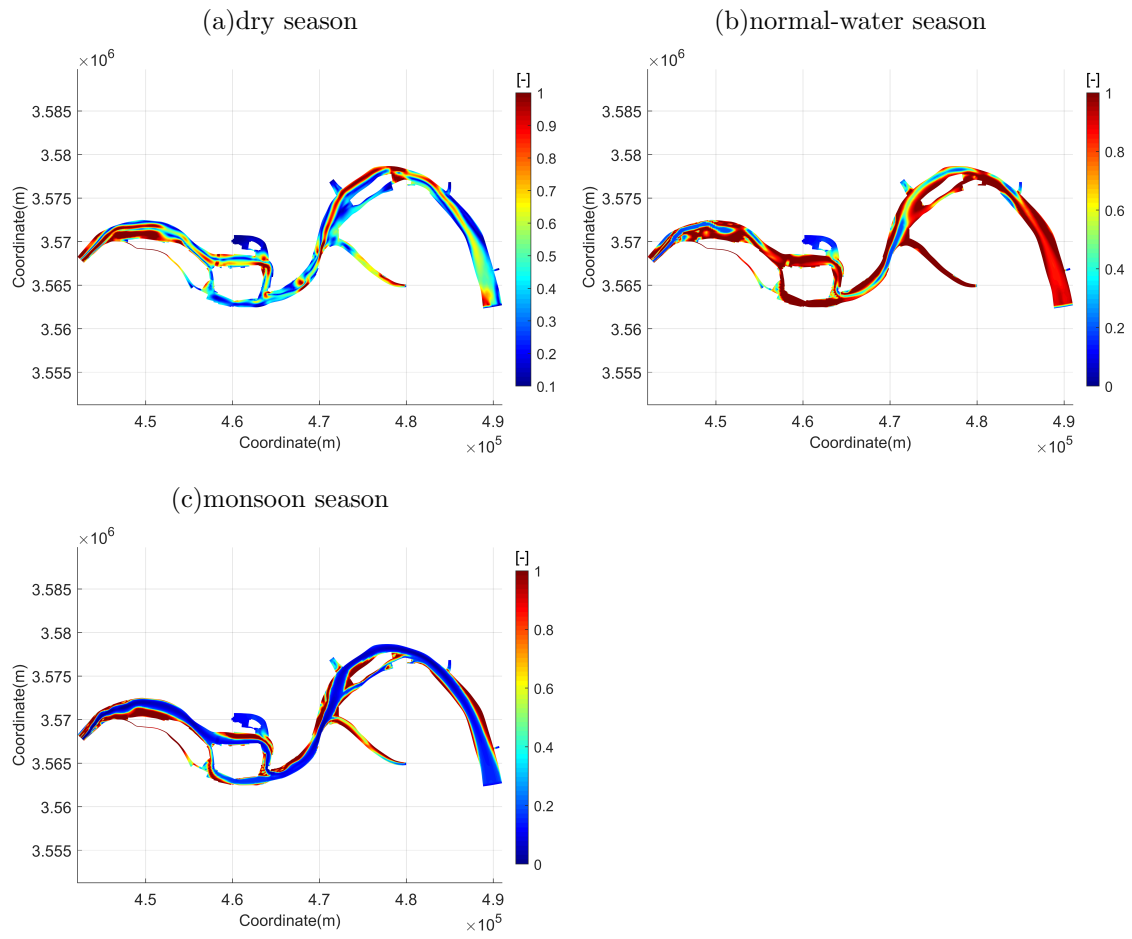


Figure A.3.3: Distribution map of SI of V5 without submerged sills in the three scenarios.



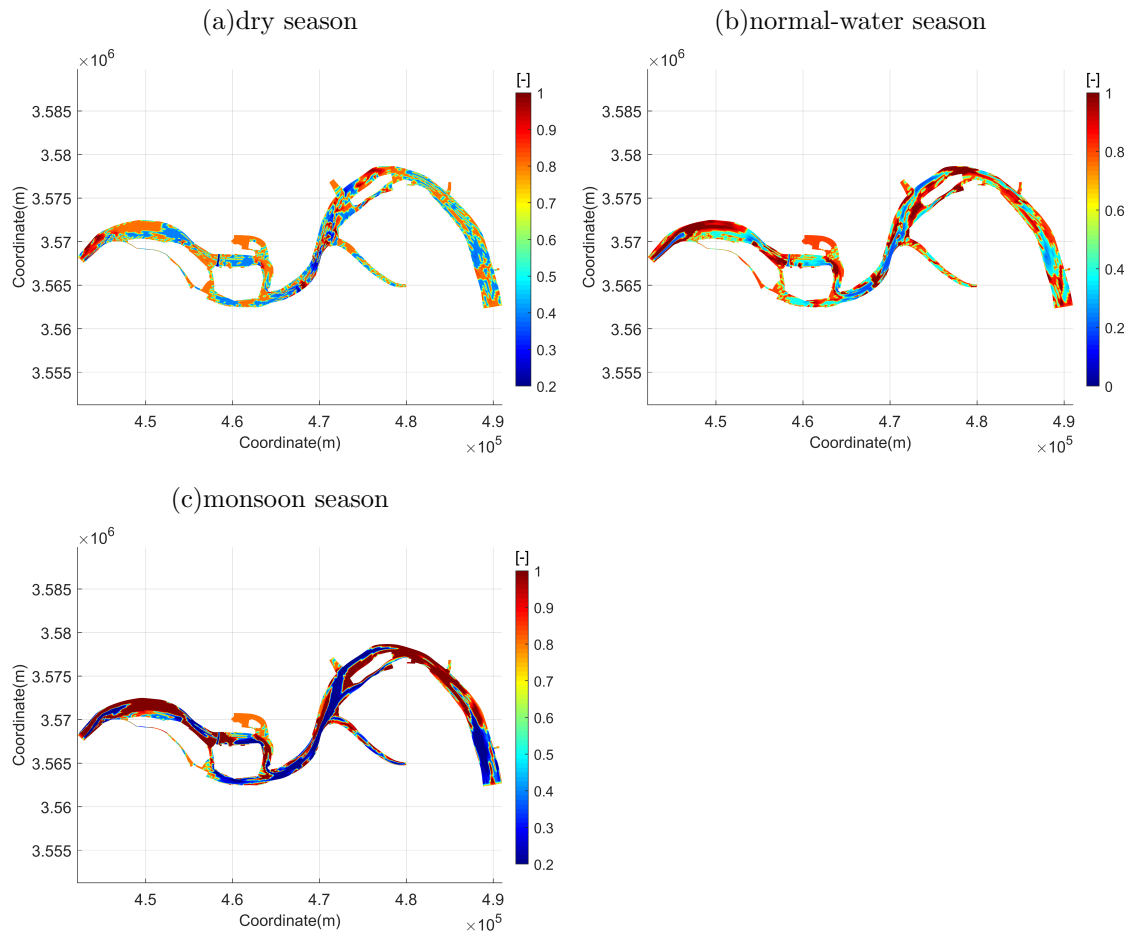


Figure A.3.4: Distribution map of SI of V6 without submerged sills in the three scenarios.

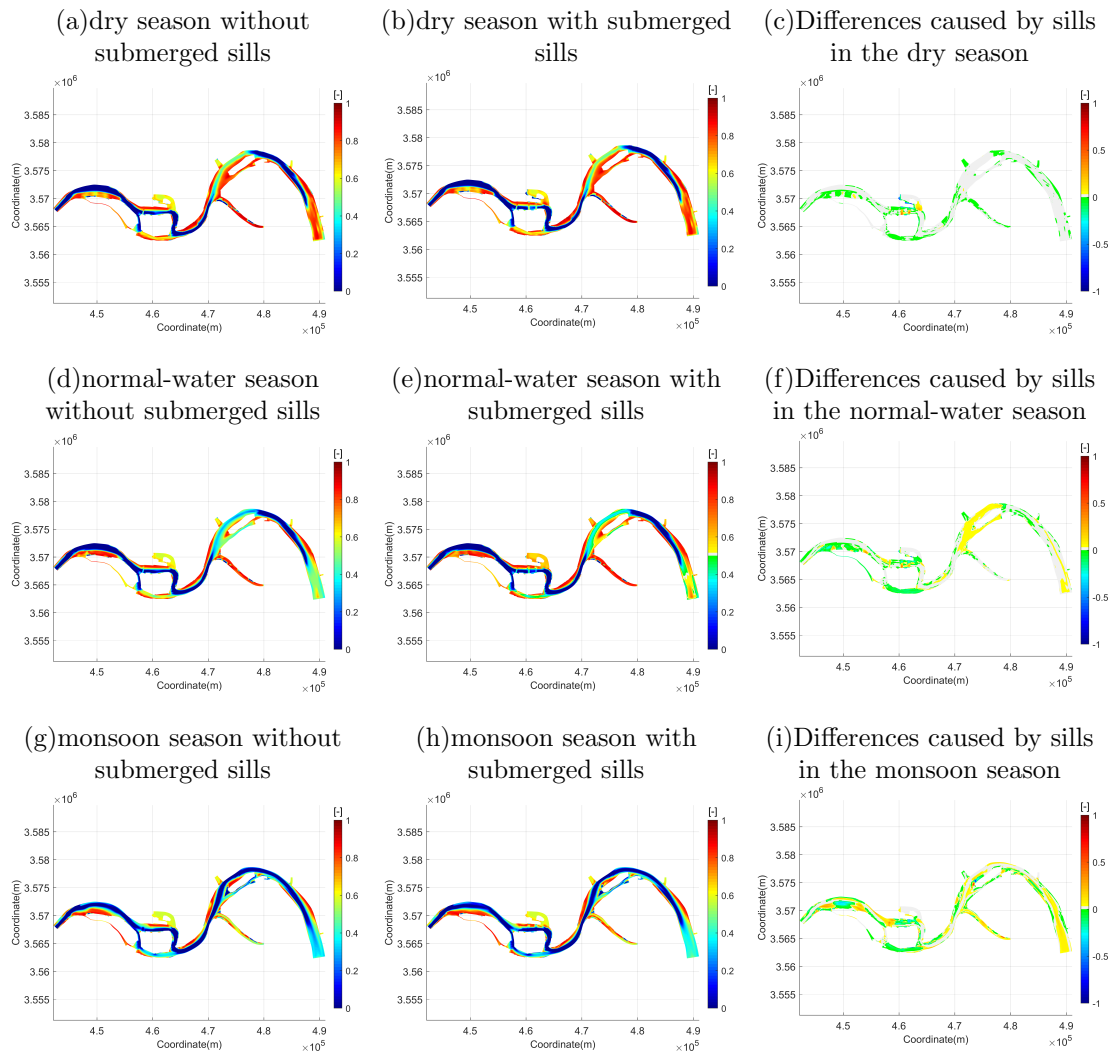
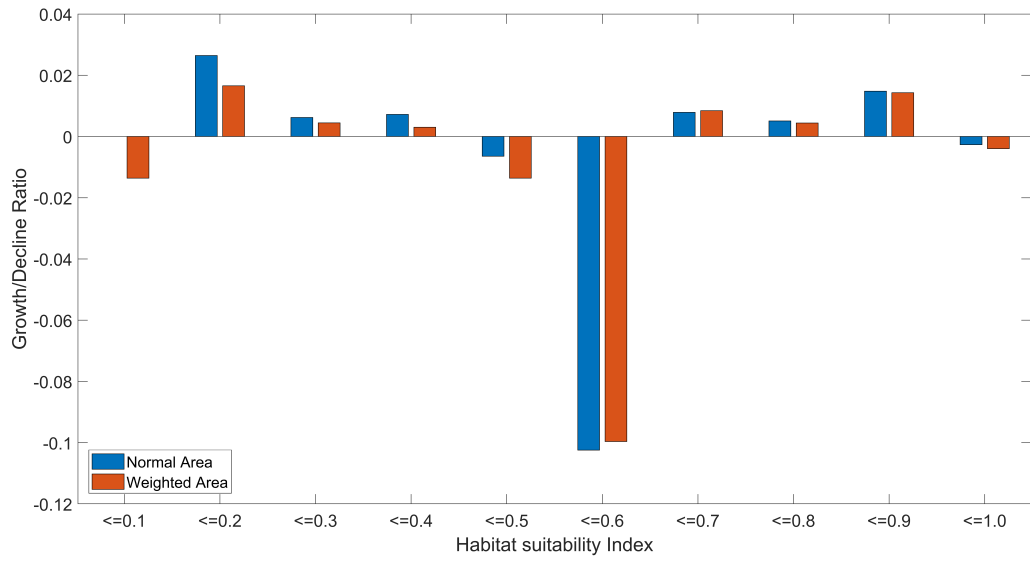
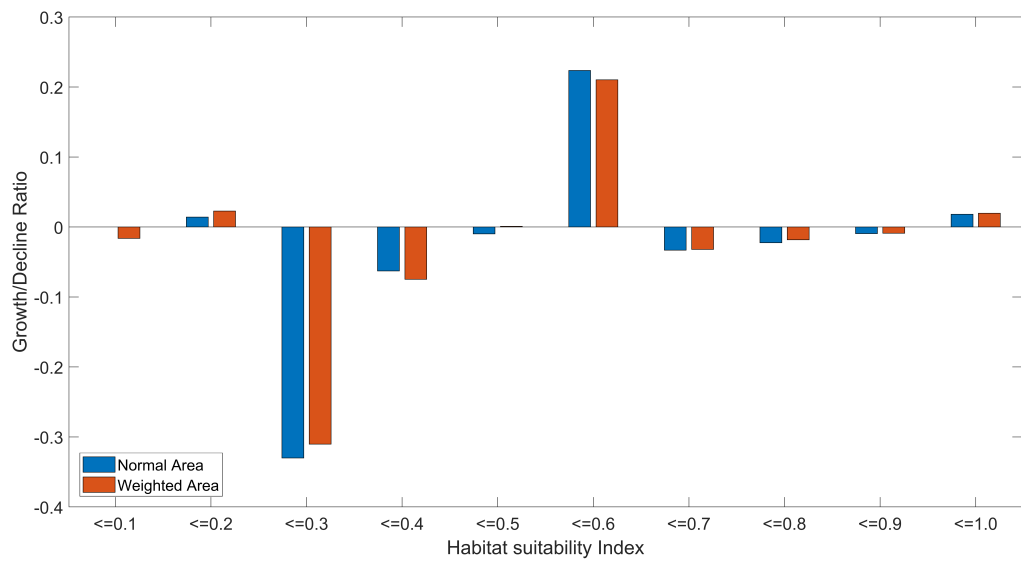


Figure A.3.5: Distribution map of CSI with- or without- submerged sills and the distribution difference caused by the submerged sills in the three scenarios during tidal ebbing period.

(a) dry season



(b) normal water season



(c) monsoon season

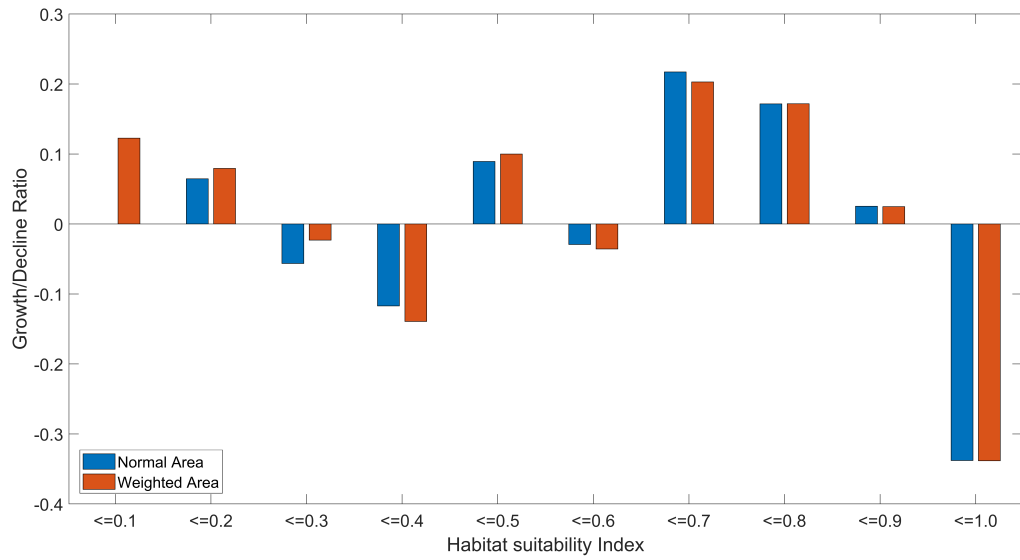


Figure A.3.6: The growth/decline ratios of habitat areas or weighted areas (product of CSI multiplied by area) with the submerged sills during tidal ebbing period in the (a) dry season (b) normal-water season and (c) monsoon season.

# Bibliography

- Ahmadi-Nedushan, B., St-Hilaire, A., Bérubé, M., Robichaud, É., Thiémonge, N., and Bobée, B. (2006). A review of statistical methods for the evaluation of aquatic habitat suitability for instream flow assessment. *River Research and Applications*, 22(5):503–523.
- Ai, W. (2018). *Response of Riverbed Evolution to Hydrosediment Dynamics of River Basin and Tidal Changes in the Tidal Reaches of the Yangtze River*. PhD thesis, East China Normal University.
- Allen, J., Somerfield, P., and Gilbert, F. (2007). Quantifying uncertainty in high-resolution coupled hydrodynamic-ecosystem models. *Journal of Marine Systems*, 64(1-4):3–14.
- Bank, W. (2017). World development indicators database [data file].
- Brooks, R. P. (1997). Improving habitat suitability index models. *Wildlife Society Bulletin (1973-2006)*, 25(1):163–167.
- Burgman, M. A., Breininger, D. R., Duncan, B. W., and Ferson, S. (2001). Setting reliability bounds on habitat suitability indices. *Ecological Applications*, 11(1):70–78.
- Chen, P., Liu, R., Wang, D., and Zhang, X. (1997). Biology, rearing and conservation of baiji. *Science, Beijing*.
- Chou, W.-C. and Chuang, M.-D. (2011). Habitat evaluation using suitability index and habitat type diversity: a case study involving a shallow forest stream in central taiwan. *Environmental monitoring and assessment*, 172(1-4):689–704.
- Ding, W., Renjun, L., Zhang, X., Jian, Y., Wei, Z., Zhao, Q., and Wang, X. (2000). Status and conservation of the yangtze finless porpoise. *Biology and Conservation of Freshwater Cetaceans in Asia. IUCN Species Survival Commission, Gland, Switzerland*, pages 81–85.
- Dong, H. G. et al. (2000). Investigation and evaluation of ecological environment on living ground for lipotes vexillifer in anhui section of the yangtze river [j]. *CHINESE QHINGHAI JOURNAL OF ANIMAL AND VETERINARY SCIENCES*, 4.
- Dong, S. (2009). *Studies on distribution and movement pattern of Yangtze finless porpoise in Hukou area by acoustic data loggers*. PhD thesis, Master Dissertation, University of Chinese Academy of Sciences, Beijing, China.
- Dong, S.-Y., Dong, L.-J., Li, S.-H., Kimura, S., Akamatsu, T., et al. (2012). Effects of vessel traffic on the acoustic behavior of yangtze finless porpoises (*neophocaena phocaenoides asiae-orientalis*) in the confluence of poyang lake and the yangtze river using fixed passive acoustic observation methods. *Acta Hydrobiologica Sinica*, 36(2):246–254.

- Edwards, E. A. and Twomey, K. (1982). *Habitat suitability index models: common carp*. Western Energy and Land Use Team, Office of Biological Services, Fish and . . . .
- Fish, U., Service, W., et al. (1980). Habitat evaluation procedures, ecological services manual 102. *Department of Interior, Fish and Wildlife Service, Division of Ecological Services, Washington, DC, USA*, page 130.
- Foote, A. D., Osborne, R. W., and Hoelzel, A. R. (2004). Whale-call response to masking boat noise. *Nature*, 428(6986):910–910.
- Gao, A. (1995). Geographical variation of external measurements and three subspecies of neophocaena phocaenoides in chinese waters. *Acta Theriol Sin.*, 15:81–92.
- Hao, Y., Wang, D., and Zhang, X. (2006). Review on breeding biology of yangtze finless porpoise (neophocaena phocaenoides asiaeorientalis). *Acta theriologica sinica*, 26(2):191–200.
- Hardy, T. B. and Addley, R. C. (2001). Vertical integration of spatial and hydraulic data for improved habitat modelling using geographic information systems. *IAHS-AISH PUBL.*, (266):65–76.
- Im, D., Kang, H., Kim, K.-H., and Choi, S.-U. (2011). Changes of river morphology and physical fish habitat following weir removal. *Ecological Engineering*, 37(6):883–892.
- IUCN, I. (1996). Red list of threatened animals. *IUCN, Gland*.
- Jefferson, T. A. and Wang, J. Y. (2011). Revision of the taxonomy of finless porpoises (genus neophocaena): the existence of two species. *Journal of Marine Animals and Their Ecology*, 4(1):3–16.
- Jefferson, T. A., Webber, M. A., and Pitman, R. L. (2011). *Marine mammals of the world: a comprehensive guide to their identification*. Elsevier.
- Jian-jun, Z. (2016). Protective measures for finless porpoises in phase ii project of 12.5 m deepwater channel from nanjing in the yangtze river. *China Harbour Engineering*, (2016):20–23.
- Jianhua, M. (2010). Situation of water resources in yangtze river basin and countermeasures for sustainable utilization. *Yangtze River*, 41(12):1–6.
- Jin, X., Huang, Y., Yang, W., and Chen, L. (2009). Analysis of impact of future climate change on water resources in yangtze river basin. *Yangtze River*, 40(8):35–38.
- Karr, J. and Dudley, D. (1978). Biological integrity of a headwater stream: evidence of degradation, prospects for recovery. *Environmental impact of land use on water quality: final report on the Black Creek Project—supplemental comments*. US Environmental Protection Agency, Chicago, Ill. EPA-905/9-77-007-D, pages 3–25.

- Kasuya, T. (1999). Finless porpoise, *neophocaena phocaenoides* (g. cuvier, 1829). *Handbook of marine mammals, the second book of dolphins and the porpoises*, 6:411–442.
- Leclerc, M., Boudreault, A., Bechara, T. A., and Corfa, G. (1995). Two-dimensional hydrodynamic modeling: a neglected tool in the instream flow incremental methodology. *Transactions of the American Fisheries Society*, 124(5):645–662.
- LIU, X.-b., LIN, M.-s., and LI, Z.-q. (2011). Channel evolution and regulation of zhenjiang-yangzhou reach of the lower yangtze river. *Journal of Yangtze River Scientific Research Institute*, (11):2.
- Malakoff, D. (2001). A roaring debate over ocean noise.
- Mei, Z., Huang, S.-L., Hao, Y., Turvey, S. T., Gong, W., and Wang, D. (2012). Accelerating population decline of yangtze finless porpoise (*neophocaena asiaeorientalis asiaeorientalis*). *Biological Conservation*, 153:192–200.
- Nash, J. E. and Sutcliffe, J. V. (1970). River flow forecasting through conceptual models part i—a discussion of principles. *Journal of hydrology*, 10(3):282–290.
- Orth, D. J. (1987). Ecological considerations in the development and application of instream flow-habitat models. *Regulated rivers: research & management*, 1(2):171–181.
- Poff, N. L. and Ward, J. (1990). Physical habitat template of lotic systems: recovery in the context of historical pattern of spatiotemporal heterogeneity. *Environmental management*, 14(5):629.
- Raleigh, R. F., Zuckerman, L. D., and Nelson, P. C. (1984). *Habitat suitability index models and instream flow suitability curves: brown trout*. Western Energy and Land Use Team, Division of Biological Services, Research . . . .
- Renjun, C. P. L. P. L. and Kejie, L. (1986). Studies on the rearing of lipotes [j]. *Acta Hydrobiologica Sinica*, 2.
- Roelvink, J. (2006). Coastal morphodynamic evolution techniques. *Coastal engineering*, 53(2-3):277–287.
- Salaam, D. (2017). National bureau of statistics. *NBS (National Bureau of Statistics) and MOFP*.
- Sawyer, A. M., Pasternack, G. B., Moir, H. J., and Fulton, A. A. (2010). Riffle-pool maintenance and flow convergence routing observed on a large gravel-bed river. *Geomorphology*, 114(3):143–160.
- Shuwei, Z., Heqin, C., Shuaihu, W., Shengyu, S., Wei, X., Quanping, Z., and Yuehua, J. (2017). Morphology and mechanism of the very large dunes in the tidal reach of the yangtze river, china. *Continental Shelf Research*, 139:54–61.

- Statzner, B., Gore, J. A., and Resh, V. H. (1988). Hydraulic stream ecology: observed patterns and potential applications. *Journal of the North American benthological society*, 7(4):307–360.
- SUITABILITY, I. F. (1986). Habitat suitability index models: And instream flow suitability curves: Shortnose sturgeon.
- Tan, Y., Wang, Y., Li, J., and Liu, M. (2011). Simulation research on fish habitats in reducing reach of jinping dahewan in yalong river. *Water Resour Power*, 29(3):40–43.
- Terrell, J. W. (1982). *Habitat suitability index models: Appendix A. Guidelines for riverine and lacustrine applications of fish HSI models with the Habitat Evaluation Procedures*. Western Energy and Land Use Team, Office of Biological Services, Fish and . . . .
- Wang, D. (2009). Population status, threats and conservation of the yangtze finless porpoise. *Chinese Science Bulletin*, 54(19):3473.
- Wang, D., Wang, K., Zhang, G., et al. (1997). Observations on behaviors of the changjiang finless porpoise in a net circle in river and in pools. *Acta Hydrobiologica Sinica*, 21(4):306–311.
- Wang, D., Zhang, X., and Liu, R. (1998). Conservation status and its future of baiji and yangtze finless porpoise in china. *Ecology and environmental protection of large irrigation projects in Yangtze River in 21st century*, pages 218–226.
- WANG, J., DONG, M.-l., FANG, S.-g., et al. (2003). Discussion on stress factors and conservation strategy of anhui tongling river dolphin nature reservation. *Journal of Zhejiang Ocean University*, (1):6.
- Wang, J., Fan, H., Zhu, L., and Ying, H. (2014). Hydrodynamic improvement measures of channel regulation of the right branch of hechangzhou waterway. *Port & Waterway Engineering*, 9:11–17.
- Wang, P. (1992). On the taxonomy of the finless porpoise in china. *Fisheries Science*, 11(6):10–14.
- WANG, Q.-g., LI, J., LI, K.-f., and DENG, Y. (2009). Effectiveness of hydraulic ecological rehabilitation measures in flow reduced river reaches [j]. *Journal of Hydraulic Engineering*, 6.
- WANG, X.-g. and YAN, Z.-m. (2008). Effect of hydraulic characteristics of confluent channel on physical habitat for fish communities [j]. *Journal of Tianjin University*, 2.
- Wei, Z., Wang, D., Zhang, Q., Wang, K., and Kuang, X. (2002). Population size, behavior, movement pattern and protection of yangtze finless porpoise at balijiang section of the yangtze river. *Resources and Environment in the Yangtze Valley*, 11(5):427–432.
- Wei, Z., Wang, D., Zhang, X., Wang, K., and Gao, D. (2004). Aggregation and spatio-temporal distribution of the yangtze finless porpoise *neophocaena phocaenoides asiaorientalis* in tian-e-zhou. *Acta Hydrobiologica Sinica*, 28(3):247–252.



- Wei, Z., Zhang, X., Wang, K., Zhao, Q., Kuang, X., Wang, X., and Wang, D. (2003). Habitat use and preliminary evaluation of the habitat status of the yangtze finless porpoise in the balijiang section of the yangtze river, china. *Acta Zoologica Sinica*, 49(2):163–170.
- Wen-hua, J. (2000). Observation on the group of the changjiang finless porpoise and conserved in semi-nature conditions. *Journal of Anhui University (Natural Sciences)*, (4):19.
- Wu, M., Chen, L., Yan, L., Deng, X., and He, X. (2006). Analysis of effect of a doption of fries by filling with river flows on water quality and sediment of tianezhou wetland. *Engineering Journal of Wuhan University*, 39(3):36–40.
- Xian-feng, J. G.-z. Z. and Jian-bo, C. (2001). Influence of yangtze flood control projects on rare aquatic animals and fishes. *Yangtze River*, (7):13.
- Xiao, W. and Zhang, X. (2002). Distribution and population size of yangtze finless porpoise in poyang lake and its branches. *Acta Theriologica Sinica*, 22(1):7–14.
- Xiong, Y. and Zhang, X. (2011). Population size, distribution and activities of the yangtze finless porpoise in the yangtze xinluo baui national nature reserve, hubei. *Resources and Environment in the Yangtze Basin*, 20(2):143–149.
- Yang, J. and Chen, P. (1996). Movement and behavior of finless porpoise (*neophocaena phocaenoides cuvier*) at swan oxbow, hubei province. *Acta Hydrobiologica Sinica*, 20(1):32–40.
- Yang, J., Wan, X., Zeng, X., Zheng, J., Han, Y., Fan, F., Hao, Y., Wang, K., Mei, Z., and Wang, D. (2019). A preliminary study on diet of the yangtze finless porpoise using next-generation sequencing techniques. *Marine Mammal Science*, 35(4):1579–1586.
- Yang, J., Xiao, W., Kuang, X., Wei, Z., and Liu, R. (2000). Studies on the distribution, population size and the active regularity of *lipotes vexillifer* and *neophocaena phocaenoides* in dongting lake and boyang lake. *Resources and Environment in the Yangtze Valley*, 9(4):444–450.
- Yang, Z.-F., Yu, S.-W., Chen, H., and She, D.-X. (2010). Model for defining environmental flow thresholds of spring flood period using abrupt habitat change analysis. *Advances in Water Science*, 21(4):567–574.
- Yu, D., Dong, M., Wang, J., and Zhang, X. (2001). Population status of yangtze finless porpoise in the yangtze river section from hukou to nanjing. *Acta theriologica sinica*, 21(3):174–179.
- Yu, D., Huang, M., Zhao, K., and Chen, S. (2012). Impact of river training on the population abundance of yangtze finless porpoise in dongliu section of the yangtze river. *Acta Theriol Sin*, 21:174–179.
- Yu, D., Jiang, W., and Mi, L. (2003). Preliminary observations on feeding behavior of finless porpoises in a semi-nature reserve of yangtze river. *Acta theriologica sinica*, 23(3):198–202.

- Yu, D., Tang, H., and Wang, K. (2002). The impact of tongling yangtze bridge on the dolphins' habitats. *Acta ecologica sinica/Shengtai Xuebao*, 22(12):2079–2084.
- Yu, D., Wang, J., Yang, G., and Zhang, X. (2005). Primary analysis on habitat selection of yangtze finless porpoise in spring in the section between hukou and digang. *Acta theriologica sinica*, 25(3):302–306.
- Zhang, X., Liu, R., Zhao, Q., Zhang, G., Wei, Z., Wang, X., and Yang, J. (1993). The population of finless porpoise in the middle and lower reaches of yangtze river. *Acta Theriologica Sinica*, 13(4):260–270.
- Zhao, X., Barlow, J., Taylor, B. L., Pitman, R. L., Wang, K., Wei, Z., Stewart, B. S., Turvey, S. T., Akamatsu, T., Reeves, R. R., et al. (2008). Abundance and conservation status of the yangtze finless porpoise in the yangtze river, china. *Biological Conservation*, 141(12):3006–3018.
- Zhao, X. and Wang, D. (2011). Abundance and distribution of yangtze finless porpoise in balijiang section of the yangtze river. *Resources and Environment in the Yangtze Basin*, 20(12):1432–1439.
- Zhou, K., Yang, G., Gao, A., Sun, J., and Xu, X. (1998). Population abundance and distribution characteristics of finless porpoise in the river section from nanjing to hukou of the yangtze river. *Nanjing shida xuebao*, 21(2):91–98.